NASA/CR—2005-213333

Nozzle Aerodynamic Stability During a Throat Shift

Edwin J. Kawecki and Gregg L. Ribeiro
United Technologies Corporation, Pratt & Whitney, East Hartford, Connecticut

February 2005

The NASA STI Program Office . . . in Profile

Since its founding, NASA has been dedicated to the advancement of aeronautics and space science. The NASA Scientific and Technical Information (STI) Program Office plays a key part in helping NASA maintain this important role.

The NASA STI Program Office is operated by Langley Research Center, the Lead Center for NASA's scientific and technical information. The NASA STI Program Office provides access to the NASA STI Database, the largest collection of aeronautical and space science STI in the world. The Program Office is also NASA's institutional mechanism for disseminating the results of its research and development activities. These results are published by NASA in the NASA STI Report Series, which includes the following report types:

- TECHNICAL PUBLICATION. Reports of completed research or a major significant phase of research that present the results of NASA programs and include extensive data or theoretical analysis. Includes compilations of significant scientific and technical data and information deemed to be of continuing reference value. NASA's counterpart of peer-reviewed formal professional papers but has less stringent limitations on manuscript length and extent of graphic presentations.

- TECHNICAL MEMORANDUM. Scientific and technical findings that are preliminary or of specialized interest, e.g., quick release reports, working papers, and bibliographies that contain minimal annotation. Does not contain extensive analysis.

- CONTRACTOR REPORT. Scientific and technical findings by NASA-sponsored contractors and grantees.

- CONFERENCE PUBLICATION. Collected papers from scientific and technical conferences, symposia, seminars, or other meetings sponsored or cosponsored by NASA.

- SPECIAL PUBLICATION. Scientific, technical, or historical information from NASA programs, projects, and missions, often concerned with subjects having substantial public interest.

- TECHNICAL TRANSLATION. English-language translations of foreign scientific and technical material pertinent to NASA's mission.

Specialized services that complement the STI Program Office's diverse offerings include creating custom thesauri, building customized databases, organizing and publishing research results . . . even providing videos.

For more information about the NASA STI Program Office, see the following:

- Access the NASA STI Program Home Page at ***http://www.sti.nasa.gov***

- E-mail your question via the Internet to help@sti.nasa.gov

- Fax your question to the NASA Access Help Desk at 301–621–0134

- Telephone the NASA Access Help Desk at 301–621–0390

- Write to:
  NASA Access Help Desk
  NASA Center for AeroSpace Information
  7121 Standard Drive
  Hanover, MD 21076

NASA/CR—2005-213333

Nozzle Aerodynamic Stability During a Throat Shift

Edwin J. Kawecki and Gregg L. Ribeiro
United Technologies Corporation, Pratt & Whitney, East Hartford, Connecticut

Prepared under Contract NAS3–26618

National Aeronautics and
Space Administration

Glenn Research Center

February 2005

Document History

This research was originally published internally as HSR026 in January 1996.

Available from

NASA Center for Aerospace Information
7121 Standard Drive
Hanover, MD 21076

National Technical Information Service
5285 Port Royal Road
Springfield, VA 22100

Available electronically at http://gltrs.grc.nasa.gov

Contents

List of Figures

List of Tables

Nozzle Aerodynamic Stability During a Throat Shift

Edwin J. Kawecki and Gregg L. Ribeiro
United Technologies Corporation
Pratt & Whitney
East Hartford, Connecticut 06108

1. Summary

An experimental investigation was conducted on the internal aerodynamic stability of a family of two-dimensional (2–D) High Speed Civil Transport (HSCT) nozzle concepts. These nozzles function during takeoff as mixer-ejectors to meet acoustic requirements, then convert to conventional high-performance convergent-divergent (CD) nozzles at cruise. The transition between takeoff mode and cruise mode results in the aerodynamic throat and the minimum cross-sectional area that controls the engine backpressure shifting location within the nozzle for all of the present concepts of interest. The stability and steadiness of the nozzle aerodynamics during this so called *throat shift* process is a concern, as it can directly affect the engine aerodynamic stability, and the mechanical design of the nozzle.

The objective of the study was to determine if pressure spikes or other perturbations occurred during the throat shift process and, if so, identify the causal mechanisms for those perturbations. This included both local pressure effects and upstream influences. The scope of the effort was to design, fabricate, and test a 5 percent scale (3 in. × 5 in. cross-section) variable geometry cold flow rig that investigated these transient pressure characteristics over the range of geometry, operating conditions, and actuation rates representative of the nozzle concepts.

The two nozzle concepts modeled in the test program were the fixed chute (FC) and downstream mixer (DSM). These 2–D nozzles differ principally in that the fixed chute has a large over-area between the forward throat and aft throat locations (three times the forward throat area), while the DSM has an over-area of only about 10 percent. Because both nozzles are symmetric about the engine horizontal centerline, only half of each nozzle was modeled. The fixed chute nozzle requires moving a translating plug and hinged rear flaps in concert to accomplish the throat shift. In the test rig, the required nozzle variable geometry was simulated with a translating plug and a variable angle rear flap. Each was independently actuated by computer controlled servo motors that allowed accurately programmed repeatable motion, with simultaneous coordinated control of the 2 degrees of freedom. The DSM nozzle has no plug, and so was simulated with a variable angle rear flap alone.

The test program included almost 300 throat shifts at a range of nozzle pressure ratios (NPRs) from 2.5 to 6, over-areas between throats of 1X to 3.5X, and actuation times ranging from 0.2 sec to 10 sec.

High-response pressure data, from Kulite sensors located on a nozzle sidewall, indicated no upstream pressure spikes occurred at any time during the entire test matrix. There were abrupt pressure changes of up to 20 percent between the throats during transitions, but the levels were always bounded by the final steady pressures and were not felt upstream of the forward throat.

The conclusions were that engine mass flow and backpressure can be held constant simultaneously during nozzle throat shifts on this class of nozzles, and mode shifts can be accomplished at constant mass flow and engine backpressure without upstream pressure perturbations. This class of nozzle concepts can be designed assuming steady flow loads, and uninterrupted engine back pressures.

2. Introduction

Nozzle Concepts

Exhaust nozzle concepts being considered for the High Speed Civil Transport (HSCT) operate in an ejector mode at low-speed for noise suppression, then transition to nonejector, convergent-divergent (CD) configurations at cruise. Two nozzles, both two-dimensional (2–D), representative of the current HSCT mixer-ejector concepts are the fixed chute (FC) and the downstream mixer (DSM).

The fixed chute nozzle shown in figure 1 is characterized by an ejector chute fixed in the flow under all conditions, and by a plug and rear flaps that move as required to meet the necessary flow areas. In the ejector/low-speed mode, the auxiliary inlet doors are opened, the plug is forward under the ejector/secondary chutes, and the rear flaps are full open. In this configuration, the plug blocks the flow from passing under the chutes, causing the primary flow to be directed between the chutes. The primary flow side of the chutes is the minimum area of the flow and controls the engine backpressure. The secondary area of the nozzle is about twice the primary area, so the resulting mixed area is about three times the primary area. Because the rear flaps are full open, the mixed flow is not backpressured by the nozzle.

The fixed chute high-speed mode is also given in figure 1 and shows that the plug has moved aft and the rear flaps have rotated into the flow. Moving the plug to the aft position unblocks the passage under the ejector/secondary chutes and increases the area by about 2X. In this configuration, the rear flaps are partially closed, causing a new minimum area to be formed in the nozzle at the rear flaps. The plug motion has opened the area at the chute exit, reducing the local Mach number to the M = 0.2 range and greatly reducing the aerodynamic losses through the chutes.

The DSM nozzle is characterized by rotating ejector/secondary chutes that are in the flow only during the ejector mode and a split divergent flap (fig. 2). In the ejector/low-speed mode, the auxiliary inlet doors are opened, the chutes are rotated into the flow through slots in the forward divergent flaps, and the aft divergent flaps are full open. Because the chutes extend close to the engine centerline, the primary flow is directed between the chutes. As in the fixed chute concept, the primary side of the chutes is the minimum or controlling area of the flow; and with the flaps full open, the mixed flow is not backpressured by the nozzle.

Figure 2 also shows the DSM in high-speed mode. The ejector/secondary chutes have rotated out of the flowpath to form smooth forward divergent flaps, and both forward and aft divergent flaps have rotated into the flow. The flowpath now resembles a classical convergent/divergent nozzle with the minimum area of the flow at the hinge between the convergent flap and the forward divergent flap.

The mode transition process for the fixed chute and the DSM adjusts the geometry from the low-speed configuration to the high-speed configuration while maintaining a constant engine backpressure. Maintaining backpressure requires maintaining a choked throat throughout the process, and adjusting the throat area during the mode transition process to compensate for differences in internal losses as the internal aerodynamics change.

The nozzle throat is not, however, located at the same physical station in the low-speed and high-speed configurations. In the low-speed configuration, the throat is located at the chute exit station; while in high-speed it is located several feet downstream in the fixed chute concept (fig. 1), and upstream in the DSM concept (fig. 2) at the convergent-divergent nozzle throat. The throat must transition (or *shift*) between these positions during the mode transition process.

Aerodynamics

The aerodynamics of a throat shift process, and related issues of stability and loads, have not received identified treatment in the open literature. Some experimental and analytical work has been performed as part of certain proprietary nozzle development efforts, as well as the present HSCT effort. The conclusions of these studies are not in agreement, however. Some experimental evidence shows a significant overpressure spike during a throat shift, while the analytical efforts suggest no pressure spike effects should occur. The analytical and experimental studies to date have each looked at particular aspects of the problem and have added understanding, but together still leave significant uncertainty whether the phenomenon will occur (and if so to what severity) for the HSCT geometry and conditions. No definitive predictions of overpressure spikes were made in any of the analyses, although discontinuous pressure jumps between the throats during throat shifts were predicted.

Previous testing conducted as part of a proprietary nozzle development effort at Pratt & Whitney (P&W) (E.B. Thayer, 1970, P&W, West Palm Beach, FL, internal report) has shown severe backpressure spikes can occur in mode transitioning nozzles under some conditions. This testing was not reported in the open literature, but is summarized in figure 3. The configuration tested was a l/l0-scale balance beam nozzle that created a throat upstream of the balance point, at the balance point, or downstream of the balance point, depending upon the amount of flap rotation about the balance point. A low-speed to high-speed transition of this nozzle corresponded to starting at the convergent geometry shown by the dashed line of figure 3. The flaps then rotated, passing through a point where the aft flap was parallel to the centerline. At this position, the throat is larger than in the convergent or the convergent-divergent configuration. The flaps continued to rotate counterclockwise until a new throat formed upstream, and further still until the final throat area was reached. This configuration does not maintain a constant nozzle throat area during the throat shift, and so would be expected to induce an engine backpressure variation inversely proportional to the area variation during the transition.

Analyses at P&W (E.J. Kawecki, 1994, P&W, West Palm Beach, FL, internal study) and General Electric Aircraft Engines (GEAE) (M. Pearson, 1993, GEAE, Cincinnati, OH, internal study), shown in figures 4 and 5, respectively, predict an upstream static pressure variation during the throat shift of the referenced geometry. This is the static pressure upstream of the forward throat and corresponds to the backpressure felt by the engine during the throat shift process. The analysis of Kawecki was one-dimensional (1-D) quasi-steady and assumed subsonic flow upstream of the throat at all times. This 1-D quasi-steady analysis predicted a continuous, regular variation in pressure that never exceeded the end point pressures (fig. 4). The analysis of Pearson is 1-D unsteady and also assumed subsonic flow upstream of the forward throat at all times. This analysis yields a pressure variation from 88 psia to 47 psia (fig. 5) as the throat height varies from 8.6 $in.^2$ to 16 $in.^2$. This is a pressure ratio of 1/1.87, which is the same to within measurement accuracy of the area ratio of 1.86. The pressure is then seen to vary inversely with the throat height in the Pearson study, demonstrating the flow to be quasi-steady. It was concluded that "the short fluid residence time compared to the rate of actuation, even for the assumed 0.1 sec actuation times, resulted in no identifiable time dependent or unsteady effects" (M. Pearson, 1993, GEAE, Cincinnati, OH, internal study).

These analytical results are in contrast to the recalled test data of figure 3, where the pressure initially drops as well, but at some point undergoes a rapid, nearly discontinuous rise to a level exceeding the endpoint pressures by a significant amount. This disagreement suggests that the flow during this particular test was not 1-D quasi-steady, but rather was unsteady or discontinuous at some point during the throat shift. Mechanisms other than quasi-steady or l-D unsteady flow must then be responsible for the observed phenomenon.

A further analysis of the throat shift nozzle mode transition was performed assuming 1-D quasi-steady flow, but also included both subsonic and supersonic branch solutions (E.J. Kawecki, 1994, P&W, West Palm Beach, FL, HSCT Coordination Memo PW94-054N). This analysis was performed to determine if phenomenon may occur due to supersonic to subsonic branch changes that could generate the observed upstream pressure disturbances. The nozzle aerodynamics at each station were calculated for a

representative mode transition, with the geometry changing from the ejector mode position to the high-speed position in an arbitrary 16 steps.

The fixed chute nozzle modeled in the calculations is shown in figure 6, representing the low-speed and high-speed modes. The aerodynamics were assumed steady and calculated for the initial, intermediate, and final positions at each of the following stations. The station numbers and names listed below are shown in figure 6.

Station	Description
1	Engine Plenum
2	Engine Choke (Modeled as a perforated plate operating choked)
3	Transition Section
4	Chutes
5	Chute/Forward Throat
6	Inter-choke Plenum
7	Aft Throat
8	Divergent Flap
9	Ambient Static

Results of those calculations are given in figures 7 through 11. The mode transition is modeled as occurring in 16 steps, which, for convenience, are shown as *Time Steps* (hereafter called out in text as Step 1, Step 2, etc.). The actual calculations are not time-dependent, so the process, in effect, is assumed to be quasi-steady.

Figure 7 shows how the areas were assumed to vary during the mode transition. Four of the stations are shown: the engine choke upstream of the chutes, the chute throat, the inter-choke plenum (plenum between the chute throat and the aft throat), and the aft throat. The only two areas that actually vary in the calculation are the chute throat and the aft throat, although, in general, the aerodynamic conditions can vary to some degree at all stations. At Step 1 in figure 7, the chute throat is at its minimum area, and the aft throat is at its maximum area. The aft throat is closing in Steps 2 through 9, while the chute throat remains at constant area. After Step 9, the chute throat area opens as the plug is moved aft. To maintain a constant engine pressure, note that the aft throat must continue to close as the plug moves. This is a result of the chute losses dropping as the chute exit area opens, and the local Mach number drops. The aft throat must then close incrementally to compensate as the total pressure approaching the aft throat increases.

Corresponding to these geometry variations, figure 8 shows the Mach number variation at each station through the nozzle. At Step 1 the chute throat is choked, and the downstream throat is unchoked (M = 0.3). The aft throat Mach number increases as it closes, until it finally chokes at Step 9. The chute throat is also choked at Step 9. At Step 10 the plug has moved slightly, opening the chute area and dropping the chute Mach number. For all later times the area continues to increase, so the Mach number continues to decrease at the chutes. The aft throat is kept choked at Step 10 and for all times after.

The static pressures through the rig are shown in figures 9 through 11. Figure 9 assumes the flow leaving the chutes expands isentropically to the available area between the chutes and the aft throat. The flow can expand supersonically or subsonically in this process. Figure 12 shows the isentropic relation for pressure ratio versus area, including the range of pressure ratios from takeoff (ejector/low-speed mode) through climb (high-speed mode), and the area ratio for the fixed chute design. In the absence of any backpressure, the area available and the range of pressures expected suggest the flow expands to the supersonic branch solution. In figure 9, the flow coming out of the chutes wants to initially over-expand below ambient pressure. The flow in the actual case will likely separate rather than fully over-expand, and so only expand to ambient pressure or a little below. The flow may remain supersonic throughout the nozzle, or shock down within the nozzle after a short distance. The extent of the supersonic region depends on the particular aerodynamics of the primary pluming, and is not known *a priori*, although some supersonic region is expected. As the exit nozzle closes, the static pressure at the throat rises, until at Step 7 the ideal isentropic pressure at the aft throat is above ambient. At this point, the aft throat starts to

backpressure the assumed supersonic stream coming from the chutes. Further closing of the aft throat will increase the backpressure on the flow as shown.

Traditionally, adverse pressure gradient supersonic flows like this are unstable and must be controlled carefully or the flow will shock down to the subsonic solution. An example of this is the unstart of a supersonic inlet due to over-backpressuring. This nozzle flow is not well behaved or controllable like an inlet, nor can it easily be. The flow exiting the chutes is then not expected to sustain the adverse pressure gradient that occurs when the aft throat closes. This will induce a shock that travels upstream from the throat to the chute, which will abruptly raise the pressure as the flow transitions to subsonic conditions.

During this process, there can also be an overpressure spike in the supersonic flow region that follows behind the shock. The strength of the overpressure is not readily predictable, as it depends on the degree of backpressure and the state of the boundary layer adjacent to the flow, neither of which are well known. Inlet unstart tests in this Mach number range can produce overpressure spikes of 2X the subsonic pressure levels, or no excess above the subsonic branch steady pressure solution, depending on the backpressure. The transition from supersonic to subsonic flow is illustrated by the inter-choke plenum line in figure 11, between Steps 7 and 8. No overpressure spike is predicted, just the quasi-steady pressure discontinuity (pressure jump) occurring when the flow adjusts from the supersonic branch to the subsonic branch solution. In this model, the pressure jump is confined to the region between the throats. The predicted pressure level never exceeds the upstream total pressure, so no significant pressure disturbance is expected upstream of the forward throat unless a backpressure-induced overpressure spike occurs within the nozzle.

Analysis results suggest that an abrupt pressure change can occur within the nozzle during the low-speed to high-speed mode transition process. Specifically, a pressure discontinuity can occur when the primary flow is backpressured by the closing of the aft throat, and thus shocks down in the over-area region from the supersonic branch solution to the subsonic branch solution. Distinct from the throat shift process, this phenomenon can occur before the second choke is established at the aft throat and prior to the actual throat shift.

Based on this analysis, a possible, but unsubstantiated, mechanism for the observed historical test results (E.B. Thayer, 1970, P&W, West Palm Beach, FL, internal report) is that the flow upstream of the forward throat was initially subsonic when either the forward or aft throats were established, but then went supersonic when the controlling area increased as the forward throat opened during the throat shift. This would result in the observed pressure drop upstream of the forward throat during the process. As the throat shift continued, the pressure would remain low, corresponding to supersonic flow, until the aft throat began to close down. At some point the decreasing throat area backpressured the flow to become subsonic, with the resulting shock traveling upstream of the nozzle and causing an abrupt pressure rise. This pressure could exceed the steady subsonic pressures if the backpressures were sufficient, as in a mixed compression supersonic inlet.

No actual data from the historical test are available, so the proposed possible mechanism cannot be evaluated or confirmed. The analysis does suggest that the behavior may occur only if there is both a significant change in the controlling area, and certain facility-to-nozzle geometries. The present HSCT nozzles, however, are designed to always maintain a nearly constant controlling area so as to maintain a constant backpressure. Substantially different than the historical test results, this suggests that at least one mechanism that could explain the previous results is not present in the HSCT nozzles. Due to this mechanism then, the observed pressure spike would then not occur in the HSCT nozzles.

Allowable Limit of Upstream Traveling Pressure Spike

The allowable backpressure variations are set by the fan surge and stall margins, and the duct pressure wave transmission characteristics. For the present HSCT engines, the allowable backpressure variations based on design margins have been summarized (E.J. Kawecki, 1994, P&W, West Palm Beach, FL, HSCT Coordination Memo PW94-024N). The results were that the present 25 percent $\Delta P/P$ fan stall

margin is the controlling factor and limits the backpressure increase to less than this amount. The pressure increase may have to be reduced to the 10 to 15 percent range once planned transient cycle analyses and stability audits are accomplished. The backpressure decrease is limited to the fan choke pressure, where flutter problems can occur. The fan will choke at about −40 percent ΔP/P, which sets the lower limit of allowable nozzle backpressure. Both of these limits are independent of frequency for 1/10-second duration events and longer. Kuchar reported results of a duct transmission study that evaluated the duct transfer function and fan sensitivity to the pulses for several assumed pulse shapes, over a range of pulse durations and amplitudes (A. Kuchar, 1994, GEAE, Cincinnati, OH, HSCT Coordination Memo GE94-079N Revision G). The duct transfer function is defined as the ratio of percent increase in the total pressure at the fan outlet guide vane (OGV) exit to pulse amplitude. The pulse amplitude is the percent increase in static pressure at the variable area bypass injector (VABI) discharge plane. Fan sensitivity is defined as the ratio of loss in fan stall margin to pulse amplitude. "Results indicate that pulses in the range of 20-30 milliseconds full scale would have the largest impact on fan stall margin" (A. Kuchar, 1994, GEAE, Cincinnati, OH, HSCT Coordination Memo GE94-079N Revision G). Results above 1/10-second duration agree with the previously quoted results (E.J. Kawecki, 1994, P&W, West Palm Beach, FL, HSCT Coordination Memo PW94-054N), and results for pulses of duration less than 10 milliseconds show a decrease in sensitivity due to attenuation of the pulse passing through the duct. The results are summarized in figure 13, where the fan sensitivity to pressure perturbations are given for different pulse widths and shapes.

Combining the absolute level of allowable pressure perturbation (E.J. Kawecki, 1994, P&W, West Palm Beach, FL, HSCT Coordination Memo PW94-024N), and the duct transmission characteristics (A. Kuchar, 1994, GEAE, Cincinnati, OH, HSCT Coordination Memo GE94-079N Revision G) yields an approximate allowable upstream traveling pressure spike emanating from the nozzle of 15 percent allowable/1.4 gain factor = 10 percent pressure excursion. The allowable upstream traveling spike is then 10 percent above the local total pressure at the nozzle.

The result of these analyses was that no definitive explanation for the previous test results was forthcoming. A test program with HSCT configurations undergoing mode transitions is called for, with the specific purpose of characterizing the aerodynamics, measuring the pressures throughout the nozzle, and establishing whether mode transitions can be accomplished while maintaining constant engine backpressure.

3. Test Program

Dynamic Stability Rig Configurations

Three rig configurations, each with a different amount of area change between the controlling areas, were tested. The configurations are the fixed chute (FC) nozzle (with a large over-area of about 200 percent), the downstream mixer (DSM) nozzle (with a small over-area of about 50 and 10 percent), and a flat plate (with no over-area). Figure l4 shows the rig in the fixed chute nozzle configuration. Visible in the photograph are the motors and drivers for the translating plug (above the model) and the aft throat convergent flap (below the model), Kulite cables (in front of the model), and hypotubes (behind the model). The primary flow, gaseous nitrogen (GN2), was supplied from an 1800 psia tank. Valves, filters, pressure reducing controllers, and a sonic nozzle were used *en route* to the rig.

Figure 15 shows the rig in the fixed chute configuration with the sidewall removed. In the ejector/low-speed mode (fig. 16), the primary flow is forced between the secondary chutes by a translating plug positioned under the chutes. The flow exits the chutes, then plumes in the large over-area downstream of the chutes before passing through the aft throat. In this test program the chutes are not flowing, and so were modeled as solid, i.e., the secondary chutes are totally closed off. The auxiliary inlet supplying the chutes will most likely be closed in the product prior to the mode shift. This would avoid

backflowing the chutes as the backpressure starts to rise. The mode transition starts as the aft throat convergent flap begins to close, eventually forming a second throat. The plug then starts to move in concert with the still closing convergent flap such that the engine backpressure remains constant. Finally, the plug reaches the limit of travel, and a single throat remains at the convergent flap (fig. 17).

Figure l8 shows the rig in the DSM configuration with the sidewall removed. The mode transition is simulated as a 1 degree of freedom system and takes place through an over-area of about 50 or 10 percent in a nearly rectangular channel. In the ejector/low-speed mode (fig. 19), the throat is at the aft end of the plate, with subsonic flow everywhere upstream of this point. During the mode transition, the plate rotates about the front hinge, causing the aft throat to open and leaving the forward throat controlling the area (fig. 20). The flow downstream of the forward throat then becomes supersonic.

The no over-area plate configuration represents a limiting case with no plenum between the two choke stations. The DSM configuration with a flat plate installed was used to model this configuration.

Test Matrix

A test matrix was defined to evaluate the throat shift aerodynamics. The test matrix is shown in table 1, and consisted of three test series, each on a different rig configuration. In each test series, the variable geometry was actuated to induce a throat shift. Any abrupt pressure changes were noted, along with whether they occurred prior to the throat shift, during the throat shift, or after the throat shift.

The experiments were conducted over a range of nozzle pressure ratios (NPRs) representative of the takeoff through climb values. The NPR ranges from about 4 at takeoff to about 6 at 32,000 ft. The nozzle unstart and mode transition issues were expected to be active over this range of pressure ratios.

The rate of actuation was varied over a representative range to determine the effect of actuation rate on the throat shift and to include the effects of scaling on actuation rates. Throat shifts were accomplished over a range of times from 0.2 seconds to 10 seconds.

In the fixed chute configuration, suppressor area ratio (SAR) was varied from 3.5 to 1.6 by changing the number of chutes, which changed the chute throat area. These chute assemblies are shown in figure 2l. In the DSM nozzle configuration, percent over-area was varied by using two bent plates: a 50 percent over-area plate and a 10 percent over-area plate. Several plates, including the flat plate, are shown in figure 22.

For each of the configurations, a series of tests were conducted where the aft throat was swept from full open (closing sweep), to choked, then back to full open (opening sweep) again.

Table 1.—Test Matrix

NPR	Actuation Rate(s) (sec)	Configuration: Fixed Chute: No. of Chutes/SAR: 10 3.5	9 2.8	8 2.3	5 1.6	Translating Plug: Fixed Forward	Fixed Between	Fixed Aft	Programmed Motion	None	DSM: % Over-Area: 50%	10%	Flat Plate	Variable Angle Rear Flap: Closing Sweep	Opening Sweep	Programmed Motion
2	3	x				x								x	x	
2.4	0.3, 0.5, 1, 3, 5	x				x			x					x	x	x
2.4	0.3, 0.5, 1, 3, 5		x			x								x	x	
2.4	0.3, 0.5, 1, 3, 5			x		x								x	x	
2.4	0.3, 0.5, 1, 3, 5				x	x								x	x	
3	0.2, 0.3, 0.5, 1, 3, 5, 10	x				x	x	x	x					x	x	x
3	0.3, 0.5, 1, 3, 5		x			x								x	x	
3	0.3, 0.5, 1, 3, 5			x		x								x	x	
3	0.3, 0.5, 1, 3, 5				x	x								x	x	
4	0.3, 3	x							x					x		x
4.5	0.3, 0.5, 1, 3, 5, 10	x				x	x	x						x	x	
4.5	0.3, 0.5, 1, 3, 5		x			x								x	x	
4.5	0.3, 0.5, 1, 3, 5			x		x								x	x	
4.5	0.3, 0.5, 1, 3, 5				x	x								x	x	
5	0.3, 0.5, 1, 3, 5	x				x			x					x	x	x
5	0.3, 0.5, 1, 3, 5		x			x								x	x	
5	0.3, 0.5, 1, 3, 5			x		x								x	x	
5	0.3, 0.5, 1, 3, 5				x	x								x	x	
5.4	3	x												x	x	
6.1	0.2, 0.3, 0.5, 1, 3, 5	x				x								x	x	
6.1	0.3, 0.5, 1, 3, 5		x			x								x	x	
6.1	0.3, 0.5, 1, 3, 5			x		x								x	x	
2.4	0.3, 1, 3									x	x			x	x	
2.4	0.3, 0.5, 1, 3, 5									x		x		x	x	
3	0.3, 1, 3									x	x			x	x	
3	0.3, 1, 3, 5									x		x		x	x	
4.5	0.3, 1, 3									x	x			x	x	
4.5	0.3, 1, 3, 5									x		x		x	x	
5	0.3, 1, 3									x	x			x	x	
5	0.3, 1, 3, 5									x		x		x	x	
6.1	0.3, 1, 3									x	x			x	x	
6.1	0.3, 1, 3, 5									x		x		x	x	
2.4	0.3, 1, 3									x			x	x	x	
3	0.3, 1, 3									x			x	x	x	
4.5	0.3, 1, 3									x			x	x	x	
5	0.3, 1, 3									x			x	x	x	
6.1	0.3, 1, 3									x			x	x	x	

Tests were also conducted in the fixed chute configuration with the plug translating aft after a dual choke had been established. These tests most closely simulated the planned functioning of the nozzle, where the forward throat is relieved by opening up its area after the aft throat is established. Opening the forward throat area (i.e., moving the plug) is required to achieve a full throat shift without disturbing the engine backpressure or flow. Closing down the aft throat past choke initiation would also unchoke the chute station, but would induce a change in the upstream pressure, or mass flow, or both. These tests were also performed with the plug and aft throat moving in concert to maintain a constant pressure upstream of the forward throat.

Instrumentation

The rig had instrumentation locations for 16 high-response (Kulite) static pressure sensors and 25 low-response conventional static pressure sensors (hypotubes), as shown in figure 23. Pressure sensor locations are given in table 2. The Kulite sensor response was from dc to 20,000 Hz, while the conventional pressures responded from dc to about 10 Hz. Each test configuration recorded a different set of these pressure sensors consistent with the geometry of the model. For example, in the DSM configuration, pressure instrumentation in the chute station and some of the inter-choke plenum station is blocked by hardware and was not recorded. A choked sonic nozzle was used by the facility to measure the mass flow and maintain it constant during the test. The tests were conducted with ambient temperature dry nitrogen, and the temperature was measured in the upstream plenum. The position of the variable geometry was recorded during the test.

Test Results

Table 3 is a log of all of the tests for which results are presented in this report. Almost 300 tests were performed to examine the parameters detailed in the test matrix. The test log represents the specific tests chosen to present the results demonstrated by all of the tests. Shown in the table are analog data tape numbers used to record Kulite and variable geometry data and the digital data transient numbers used to record conventional pressure and variable geometry data for each test. The digital data transient numbers were used to reference the tests during the analysis of the test data and are noted on all plots in this report.

The various configurations are identified for each test in the test log. Fixed chute configurations are denoted by an *FC-#,* where the # varies between 1 (10 chutes), 2 (9 chutes), 3 (8 chutes), and 4 (5 chutes). DSM and flat plate configurations use a *DSM-#,* where # varies between 1 (flat plate), 2 (10 percent over-area plate), and 3 (50 percent over-area plate). The motion of the aft throat convergent flap for the fixed chute configurations and the variable angle rear flap for the DSM configurations is shown under *Flap Action*. Whether the flap was closing, opening, or closing then opening (abbreviated with *c/o*) and the angles bounding, the motion are detailed. The zero degree reference was for a horizontal flap, i.e., the flap was parallel to the rig top and bottom plate surfaces. For the fixed chute configuration, this corresponds to a full open aft throat convergent flap. In the DSM configuration, the zero degree reference corresponds to equal forward and aft throat areas. For the flat plate, at this position, the plate was horizontal. The translating plug action (position fixed forward, aft or at a distance from the forward location or motion moving aft or moving aft then forward then aft) is shown. The move time for the variable geometry actuation is listed. This is the time entered into the drive and motor controller for the actuated parts to complete their motion. In tests that required the actuated parts to make two moves (e.g., closing then opening a flap), the move time corresponds to the time allotted for each move (i.e., the closing move time and the opening move time). Between the two moves is a short period of time, which varied from test to test, during which no parts were actuated. Tests where the flap and translating plug were moved in concert to maintain a constant upstream pressure used a computer program to coordinate the motions. The names of the programs are identified in the log.

Table 2.—Dynamic Stability Rig Instrumentation Locations

Low-Response Pressure Sensors		
Header	**X**	**Y**
1	0.40	0.60
2	1.15	0.60
3	1.90	0.60
4	3.00	0.60
5	3.85	0.60
6	4.70	0.60
7	5.10	0.25
8	5.10	0.90
9	5.15	1.25
10	5.35	1.00
11	5.50	0.25
12	5.55	0.90
13	5.70	1.25
14	5.80	0.80
15	5.90	0.25
16	6.15	0.70
17	6.35	0.25
18	6.60	0.60
19	6.95	0.20
20	6.95	0.45
21	7.30	0.30
22	7.60	0.25
23	8.40	0.25
24	9.50	0.25
25	10.60	0.25

High-Response Pressure Sensors		
Header	**X**	**Y**
A	0.70	0.90
B	1.50	0.90
C	2.80	0.90
D	3.55	0.90
E	4.60	0.90
F	4.95	1.10
G	5.35	0.25
H	5.45	1.15
I	6.00	0.25
J	6.20	0.95
K	6.60	0.25
L	6.70	0.80
M	7.20	0.60
N	7.30	0.15
O	7.80	0.25
P	10.10	0.25

Note: Low-response pressure sensors are conventional hypotubes. High-response pressure sensors are Kulites. X is measured from the rig inlet. Y is measured from the inside surface of the rig bottom plate. (See fig. 23.) All dimensions are in inches.

Table 3.—Test Log

Test No.	Analog Data		Digital Data Transient No.	Configuration	Pressure Sensor 5 (psia)	Flap Action	Translating Plug Action	Move Time (sec)	Program Names
	Tape No.	Tape (ft)							
1	DK252014A5	600	73	FC-1	45	Closing, 15 > 45 degrees	Fixed Forward	10	N/A
2	DK252014A5	686	79	FC-1	45	Closing, 15 > 45 degrees	Fixed Forward	0.2	N/A
3	DK256014A5	700	101	FC-1	45	Closing, 1.6 > 40 degrees	Fixed Forward	5	N/A
4	DK256014A5	733	103	FC-1	45	Closing, 1.6 > 40 degrees	Fixed Forward	3	N/A
5	DK256014A5	758	105	FC-1	45	Closing, 1.6 > 40 degrees	Fixed Forward	1	N/A
6	DK256014A5	780	107	FC-1	45	Closing, 1.6 > 40 degrees	Fixed Forward	0.5	N/A
7	DK256014A5	849	113	FC-1	67	Closing, 1.6 > 40 degrees	Fixed Forward	3	N/A
8	DK259014A5	1091	137	FC-1	80	Closing, 1.6 > 40 degrees	Fixed Forward	3	N/A
9	DK259014A5	1107	138	FC-1	80	Opening, 40 > 1.6 degrees	Fixed Forward	3	N/A
10	DK259014A5	6616	217	DSM-2	90	c/o 2.8 > -2.9 > 2.8 degrees	N/A	1	N/A
11	DK259014A5	7300	251	DSM-2	35	c/o 2.8 > -2.9 > 2.8 degrees	N/A	3	N/A
12	DK259014A5	7362	254	DSM-2	45	c/o 2.8 > -2.9 > 2.8 degrees	N/A	3	N/A
13	DK259014A5	7383	255	DSM-2	45	c/o 2.8 > -2.9 > 2.8 degrees	N/A	1	N/A
14	DK259014A5	7399	256	DSM-2	45	c/o 2.8 > -2.9 > 2.8 degrees	N/A	0.3	N/A
15	DK259014A5	7414	257	DSM-2	67	c/o 2.8 > -2.9 > 2.8 degrees	N/A	3	N/A
16	DK259014A5	7464	260	DSM-2	75	c/o 2.8 > -2.9 > 2.8 degrees	N/A	3	N/A
17	DK259014A5	7514	263	DSM-2	90	c/o 2.8 > -2.9 > 2.8 degrees	N/A	3	N/A
18	DK259014A5	7536	264	DSM-2	90	c/o 2.8 > -2.9 > 2.8 degrees	N/A	1	N/A
19	DK259014A5	8209	269	DSM-1	45	c/o 2.8 > -2.9 > 2.8 degrees	N/A	3	N/A
20	DK285014A5	665	285	DSM-3	45	c/o 4.4 > -1.4 > 4.4 degrees	N/A	3	N/A
21	DK285014A5	2043	323	FC-3	67	c/o 1.6 > 40 > 1.6 degrees	Fixed Forward	3	N/A
22	DK285014A5	2429	344	FC-2	45	c/o 1.6 > 40 > 1.6 degrees	Fixed Forward	3	N/A
23	DK285014A5	2519	349	FC-2	67	c/o 1.6 > 40 > 1.6 degrees	Fixed Forward	3	N/A
24	DK285014A5	2613	354	FC-2	75	c/o 1.6 > 40 > 1.6 degrees	Fixed Forward	3	N/A
25	DK285014A5	2706	359	FC-2	90	c/o 1.6 > 33 > 1.6 degrees	Fixed Forward	3	N/A
26	DK285014A5	2969	374	FC-4	67	c/o 1.6 > 27.1 > 1.6 degrees	Fixed Forward	3	N/A
27	DK285014A5	3240	388	FC-1	35	c/o 1.6 > 40 > 1.6 degrees	M Aft > Fwd > Aft	5	F5PCRU, F5PORU
28	DK285014A5	3393	392	FC-1	45	c/o 1.6 > 40 > 1.6 degrees	M Aft > Fwd > Aft	5	F5PCRU, F5PORU

Fixed Chute Configurations	
FC-1	10 Chute Mixer
FC-2	9 Chute Mixer
FC-3	8 Chute Mixer
FC-4	5 Chute Mixer

Downstream Mixer Configurations	
DSM-1	0% Over-Area Plate
DSM-2	10% Over-Area Plate
DSM-3	50% Over-Area Plate

Typical data recorded during the tests is shown in figures 24, 25, and 26. Figure 24 shows variable geometry positions and several low-response static pressure sensor readings for a test of the fixed chute configuration with 10 chutes (FC-1). During this test, the aft throat convergent flap and the translating plug were moved in concert to maintain a constant pressure (low-response Pressure Sensor 5) upstream of the forward throat. Each plot contains a drawing of the model showing how the moving parts were actuated. The actuation began in the position denoted by solid lines, moved to the position denoted by dashed lines, then back to the start position. When the throat shifts occurred is also noted on the plots. The location of the throat shifts was determined from the aft throat convergent flap and translating plug positions. As the aft throat convergent flap closes, the aft throat area will eventually equal, then drop below the forward throat area causing the upstream pressure to rise. By translating the plug aft to increase the forward throat area, reducing the aerodynamic loses through the chutes, the upstream pressure can be maintained constant. The throat shifts aft when the translating plug moves aft. Similarly, the throat shifts forward when the translating plug stops moving forward. Figures 25 and 26 show the same test as figure 24, but with high-response pressure sensors. In figure 25 the throat is being shifted aft while in figure 26 the throat is being shifted forward.

Many of the static pressure sensors located in the same stations shown in figure 6 recorded similar pressure levels. This allows a reduced number of sensors to be presented without a loss in scope of the test results. Based on figure 24 the following reduced low-response pressure sensor schedule was developed only for plotting purposes in this report:

Station	Static Pressure Sensor Number
Engine Plenum	3
Transition Section	5
Chutes	9
Chute Throat	12
Inter-Choke Plenum	18
Aft Throat	22
Divergent Flap	23

Low-response Pressure Sensor 5, from the transition section, will be used to represent the pressure upstream of the forward throat in all data plots.

Test results shown in figures 24, 25, and 26 demonstrated the ability of both concepts to maintain both constant mass flow, because of the upstream choked sonic nozzle and the constant backpressure while undergoing a throat shift. Figures 27, 28, 29, and 30 illustrate a sequence of tests with the fixed chute configuration with 10 chutes (FC-1) where the variable geometry was first moved independently, then in concert. The first two cases (independent motion) are shown in figures 27 and 28 and demonstrate a wide swing in backpressure at constant mass flow. In figure 27, the aft throat convergent flap is first closed, then the plug is moved only after the flap is closed to its final position. This independent sequencing is seen to cause a significant pressure increase then decrease to the upstream pressure (Sensor 5). Similarly in figure 28, the engine pressure drops then rises if the plug is moved to fully open first, then the aft throat convergent flap closed. Finally, if the plug and flap are moved in concert as shown in figure 29 with low-response pressure sensor data and figure 30 with high-response pressure sensor data, the upstream pressure (Sensor 5) and mass flow can be maintained virtually constant for both directions of the mode shift.

For the fixed chute configuration, the effect of changes in the number of chutes, which varied the SAR, on low-response Pressure Sensor 5 is shown in figure 31 and on high-response pressure Sensor D is shown in
figure 32. During these tests, the NPR and actuation rate were held constant. The plug was fixed forward under the chutes, and the aft throat convergent flap was swept from the open position to the closed position, shifting the throat from the chutes to the aft location. The figures illustrate no change in the behavior of the upstream pressure as SAR was varied from 3.5 to l.6. The reason for the variation in the beginning of the increase in the pressure readings is because of differences in the time the actuation was

begun and therefore in the start of mode transition. It should be noted that while the readings in figure 31 for the 8-chute and 5-chute configurations went off-scale, this occurred after the throat shift. The noise in figure 32 at the beginning of the 10 chute data is because of the analog tape start-up. Figures 33 and 34 show the effect on the pressure upstream of the forward throat due to changes in the percentage of small over-area for the DSM configuration for low-response and high-response pressure sensors, respectively. These tests were conducted at the same NPR and actuation rate. The variable angle rear flap was swept from the open position to the closed position, shifting the throat from the aft location to the forward location. No change in the behavior of low-response Pressure Sensor 5 or high-response Pressure Sensor D was noted.

NPR was varied throughout the test program for all configurations. Figures 35 and 36 show the effect on the pressure upstream of the forward throat due to NPR changes in the nine-chute fixed chute configuration (FC-2) for low-response and high-response pressure sensors, respectively. During these tests, the aft throat convergent flap was swept from the open position to the closed position while the plug was fixed forward under the chutes, shifting the throat from the chutes to the aft location. No difference in the behavior of Sensor 5 or D was noted. In figures 37 and 38, the effect of NPR is shown for the DSM configuration with the 10 percent over-area plate. Again, there was no change in the behavior of the upstream pressure sensors.

The effect on the pressure upstream of the forward throat due to changes in the actuation rate is shown in figure 39 for low-response Pressure Sensor 5 and is shown in figure 40 for high-response Pressure Sensor D for the fixed chute configuration. The plug was fixed forward under the chutes and the aft throat convergent flap was swept from the open to closed position, shifting the throat from the chutes to the aft location. The slope of the curves varies due to actuation rate changes, but the sensor readings do not indicate any change in behavior. Figures 41 and 42 show the effect of actuation rate on the 10 percent over-area DSM configuration for the low-response and high-response sensors, respectively. During these tests, the variable angle rear flap was swept from the open position to the closed position, then back to the open position, shifting the throat from the forward location to the aft location and then back to the forward location. No change in the behavior of the upstream pressure sensors was noted.

Figure 43 shows high-response pressure sensor data for the fixed chute configuration with 10 chutes for a low-speed to high-speed mode transition. In this test, the translating plug was fixed 0.14 inches downstream of the chutes and did not move. The data show that the aft throat convergent flap closes some amount before the pressure starts to rise in the inter-choke plenum. The pressure in this plenum has a small (3-5 psi) jump before the throat shift. Note that there is no such jump in the upstream sensors of the transition section and the chutes, indicating that no change is felt upstream of the forward throat when the pressure in initially rising downstream of the chutes. The small bump at 7.5 seconds in all of the pressure data was a hick-up in the GN2 flow supply. The pressure in the inter-choke plenum continues to rise steadily and evenly until the throat shift, when a rapid pressure rise of about 25 percent occurs. Again, there is no such rapid pressure rise upstream of the forward throat or at the beginning of the inter-choke plenum at Sensor J. Instead, the upstream pressures rise steadily and evenly until the aft throat convergent flap stops closing. Therefore, pressure disturbances downstream of the forward throat do not propagate upstream before or after the throat shift. Figure 44 shows high-response pressure sensor data for the same configuration and test conditions with the aft throat convergent flap opening (high-speed to low-speed mode transition). The aerodynamics mirror the case in figure 43. Transition section pressures show a gradual drop in pressure as the aft throat is opened, up to the point where the pressures in the inter-choke plenum start to react. From this time on, the pressures upstream of the forward throat, in the transition section, are steady even though the pressures downstream of the forward throat, in the inter-choke plenum, continue to drop and undergo some abrupt changes. Again, no pressure spikes or jumps were observed upstream of the forward throat at anytime during the test.

The DSM configuration also showed no upstream pressure disturbances during mode transitions in either direction. Results in figure 45 show high-response pressure sensor data for a low-speed to high-speed mode shift; and in figure 46, for a high-speed to low-speed shift. The sensors upstream of the forward throat, transition section and forward throat, exhibit no abrupt changes in pressure even though

Pressure Sensor I in the inter-choke plenum does undergo an abrupt pressure rise. This abrupt pressure rise results from the flow in the channel transitioning from subsonic to supersonic (high pressure to low pressure, as in figure 45) or the reverse (as in figure 46). Again, no pressure spikes or jumps were observed upstream of the forward throat at any time during the test.

4. Conclusions

An experimental investigation was conducted on the internal aerodynamic stability of a family of two-dimensional (2–D) High Speed Civil Transport (HSCT) nozzle concepts. These nozzles function during takeoff as mixer-ejectors to meet acoustic requirements, then convert to conventional high performance convergent-divergent nozzles at cruise. The transition between takeoff mode and cruise mode results in the aerodynamic throat and the minimum cross sectional area that controls the engine backpressure shifting location within the nozzle for all of the present concepts of interest. The stability and steadiness of the nozzle aerodynamics during this *throat shift* process is a concern, as it can directly affect the engine aerodynamic stability and the mechanical design of the nozzle.

An analysis of the throat shift process has been performed at Pratt & Whitney, Boeing, and General Electric Aircraft Engines in support of the present HSCT designs. These works have been published within program channels, but are not open literature reports. They generally assume quasi-steady subsonic, aerodynamics during the throat shift process and look specifically at the local nozzle internal aerodynamics. The conclusions of these studies are not in agreement, however, with some experimental evidence showing a significant overpressure spike during a throat shift, while the analytical efforts suggest no pressure spike effects should occur. The analytical and experimental studies to date have each looked at particular aspects of the problem and have added understanding, but together still leave significant uncertainty whether the phenomenon will occur for the HSCT geometry and conditions (and if so, to what severity). No definitive predictions of overpressure spikes were made in any of the analyses, although discontinuous pressure jumps between the throats during throat shifts were predicted.

The two nozzle concepts modeled in the test program were the fixed chute (FC) and downstream mixer (DSM). These 2–D nozzles differ principally in that the fixed chute has a large over-area between the forward throat and aft throat locations (three times the forward throat area), while the DSM has an over-area of only about 10 percent. Because both nozzles are symmetric about the engine horizontal centerline, only half of each nozzle was modeled. A rig was built that could be modified into two configurations, each representing one of the nozzle concepts. The fixed chute nozzle requires moving a translating plug and hinged rear flaps in concert to accomplish the throat shift. In the test rig, the required nozzle variable geometry was simulated with a translating plug and a variable angle rear flap. The DSM nozzle has no plug, and so was simulated with a variable angle rear flap alone.

Results for the almost 300 throat shifts conducted in this test program show the following:

- No upstream (engine backpressure) pressure spike was ever observed for either of the configurations. A spike is defined as a pressure excursion where the maximum or minimum pressure reached exceeds the steady state end point pressure levels.
- No pressure jumps were ever observed upstream of the forward throat for either concept. A pressure jump is defined as any discrete discontinuous pressure rise that occurs during a gradual continuous geometry change. Pressure jumps do not over shoot the initial or final pressures.
- Pressure jumps of up to 15 percent were observed between throat stations for both concepts. These pressure jumps occurred in less than 10 percent of the cases and never resulted in the momentary instantaneous pressures exceeding the final steady state values.

Symbols

A_j	Physical Nozzle Primary Choke Area, in.^{2}
A_m	Nozzle Cross-Sectional Flow Area at Mixer Exit, in.^{2}
ALPHA	Variable Angle Rear Flap angle, deg
Fan Sensitivity	Ratio of loss in fan stall margin to pulse amplitude, where pulse amplitude is the percent increase in static pressure at the variable area bypass injector (VABI) discharge plane
M	Mach Number
NPR	Nozzle Pressure Ratio, $P_{t,j}/P_a$
P_a	Ambient Pressure, psia
$P_{t,j}$	Jet Total Pressure, psia
SAR	Suppressor Area Ratio, A_m/A_j
THETA	Aft Throat Convergent Flap Angle, deg
X	Axial Distance Downstream of the Rig Inlet, in.
XPLUG	Translating Plug Axial Location, in.
Y	Vertical Distance from the Inside Surface of the Rig Bottom Plate, in.
Y	Specific Heat Ratio

Acronyms and Abbreviations

CD	Convergent-Divergent
c/o	Closing then Opening
DC	Direct Current Representing a Zero Frequency, Hz
DSM	Downstream Mixer
DSM-1	Downstream Mixer Nozzle Configuration with Flat Plate
DSM-2	Downstream Mixer Nozzle Configuration with 10 percent Over-Area Plate
DSM-3	Downstream Mixer Nozzle Configuration with 50 percent Over-Area Plate
FC	Fixed Chute
FC-1	Fixed Chute Nozzle Configuration With 10 Chutes
FC-2	Fixed Chute Nozzle Configuration With 9 Chutes
FC-3	Fixed Chute Nozzle Configuration With 8 Chutes
FC-4	Fixed Chute Nozzle Configuration With 5 Chutes
fwd	Forward
GEAE	General Electric Aircraft Engines
GN2	Gaseous Nitrogen
HSCT	High Speed Civil Transport
OGV	Outlet Guide Vane
P&W	Pratt & Whitney
VABI	Variable Area Bypass Injector
1-D	One-Dimensional
2–D	Two-Dimensional

Bibliography

Clark, L.T: Status Report on *Unsteady Analysis of Nozzle Throat Shift*. Boeing Internal Document PROP-BNB 5B-93-020, July 1993.

Shapiro, Ascher H.: *The Dynamics and Thermodynamics of Compressible Fluid Flow*, Volume I. Ronald Press Co., c. 1953.

Long, D.F.; Hanus G.J.: *Aerodynamic Design and Analysis of Dual Throat Hypersonic Nozzle*. United Technologies Research Center, Report No. 8901706, 1989.

Pekkari, L-0: *Aeroelastic Stability of Supersonic Nozzles with Separated Flow*. AIAA/ SAE/ASME 29th Joint Propulsion Conference and Exhibit Paper, 1993.

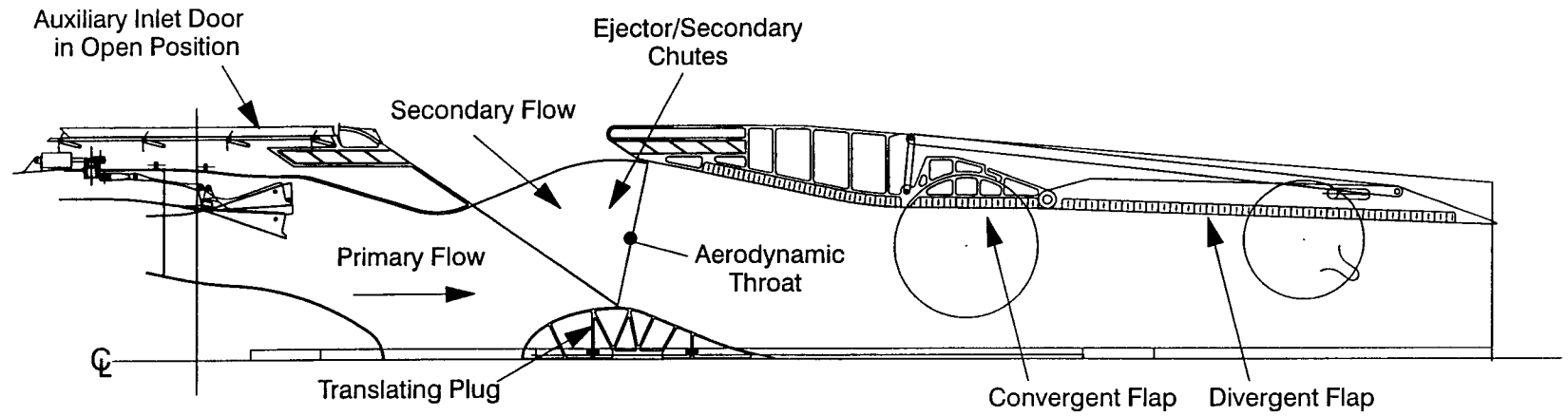

(a) Ejector/Low−Speed Mode

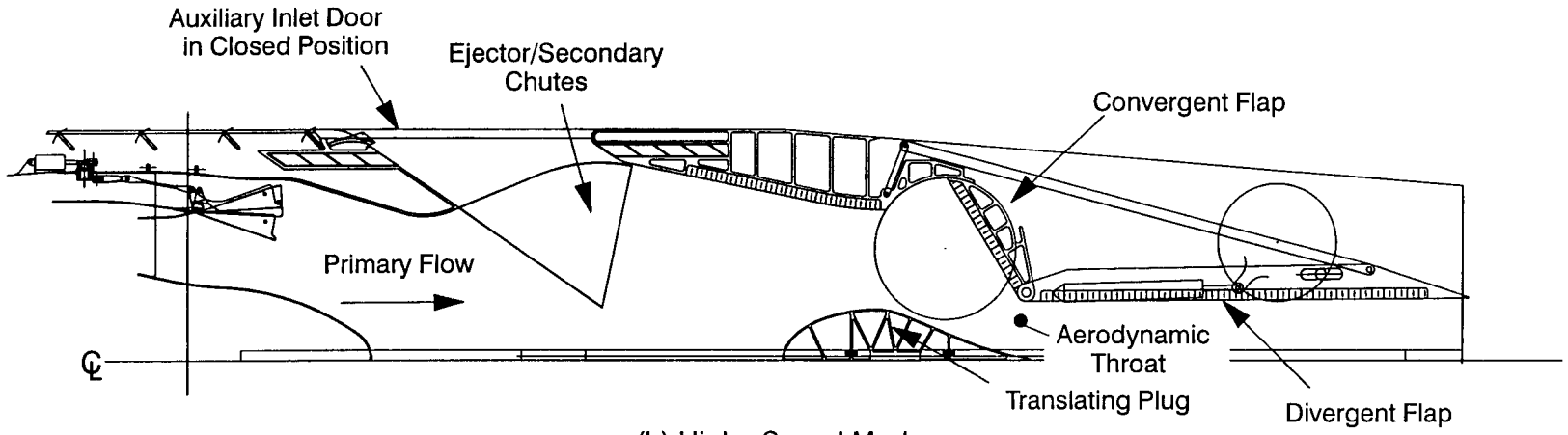

(b) High−Speed Mode

Figure 1. Fixed Chute Nozzle

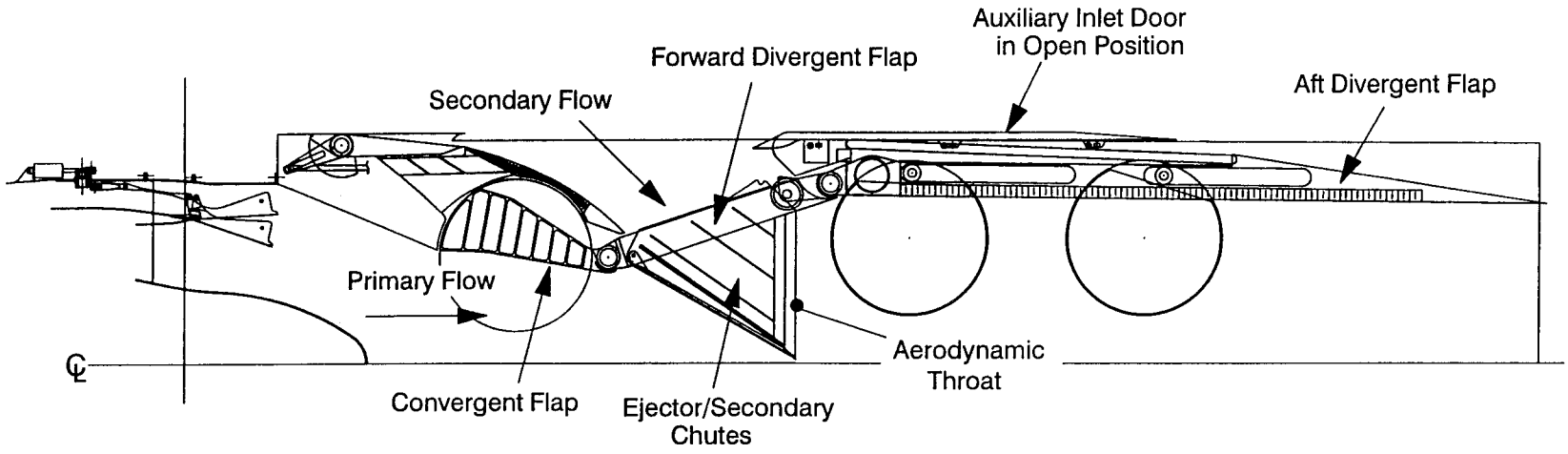

(a) Ejector/Low−Speed Mode

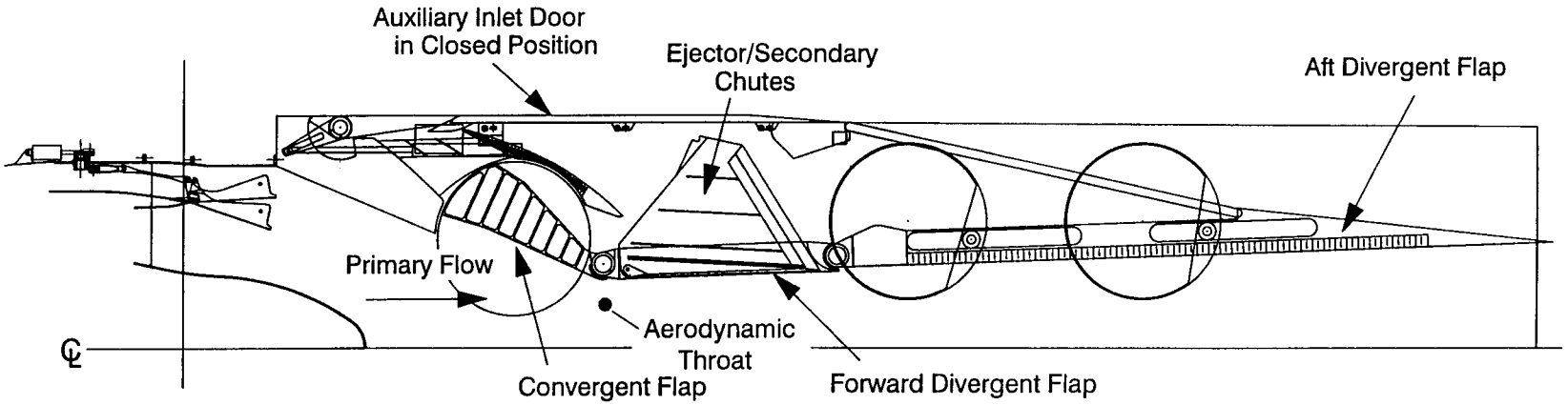

(b) High−Speed Mode

Figure 2. Downstream Mixer (DSM) Nozzle

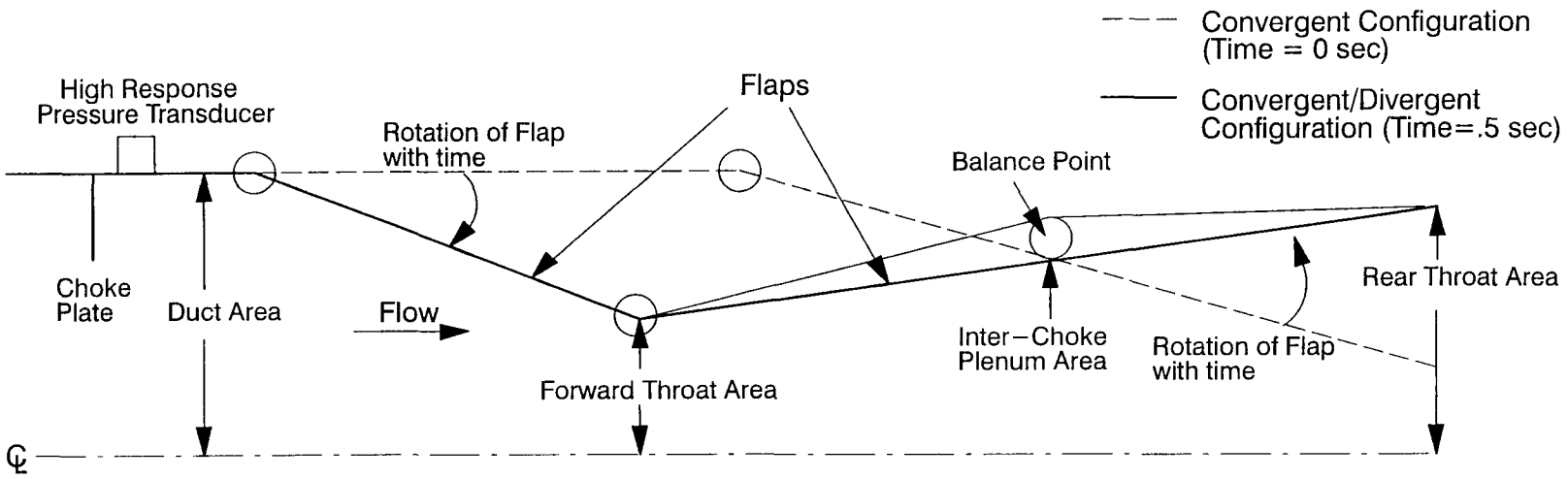

(a) 1/10 Scale Actuated 2D Balance Beam Nozzle Rig Side View

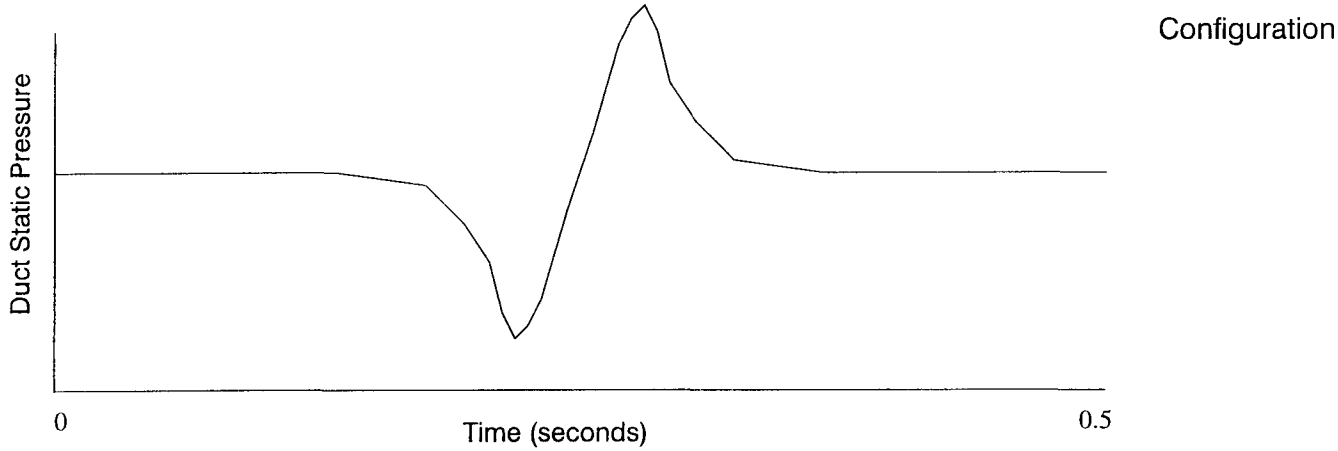

(b) Experimental Duct Static Pressure Variation During A Throat Shift From Convergent to Convergent/Divergent Configuration

Figure 3. Pratt & Whitney Experience With Throat Shift Nozzles

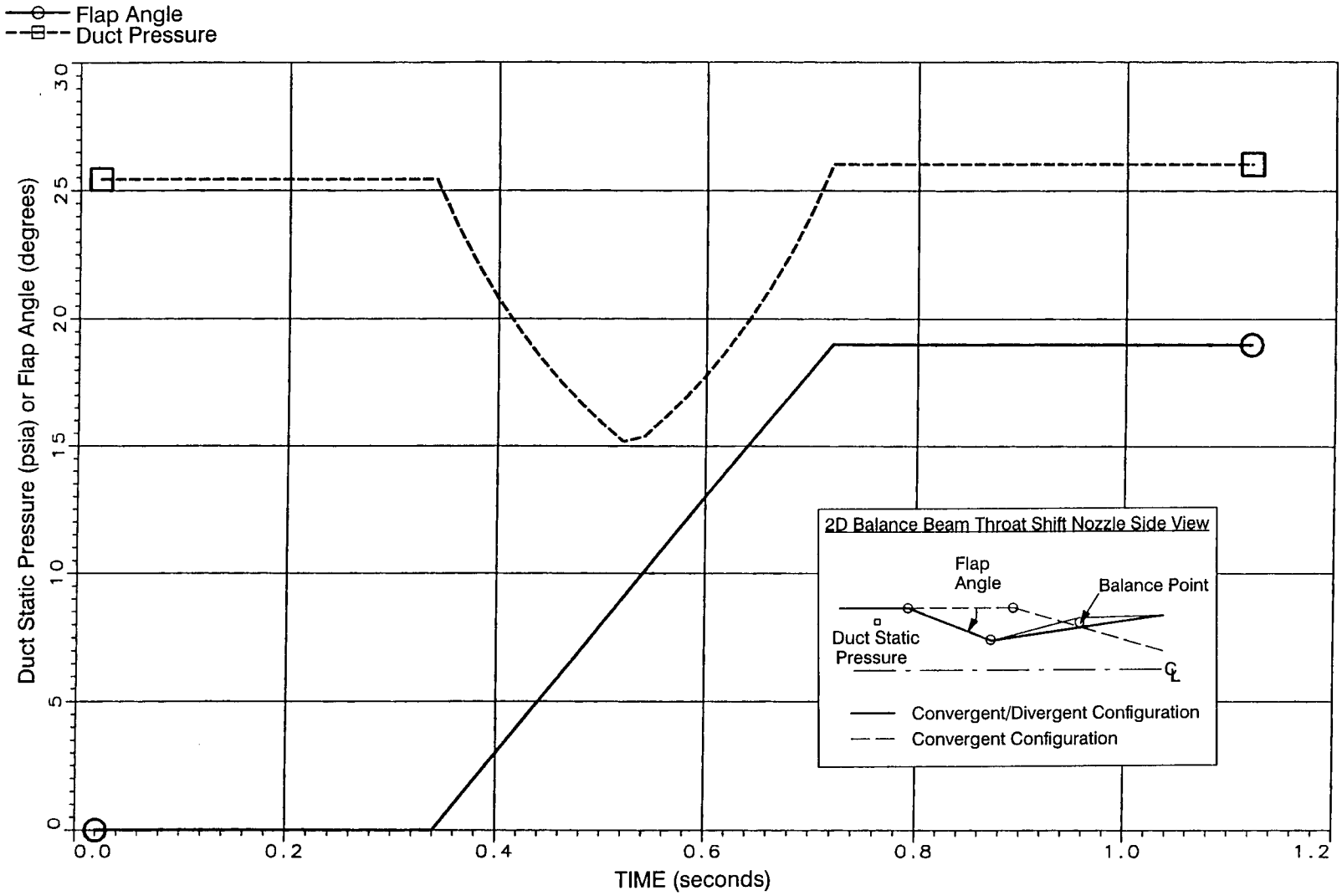

Figure 4. 1–D Quasi–Steady Analysis of a Balance Beam Throat Shift Nozzle Predicting An Upstream Static Pressure Variation

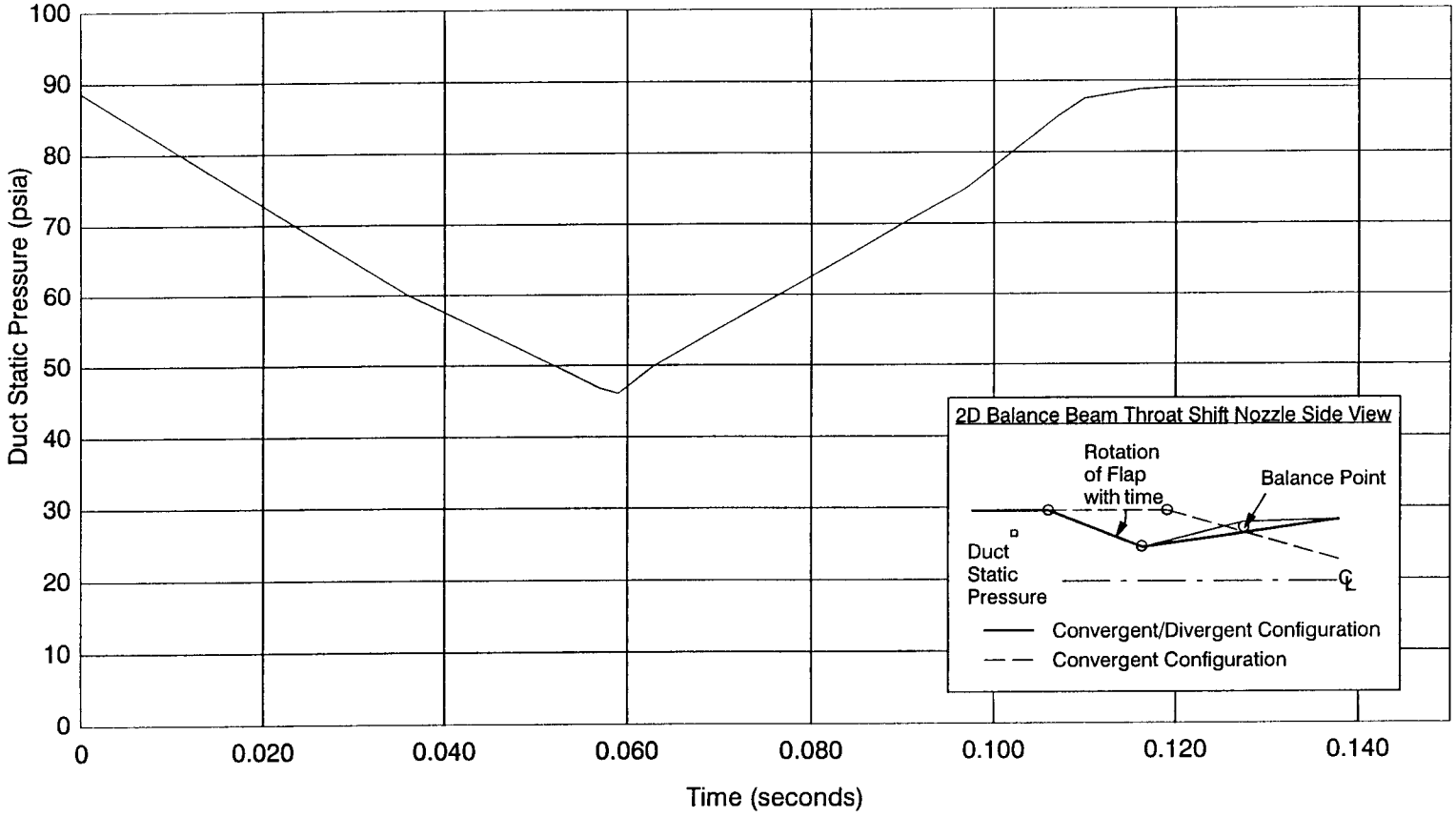

Figure 5. 1–D Unsteady Analysis of a Balance Beam Nozzle Predicting an Upstream Static Pressure Variation

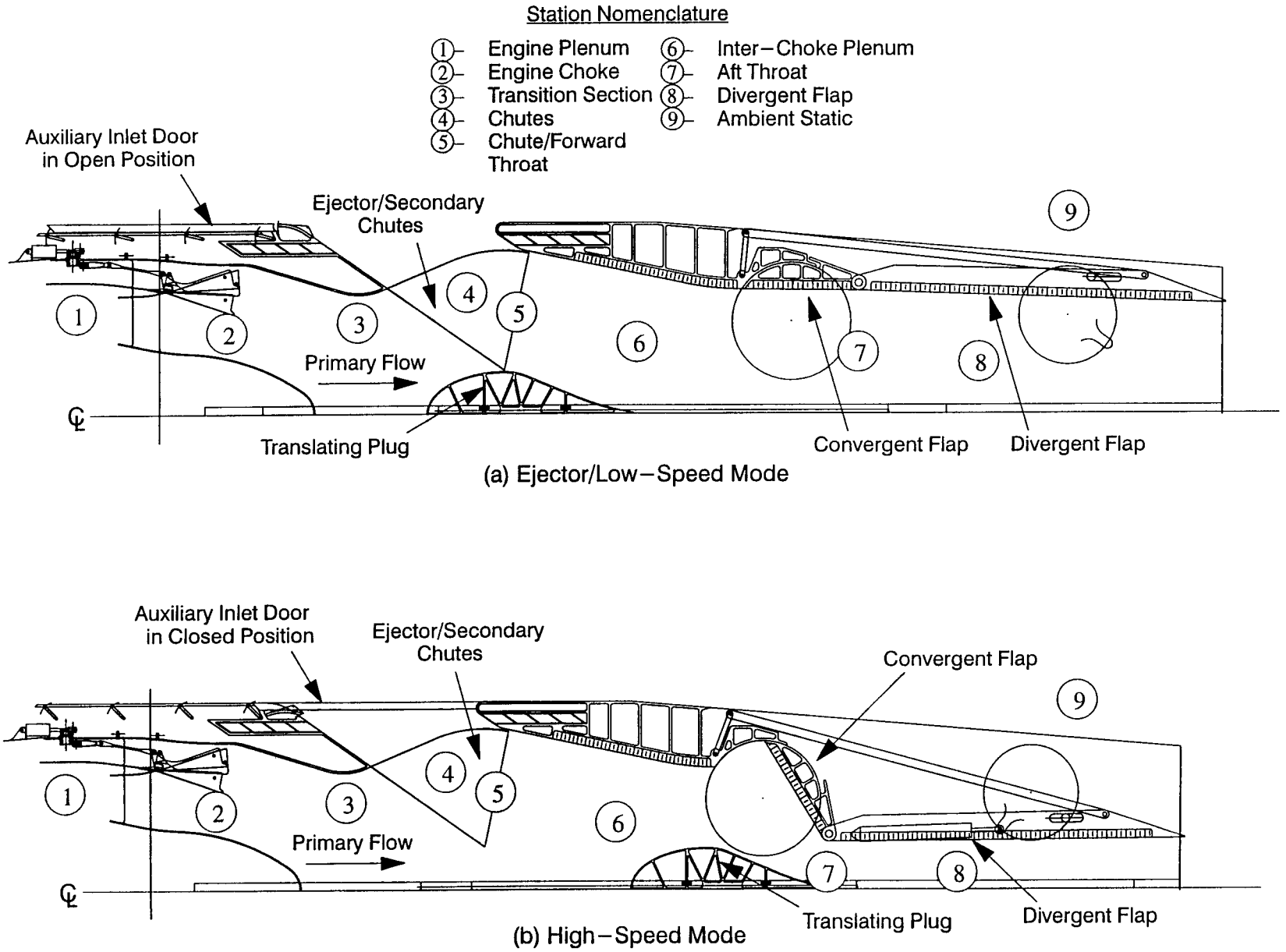

Figure 6. Station Nomenclature for Fixed Chute Nozzle 1–D Quasi–Steady Throat Shift Analysis

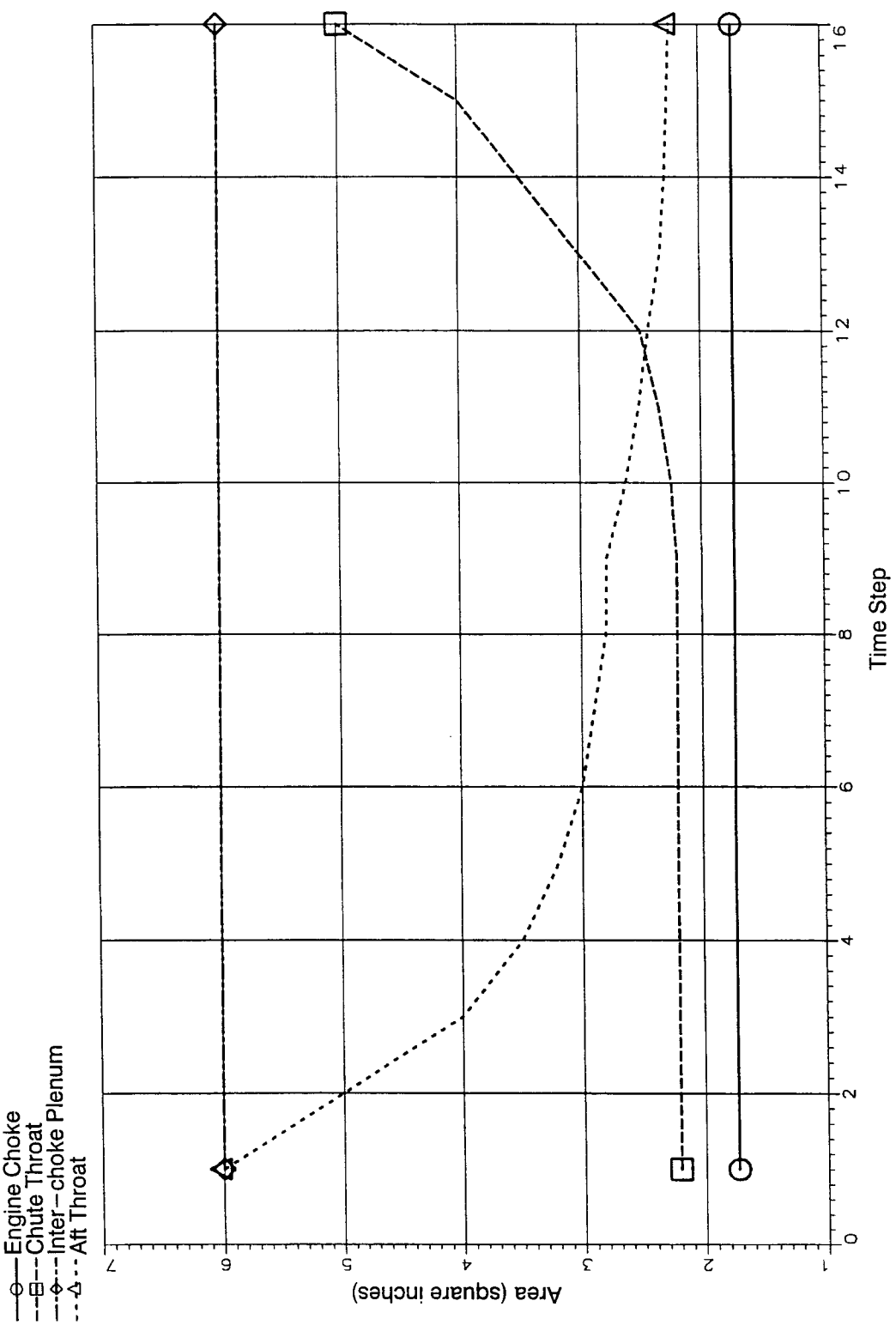

Figure 7. Area Change of Fixed Chute Nozzle 1-D Quasi-Steady Throat Shift Analytical Prediction

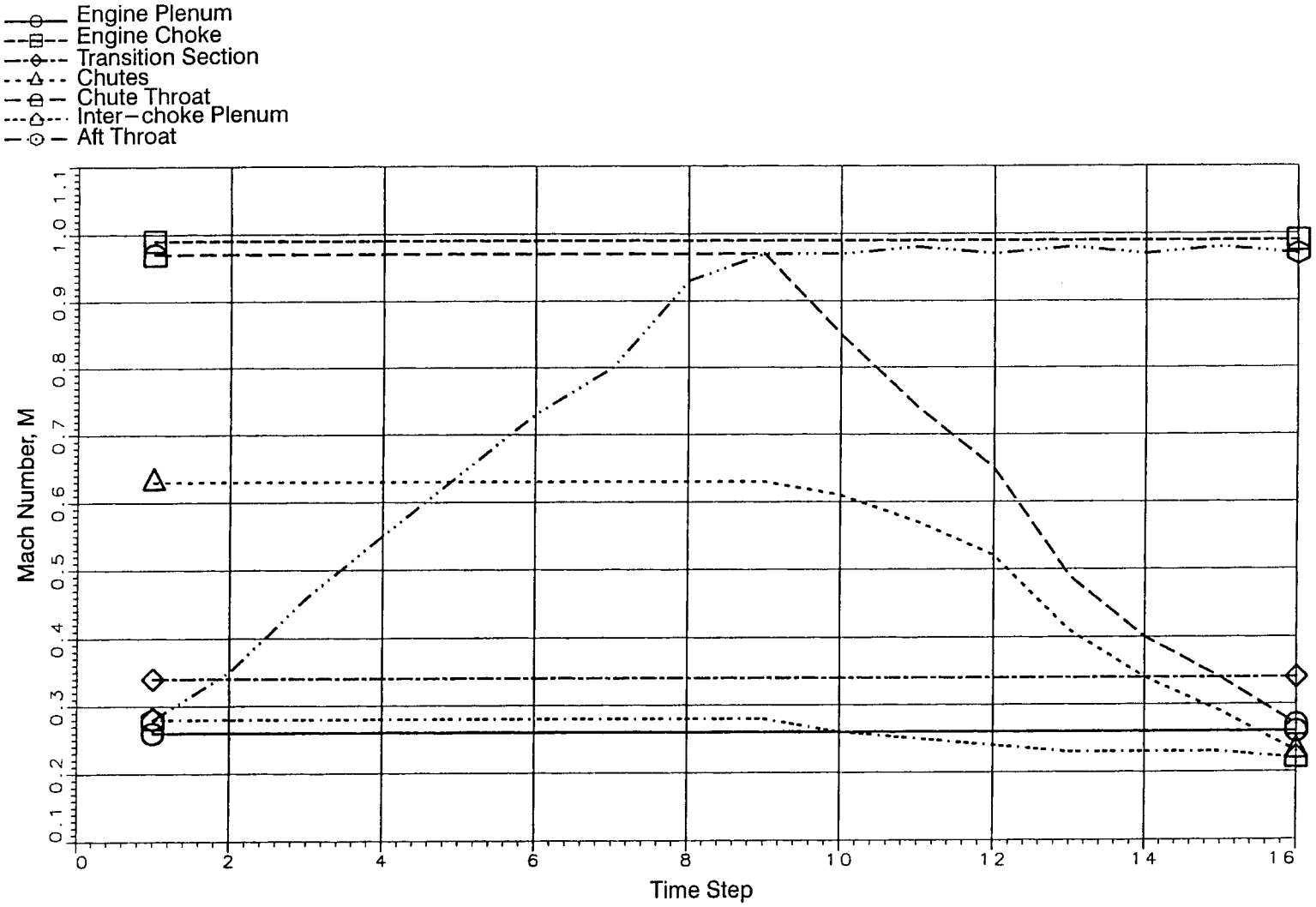

Figure 8. Mach Numbers of Fixed Chute Nozzle 1–D Quasi–Steady Throat Shift Analytical Prediction

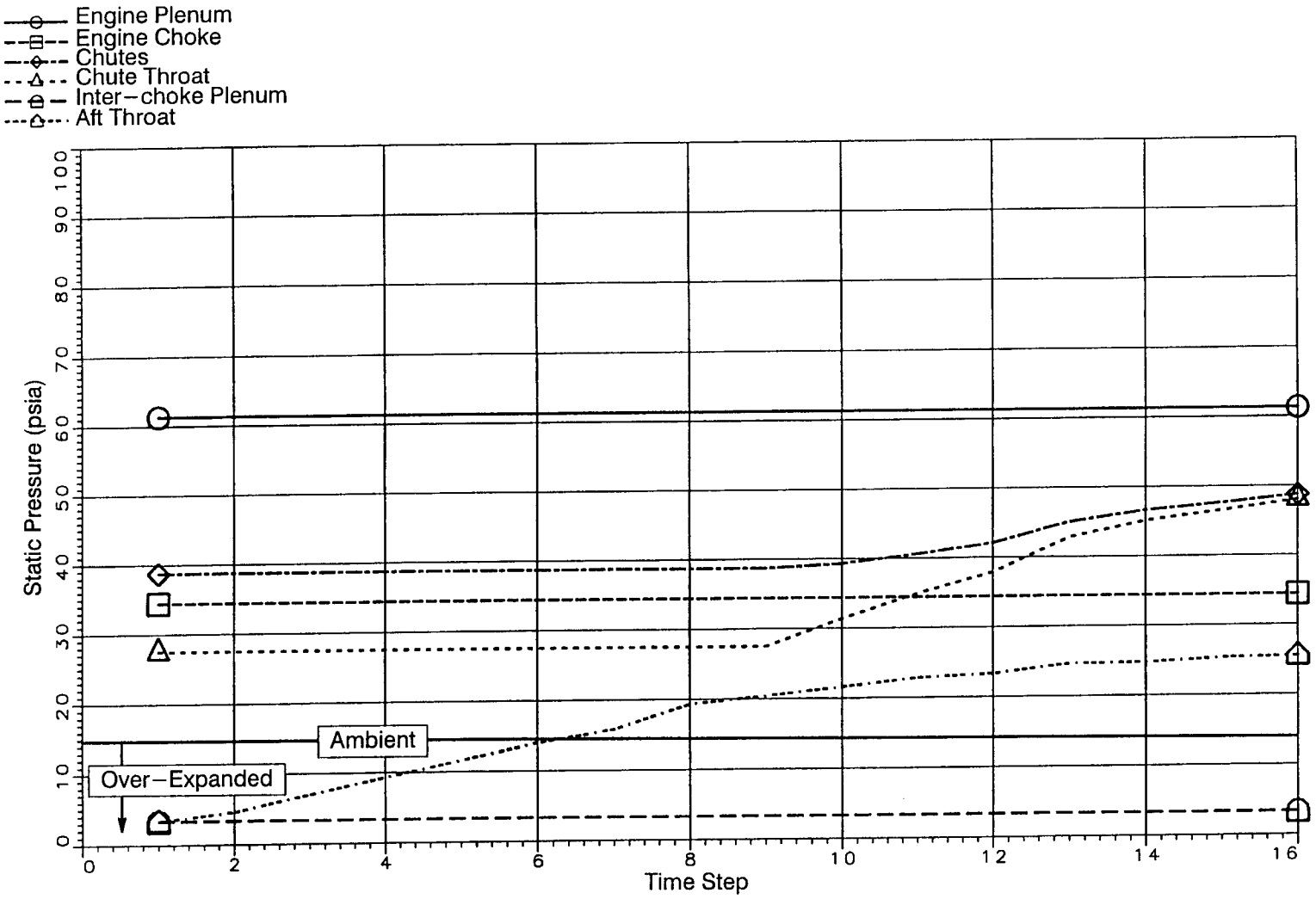

Figure 9. Static Pressures (Supersonic Solution) of Fixed Chute Nozzle 1–D Quasi–Steady Throat Shift Analytical Prediction

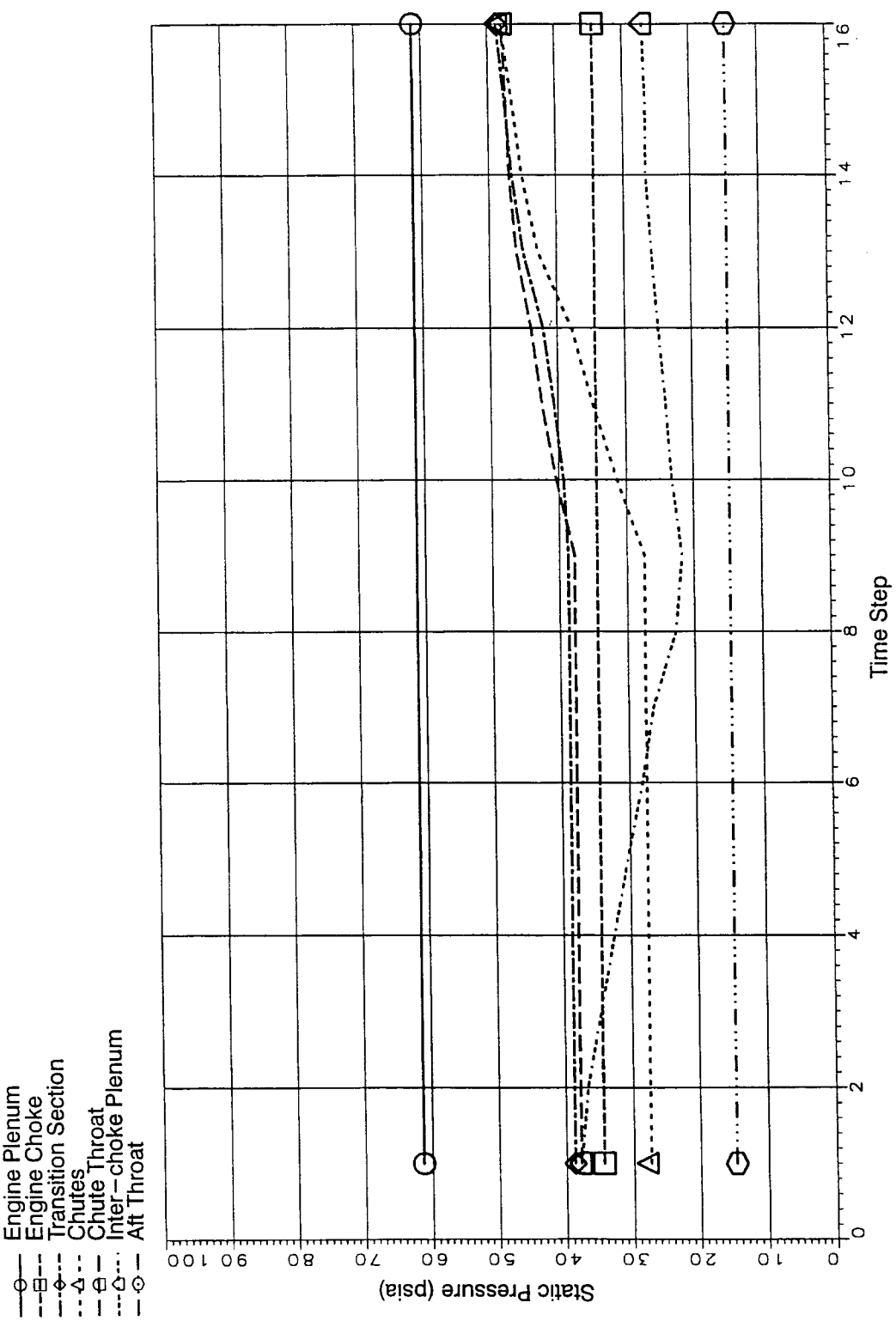

Figure 10. Static Pressures (Subsonic Solution) of Fixed Chute Nozzles 1–D
Quasi–Steady Throat Shift Analytical Prediction

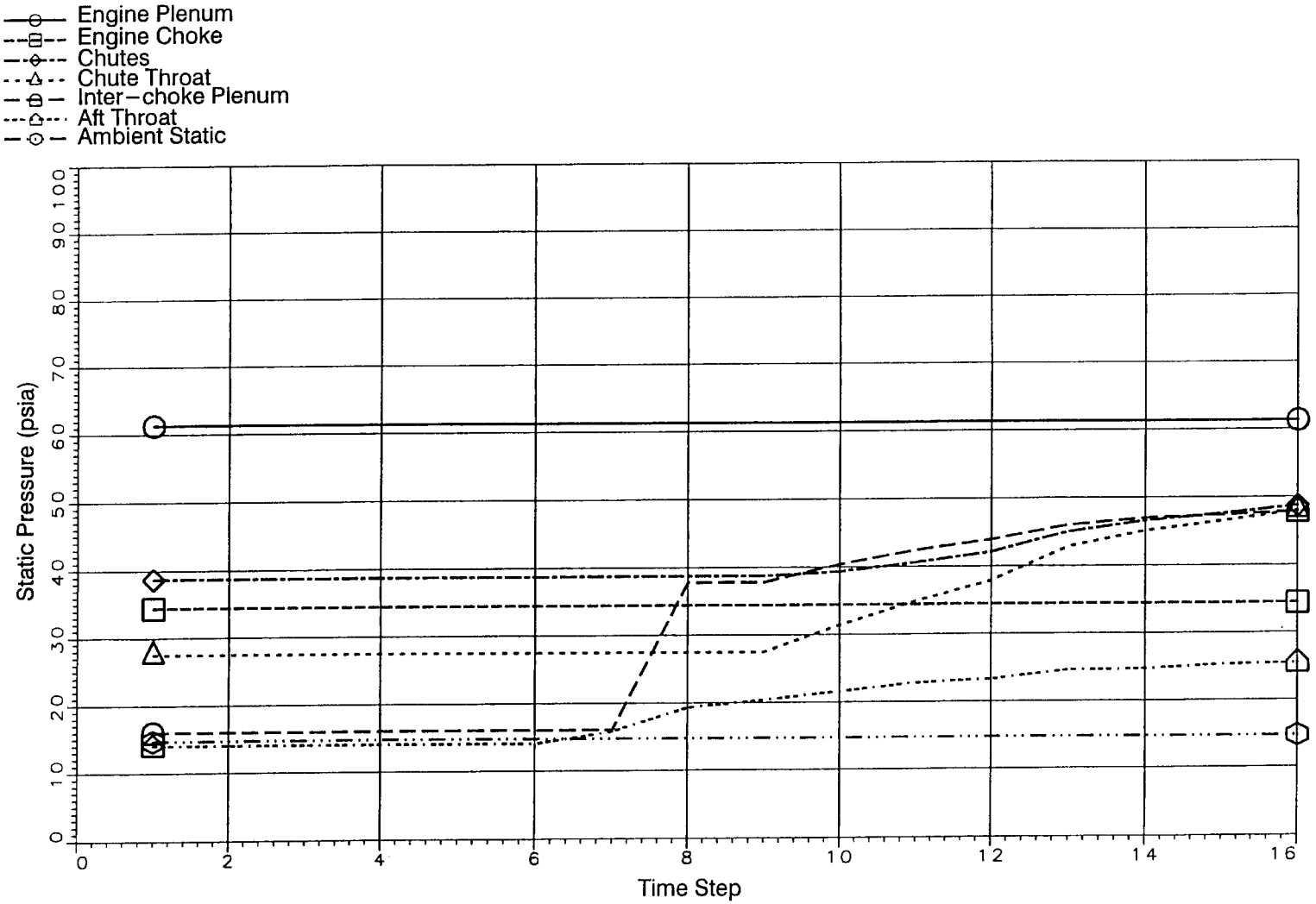

Figure 11. Static Pressures (Most Likely) of Fixed Chute Nozzle 1–D Quasi–Steady Throat Shift Analytical Prediction

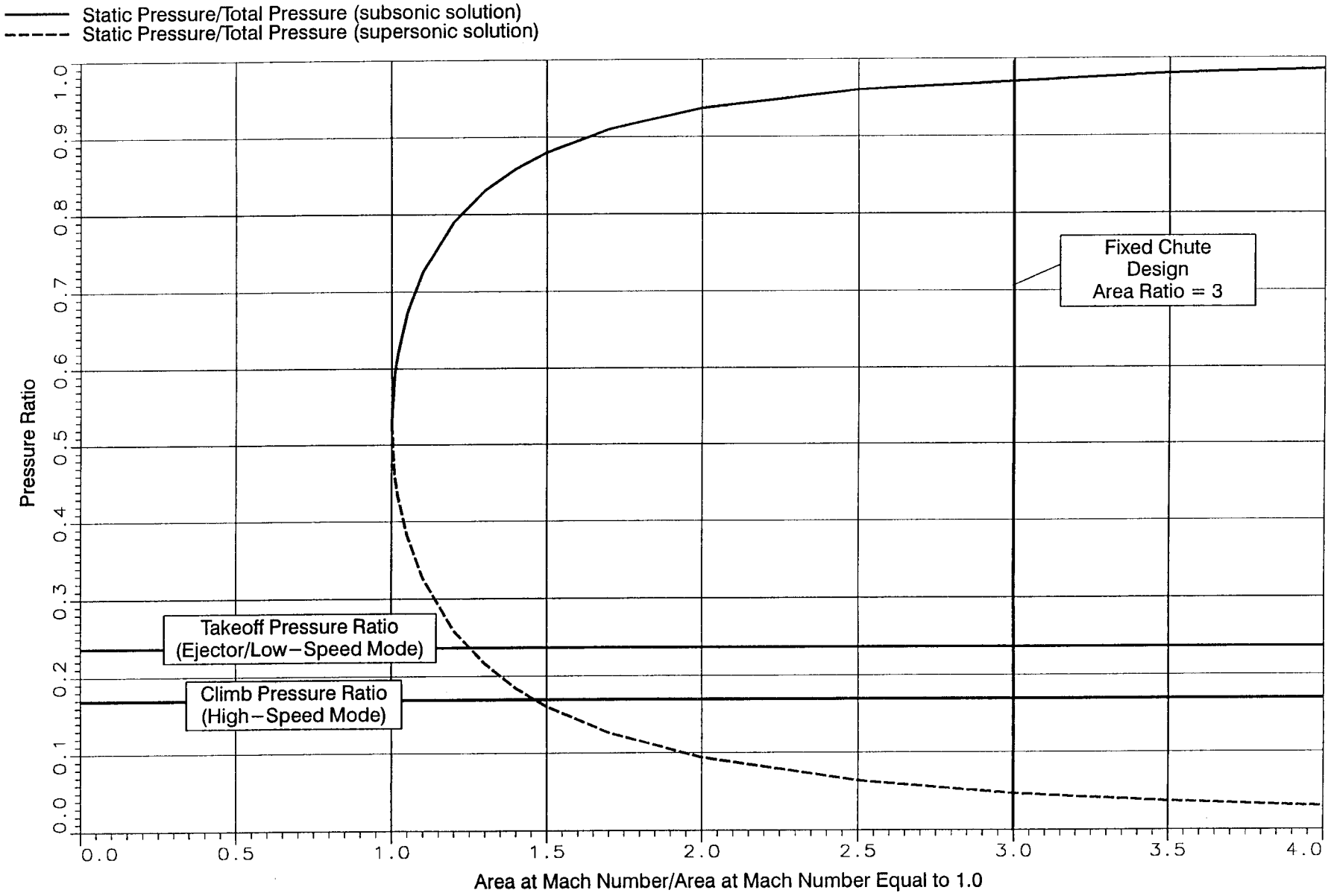

Figure 12. Nozzle Design Point Conditions with Isentropic Nozzle Pressure Ratio Area Relations for Air (γ = 1.4)

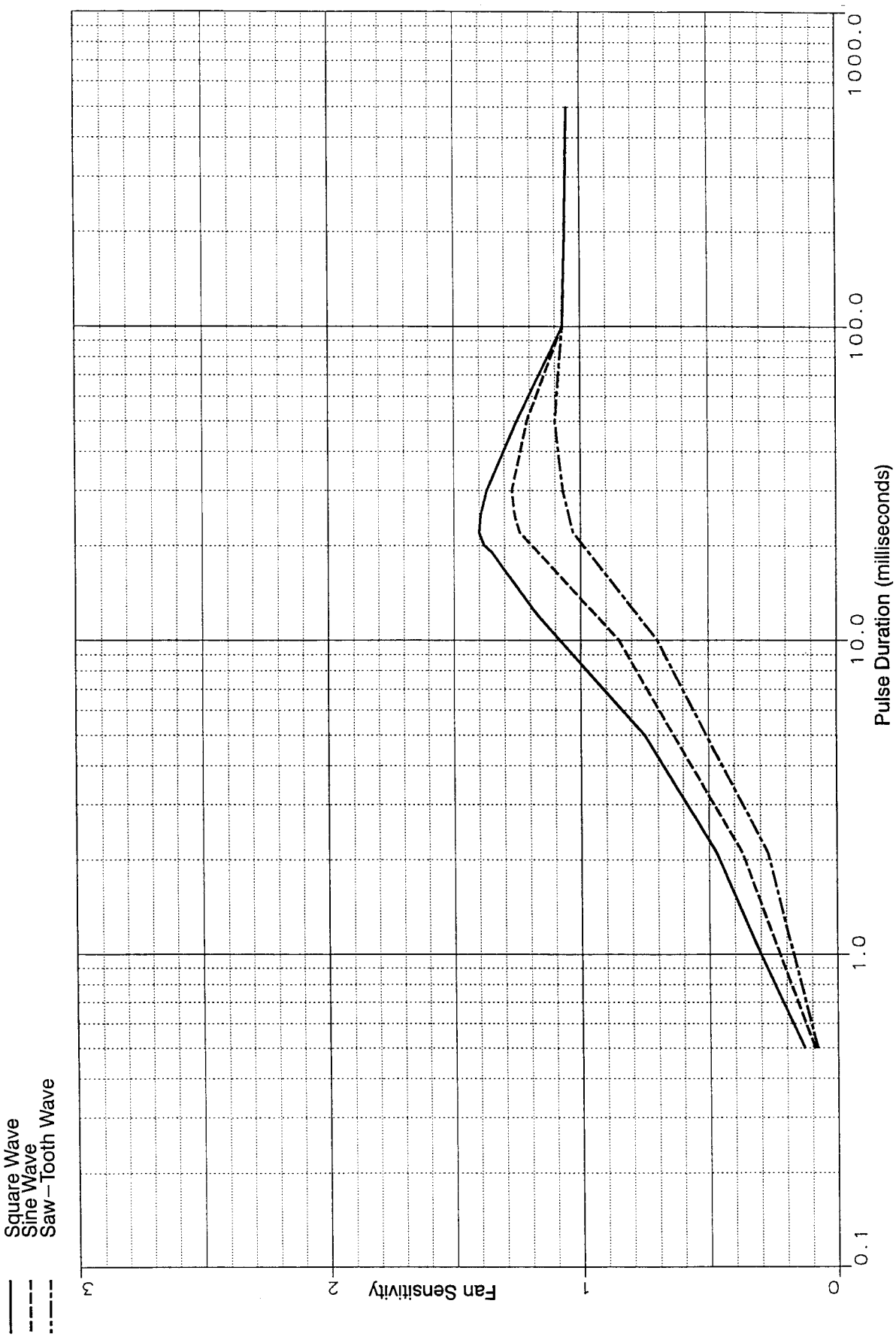

Figure 13. Fan Sensitivity to Nozzle Pressure Perturbations for Various Pulse Shapes

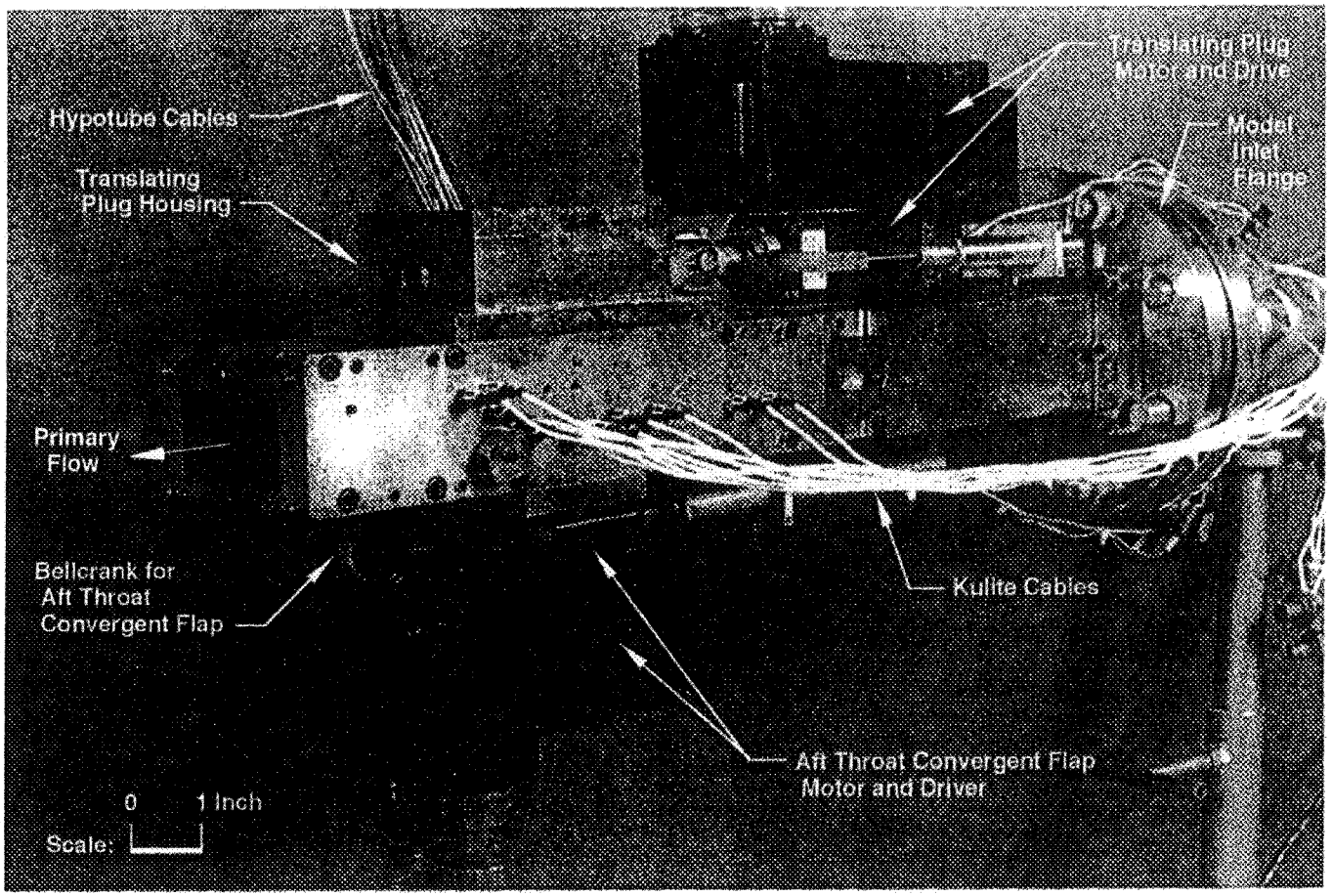

Figure 14. Dynamic Stability Rig in the Fixed Chute Configuration Showing Instrumentation, Actuators, and GN_2 Supply.

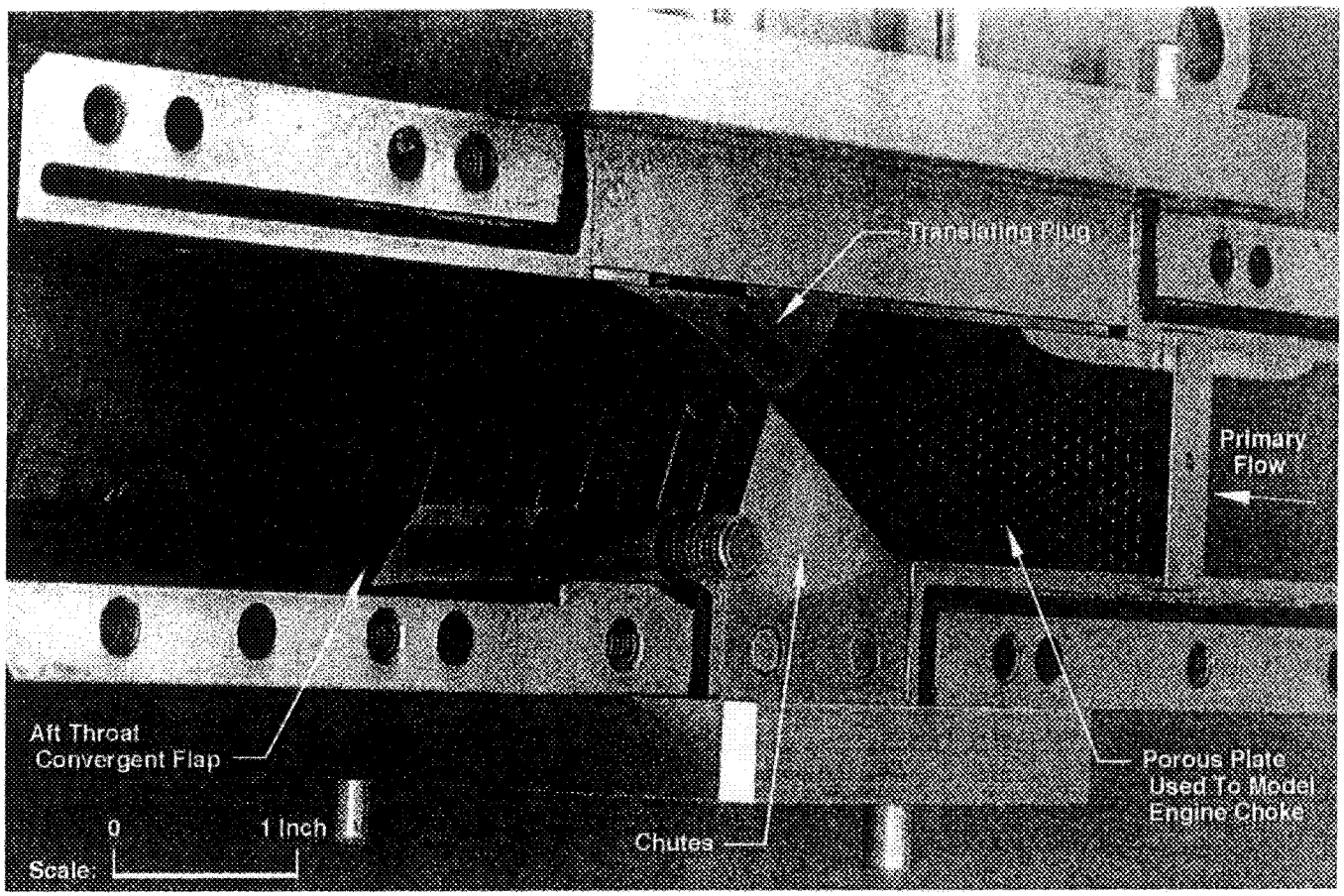

Figure 15. Dynamic Stability Rig in the Fixed Chute Configuration with 10–Chute Assembly Installed (Sidewall Removed).

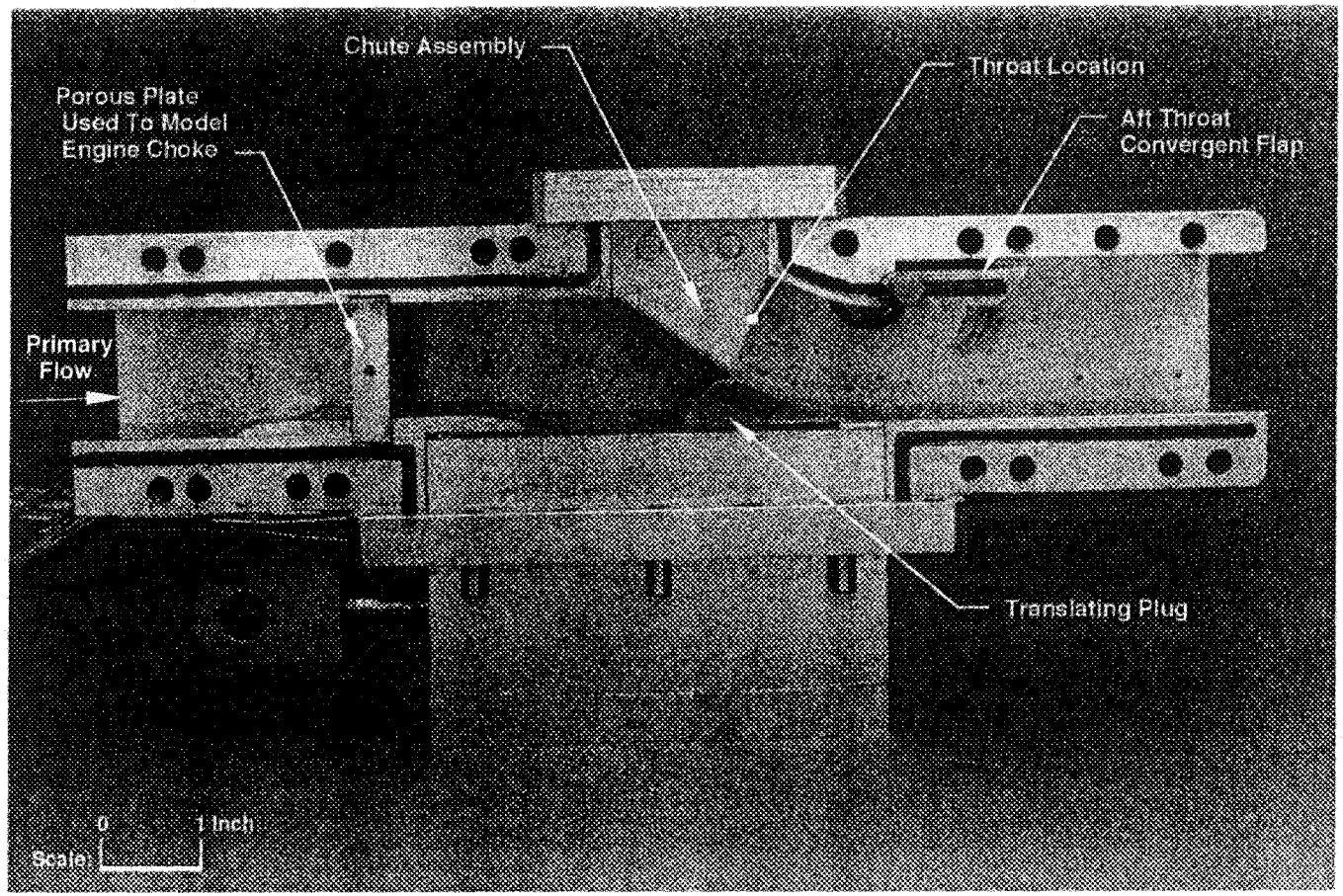

Figure 16. Dynamic Stability Rig in the Fixed Chute Configuration in the Ejector/Low–Speed Mode (Sidewall Removed). Throat Located Forward at Chute Exit.

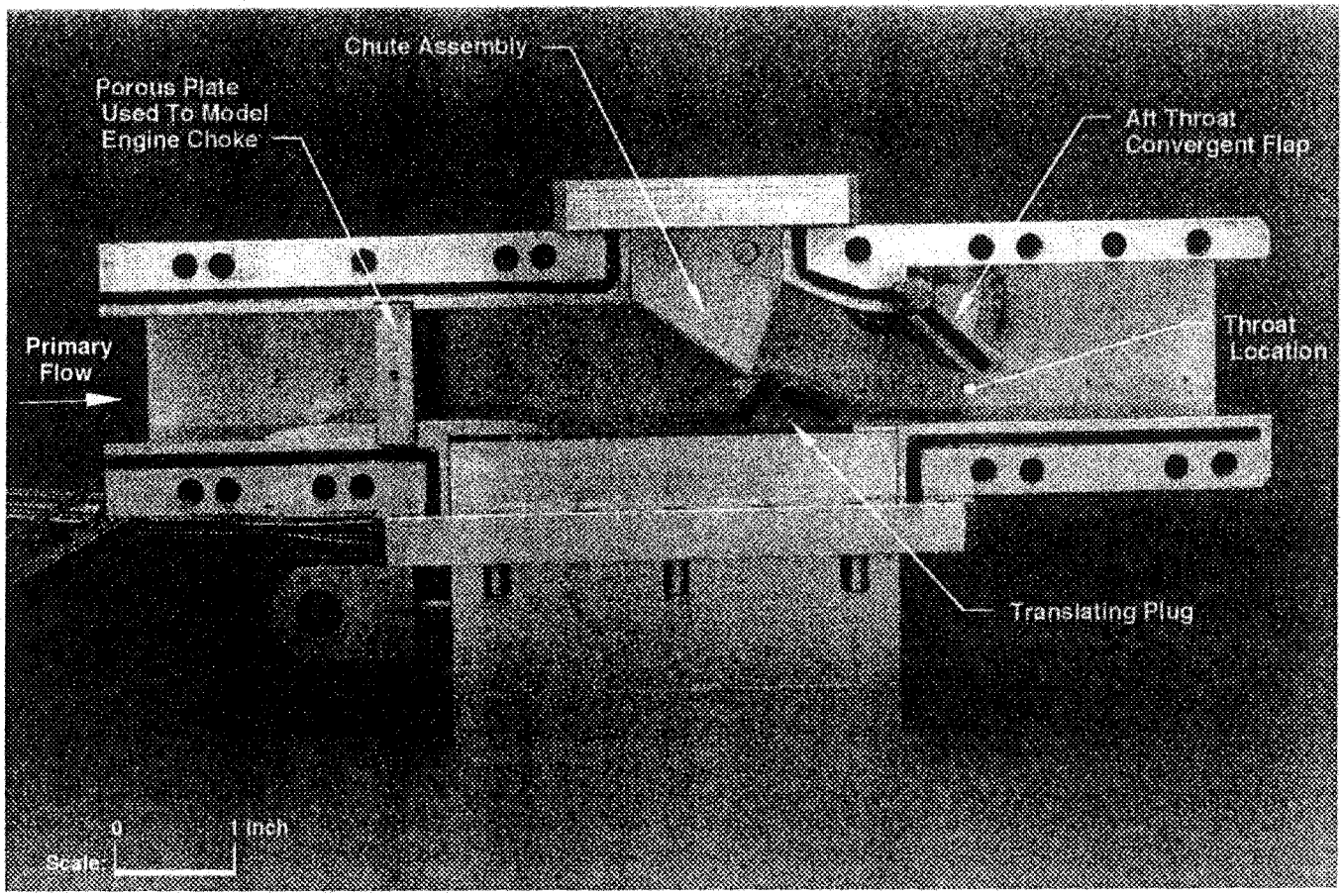

Figure 17. Dynamic Stability Rig in the Fixed Chute Configuration in the High–Speed Mode (Sidewall Removed). Throat Located Aft.

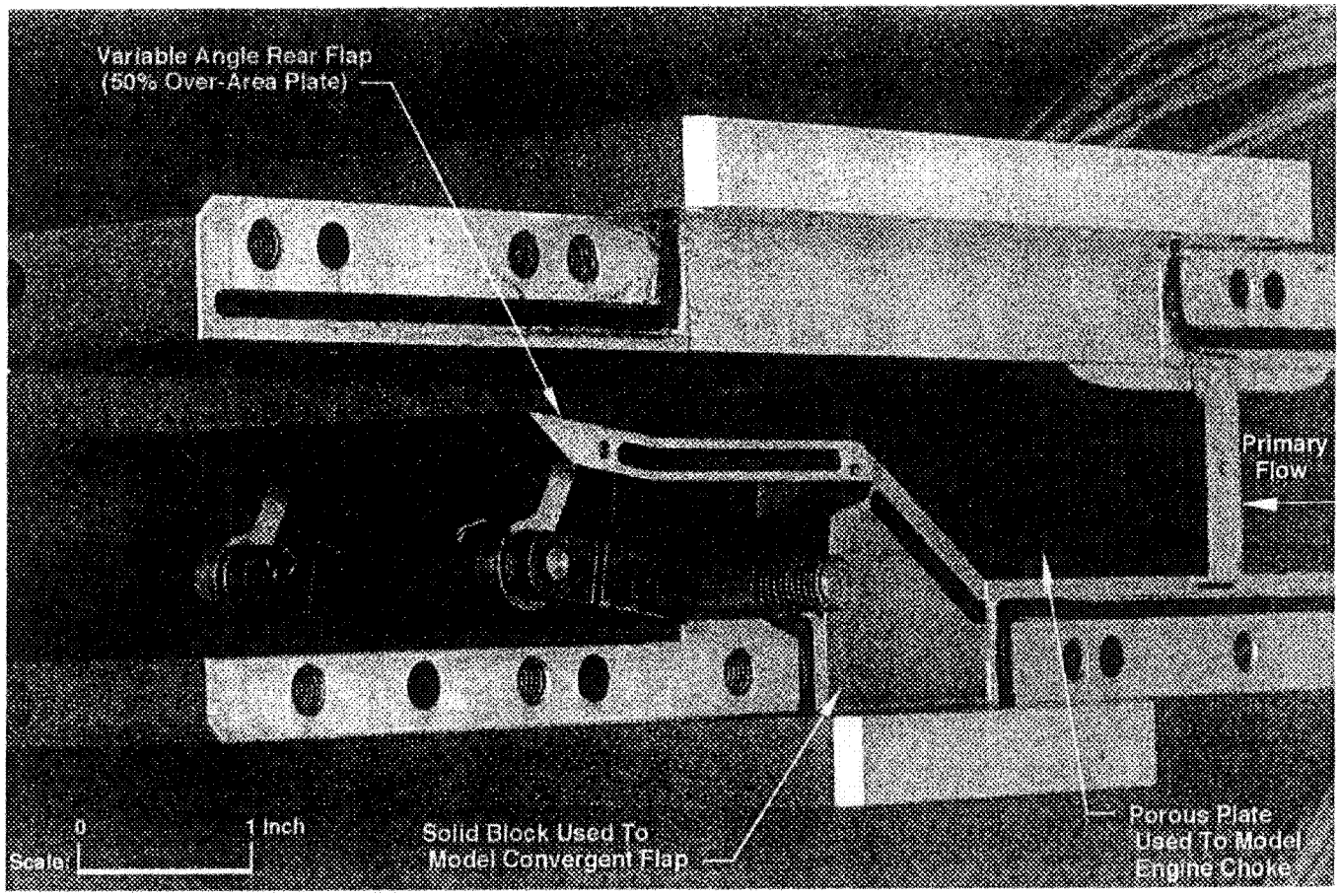

Figure 18. Dynamic Stability Rig in the DSM Configuration with the 50% Over–Area Plate Installed (Sidewall Removed)

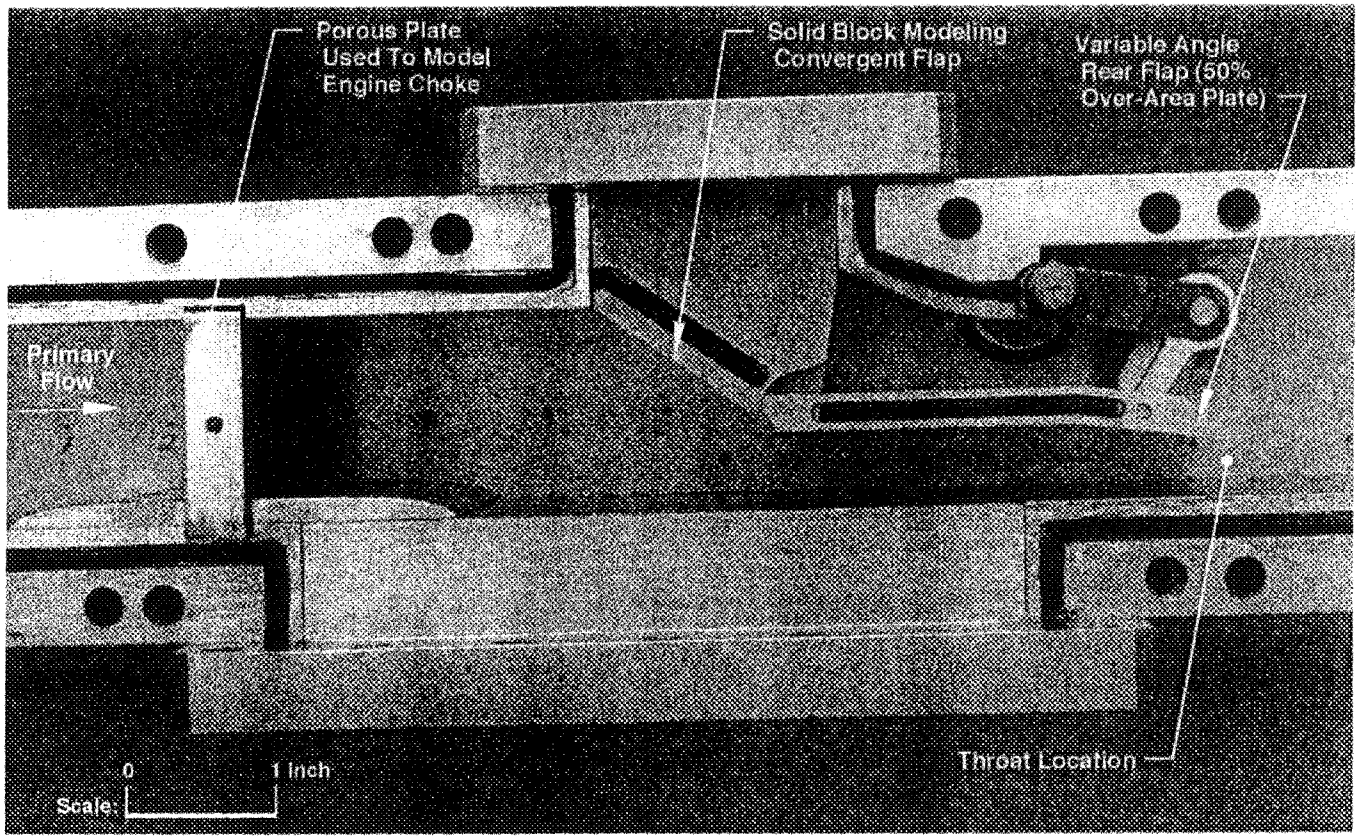

Figure 19. Dynamic Stability Rig in the DSM Configuration in the Low–Speed Mode with the 50% Over–Area Plate Installed (Sidewall Removed). Throat Located Aft.

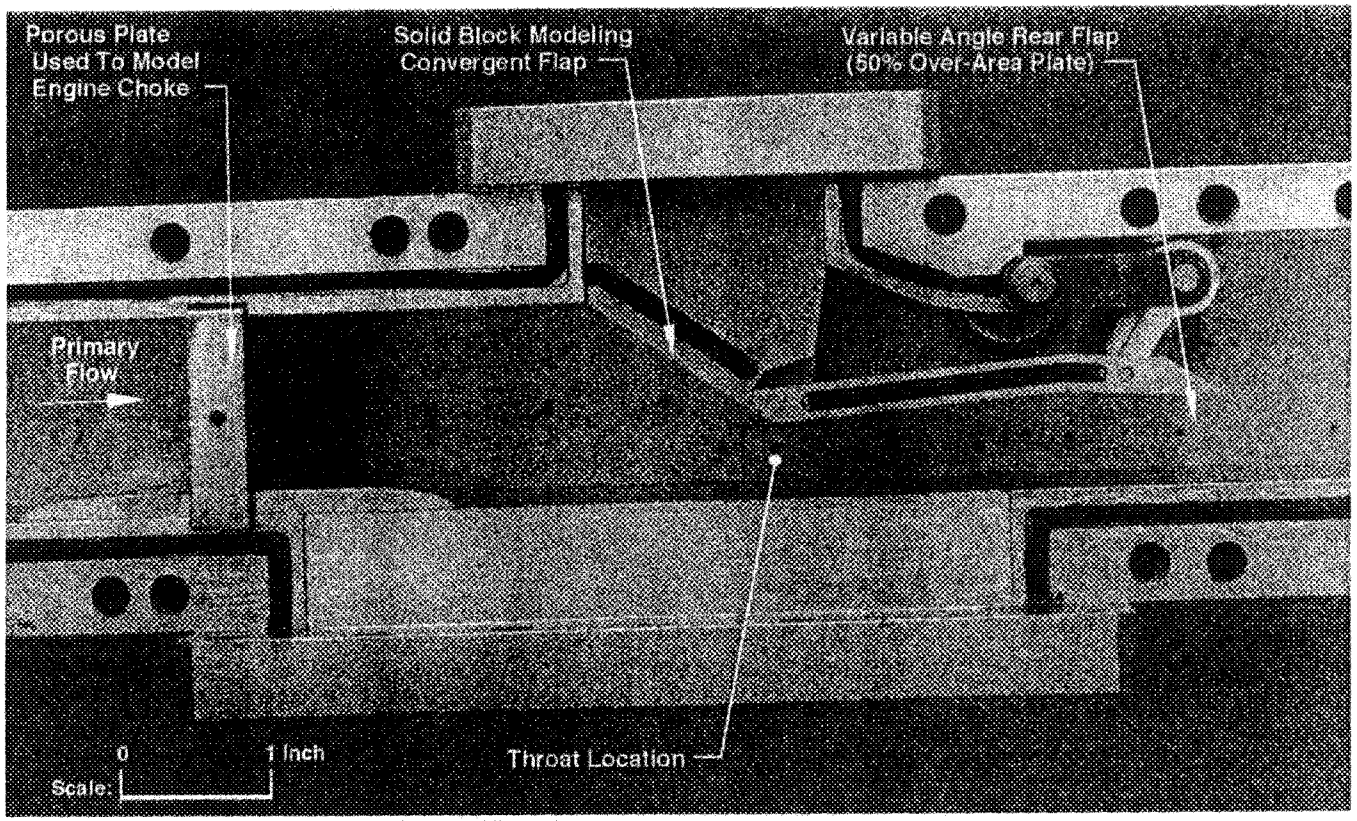

Figure 20. Dynamic Stability Rig in the DSM Configuration in the High Speed Mode with the 50% Over-Area Plate Installed (Sidewall Removed). Throat Located Forward.

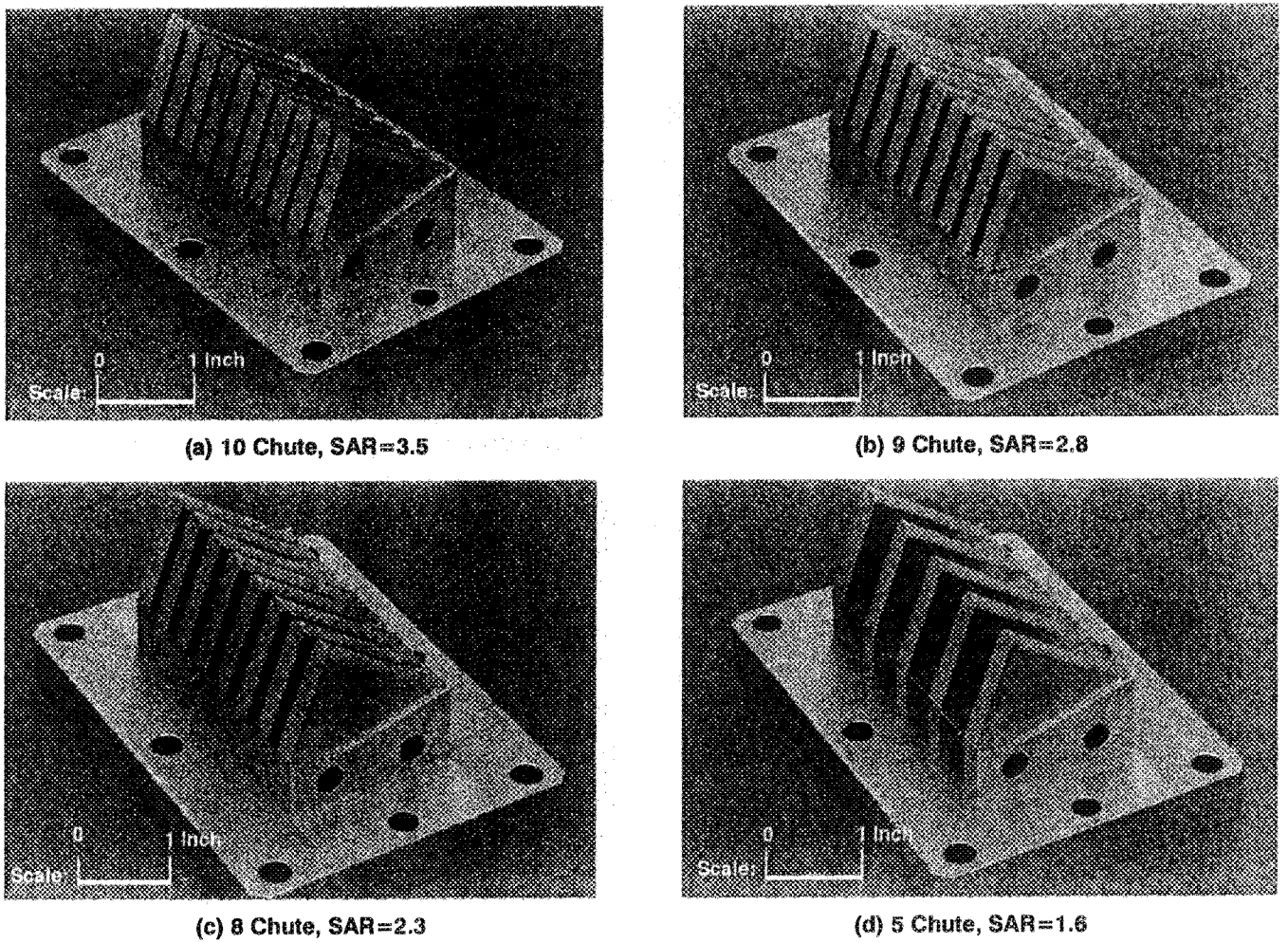

Figure 21. Chute Assemblies for Fixed Chute Configuration.

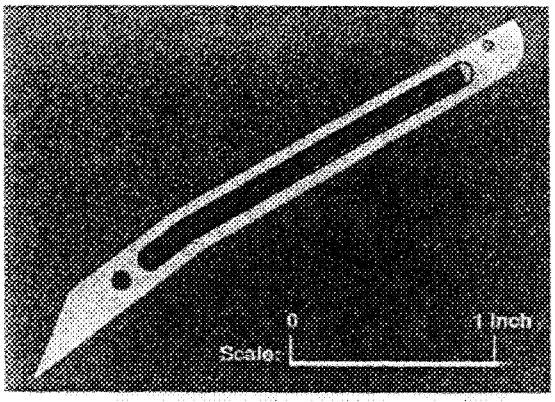

(a) 50% Over-Area

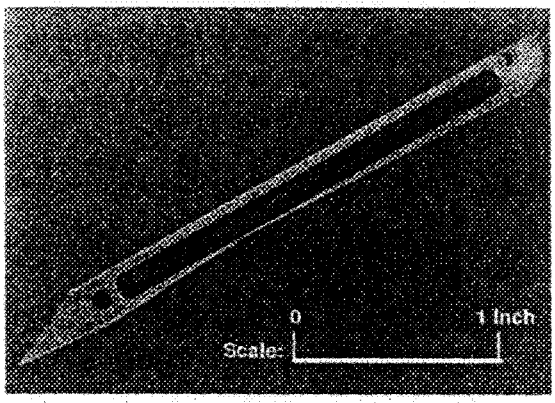

(b) 10% Over-Area

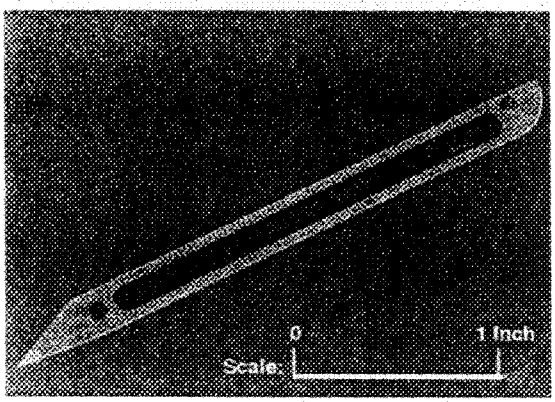

(c) No Over-Area

Figure 22. Bent and Flat Plates for DSM and No Over–Area Configurations.

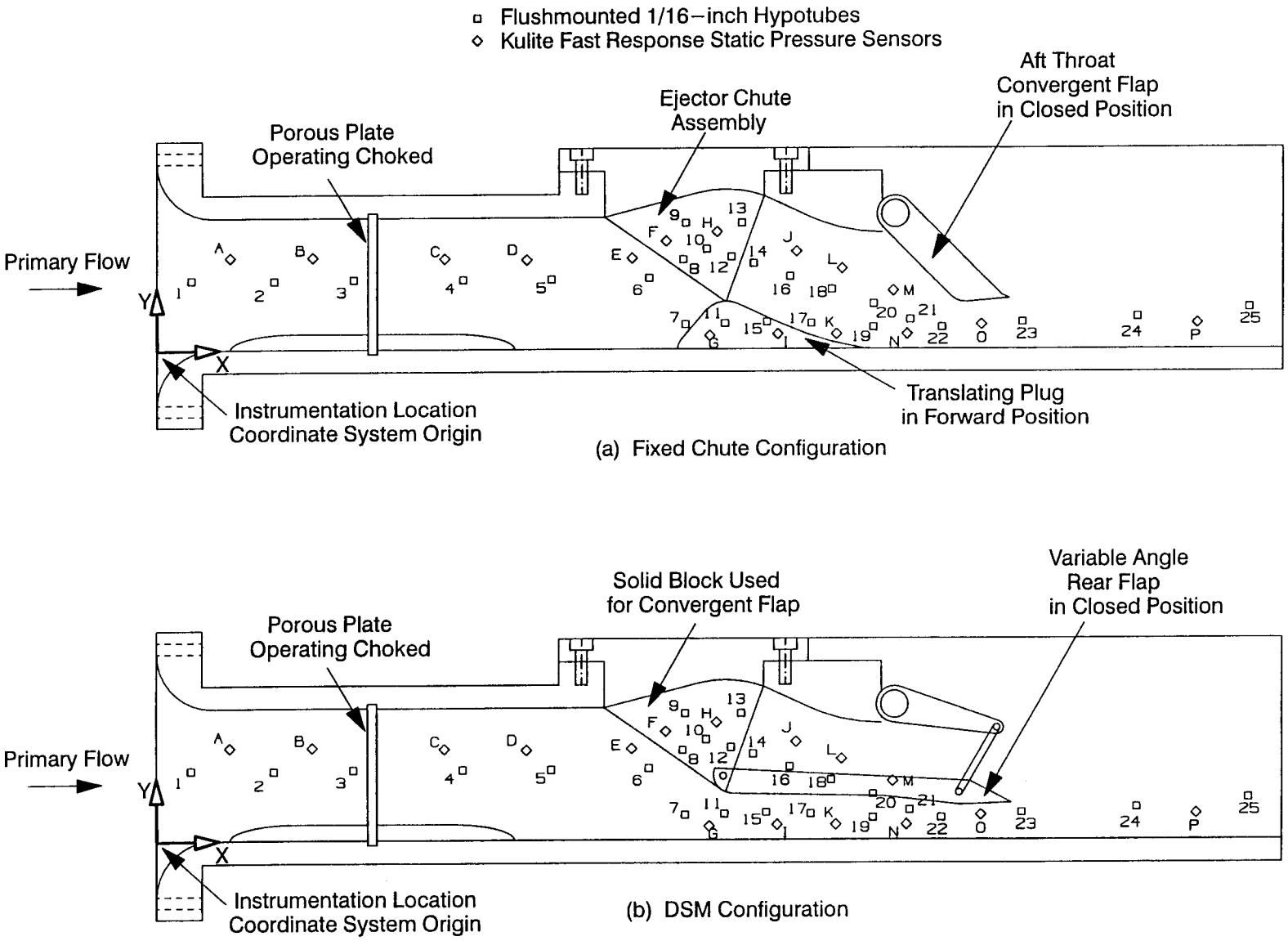

Figure 23. Dynamic Stability Rig Instrumentation Layout Showing Fixed Chute and DSM Configurations (with 10% Over–Area Plate). Hypotubes Were Located on One Sidewall and Kulites on the Other.

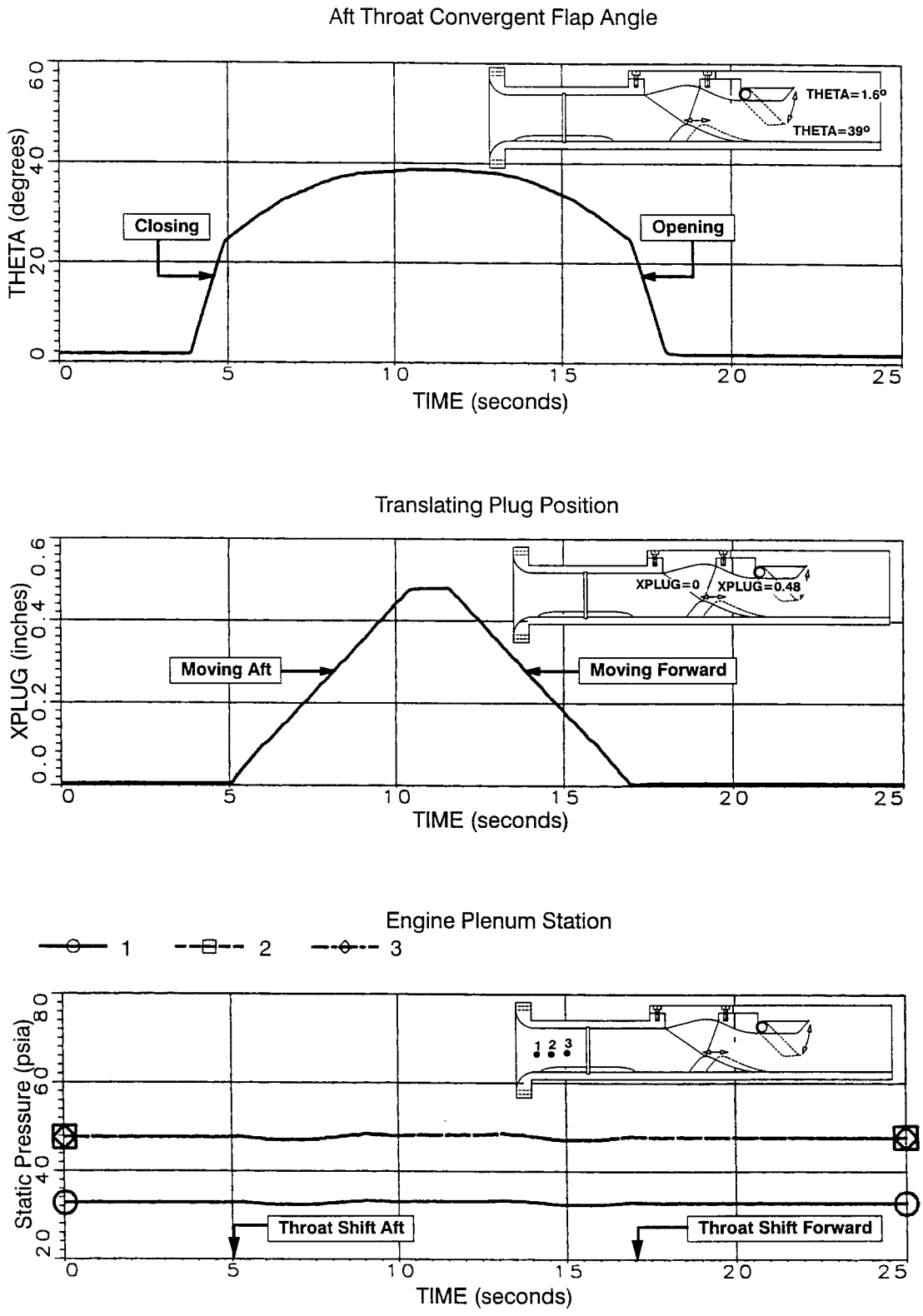

Figure 24. Low Response Static Pressures for Fixed Chute Configuration with 10 Chutes (FC−1). Aft Throat Convergent Flap and Translating Plug Moved In Concert to Maintain Constant Pressure ("5") Upstream of the Forward Throat. NPR=3. Digitial Data Transient #392 in Test Log.

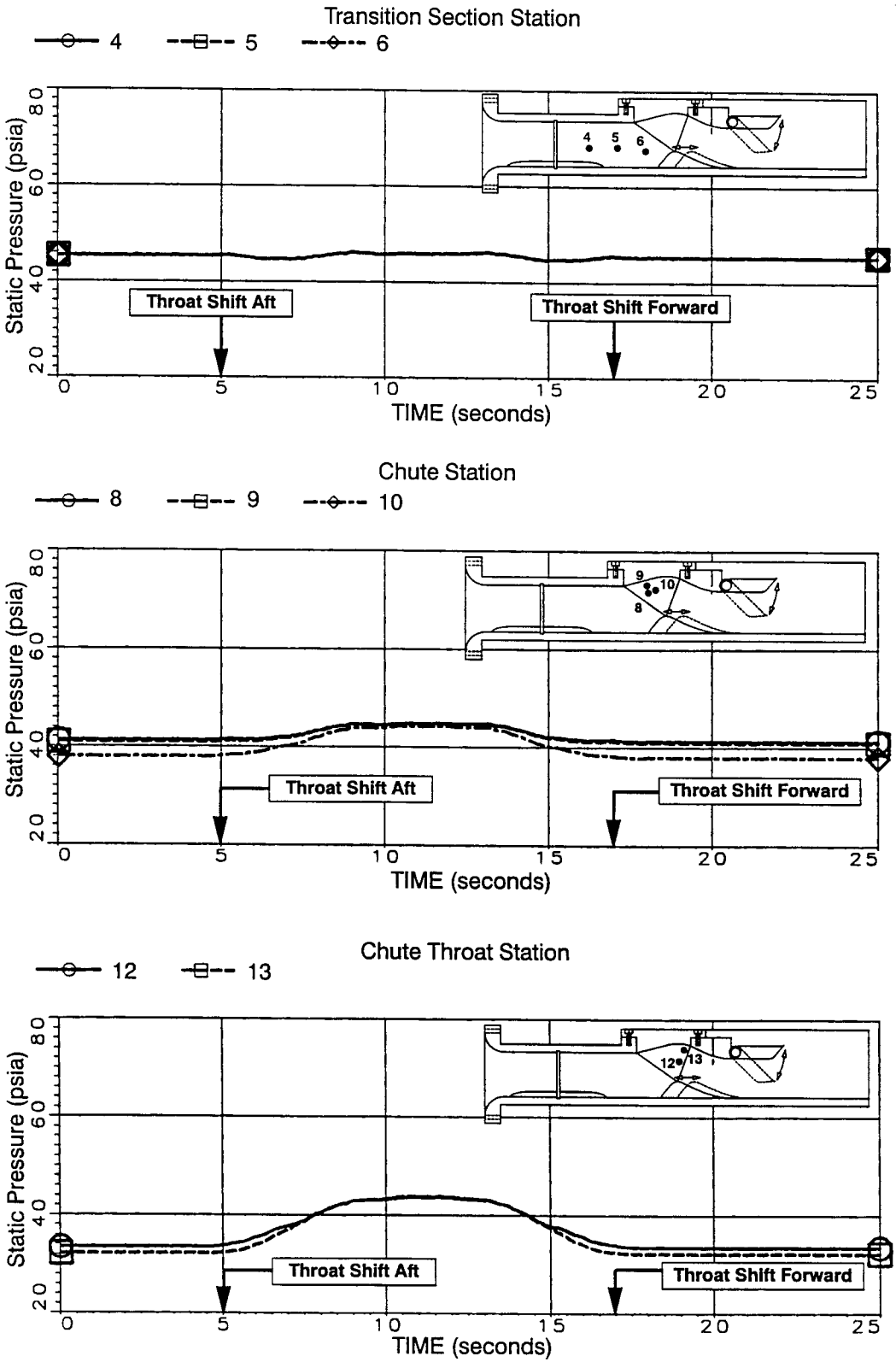

Figure 24. Low Response Static Pressures for Fixed Chute Configuration with 10 Chutes (FC−1). Aft Throat Convergent Flap and Translating Plug Moved In Concert to Maintain Constant Pressure ("5") Upstream of the Forward Throat. NPR = 3. Digitial Data Transient #392 in Test Log. (Continued).

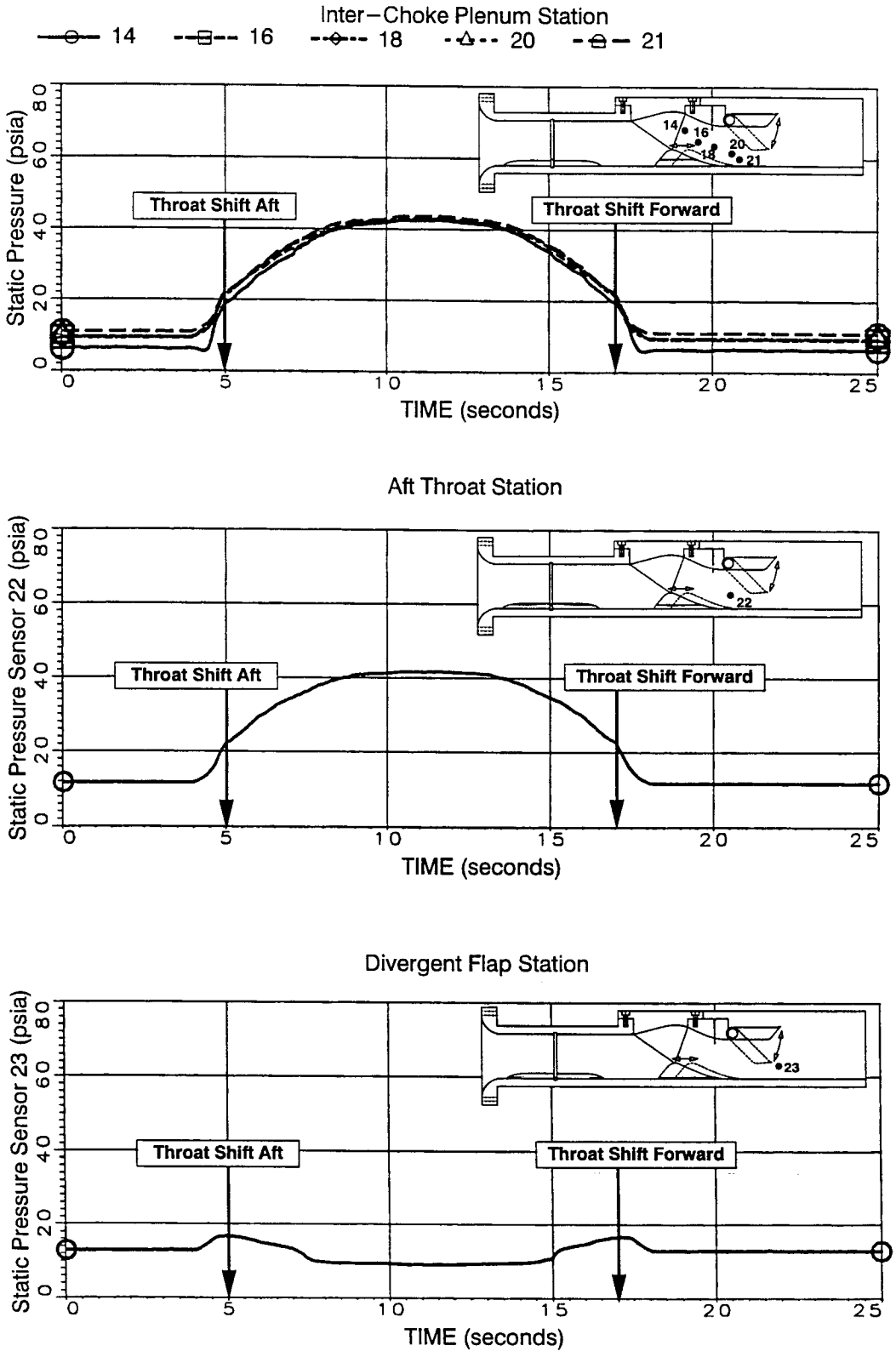

Figure 24. Low Response Static Pressures for Fixed Chute Configuration with 10 Chutes (FC–1). Aft Throat Convergent Flap and Translating Plug Moved In Concert to Maintain Constant Pressure ("5") Upstream of the Forward Throat. NPR = 3. Digitial Data Transient #392 in Test Log. (Concluded).

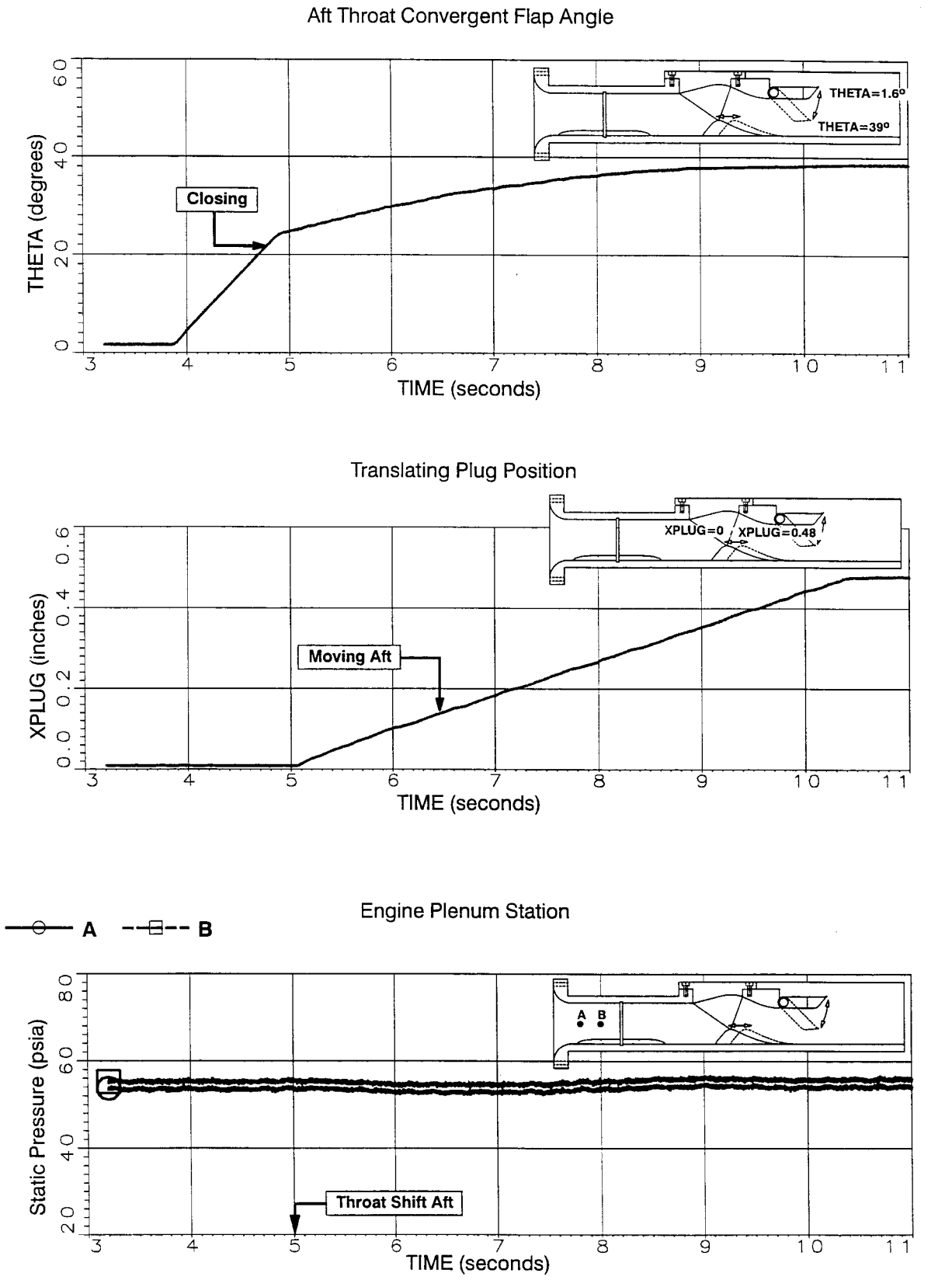

Figure 25. High Response Static Pressures for Fixed Chute Configuration with 10 Chutes (FC−1). Aft Throat Convergent Flap and Translating Plug Moved In Concert to Maintain Constant Pressure ("5") Upstream of the Forward Throat. NPR = 3. Digitial Data Transient #392 in Test Log.

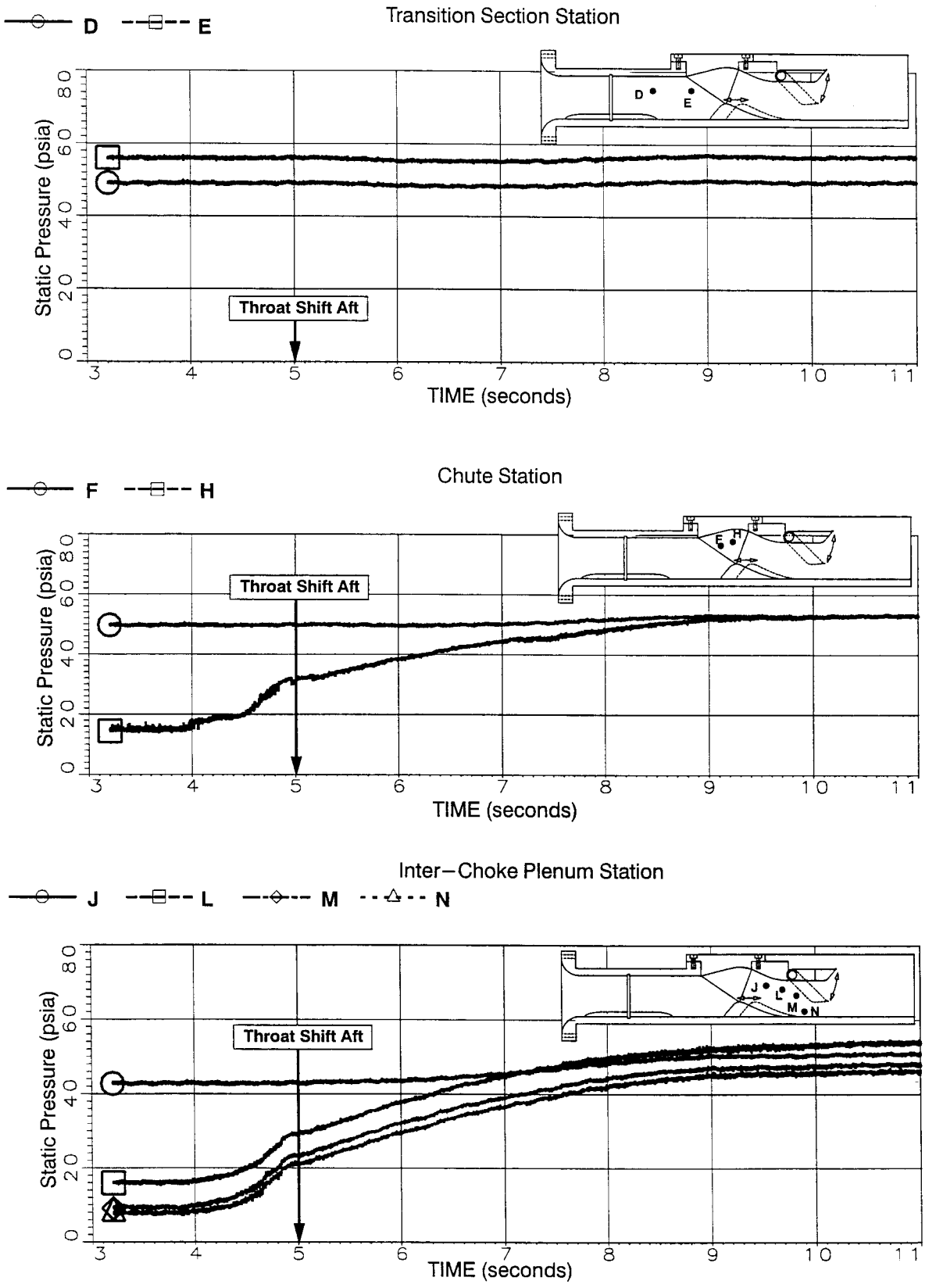

Figure 25. High Response Static Pressures for Fixed Chute Configuration with 10 Chutes (FC–1). Aft Throat Convergent Flap and Translating Plug Moved In Concert to Maintain Constant Pressure ("5") Upstream of the Forward Throat. NPR = 3. Digitial Data Transient #392 in Test Log. (Continued)

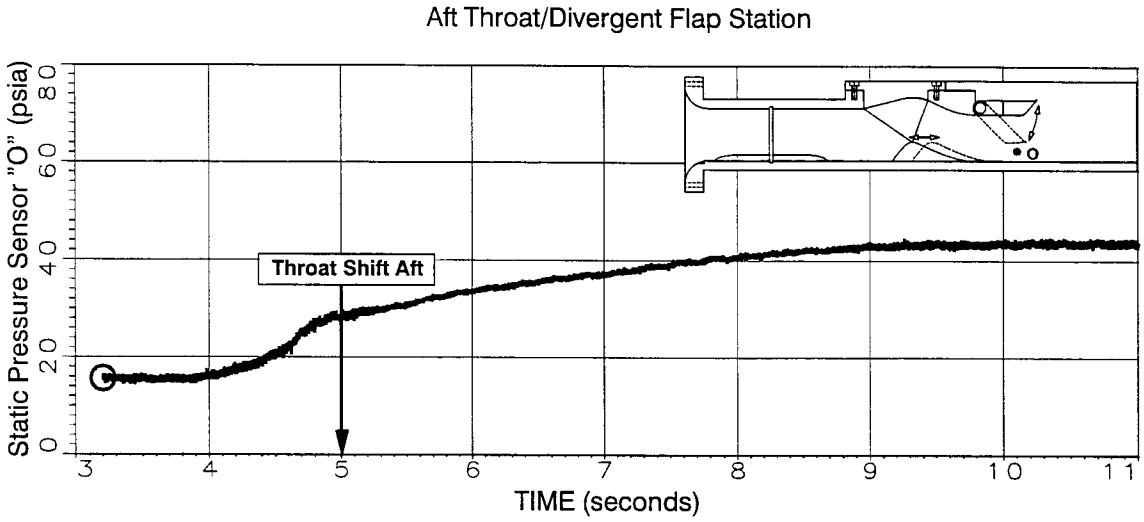

Figure 25. High Response Static Pressures for Fixed Chute Configuration with 10 Chutes (FC−1). Aft Throat Convergent Flap and Translating Plug Moved In Concert to Maintain Constant Pressure ("5") Upstream of the Forward Throat. NPR = 3. Digitial Data Transient #392 in Test Log. (Concluded)

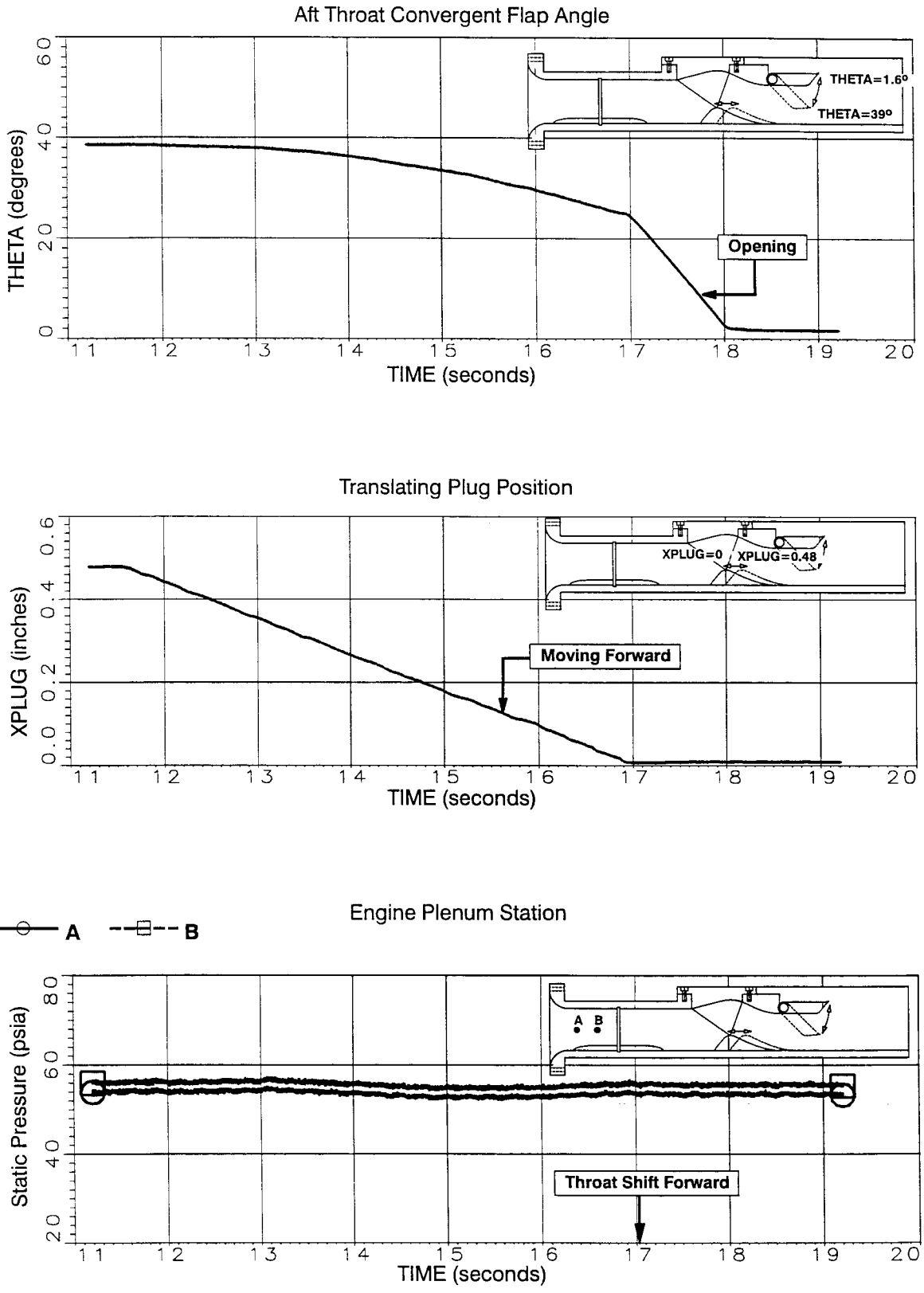

Figure 26. High Response Static Pressures for Fixed Chute Configuration with 10 Chutes (FC−1). Aft Throat Convergent Flap and Translating Plug Moved In Concert to Maintain Constant Pressure ("5") Upstream of the Forward Throat. NPR = 3. Digitial Data Transient #392 in Test Log.

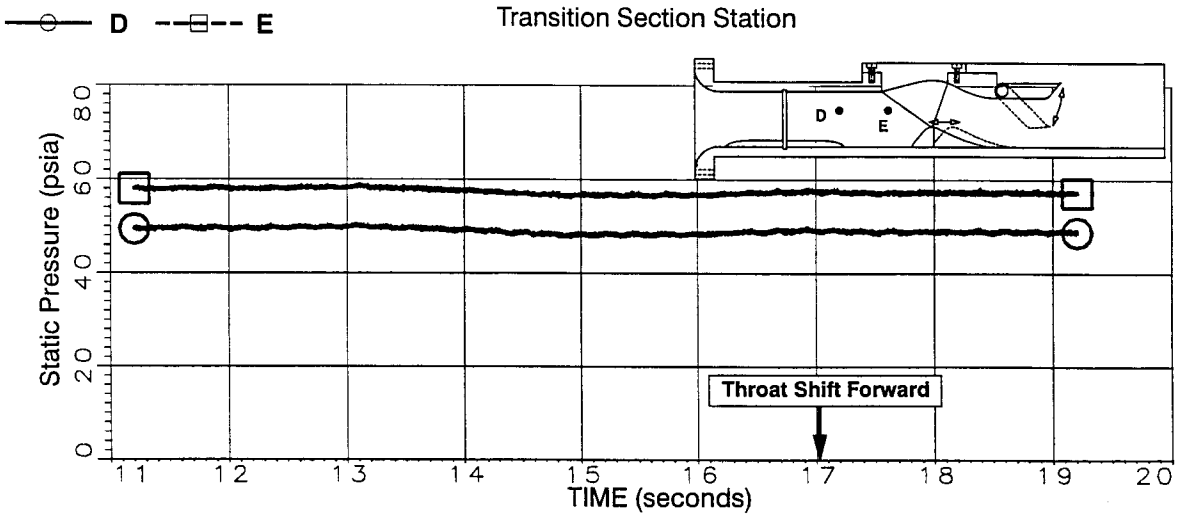

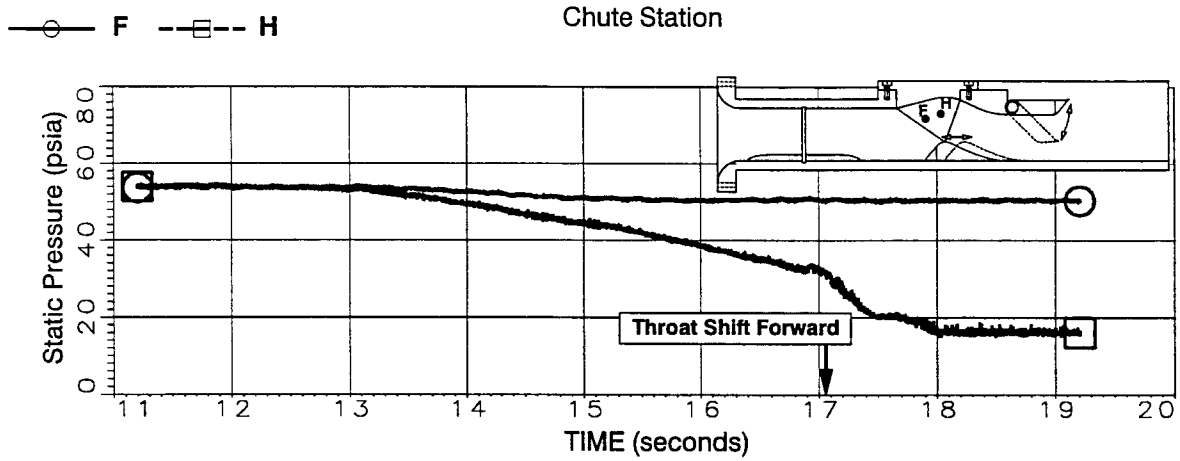

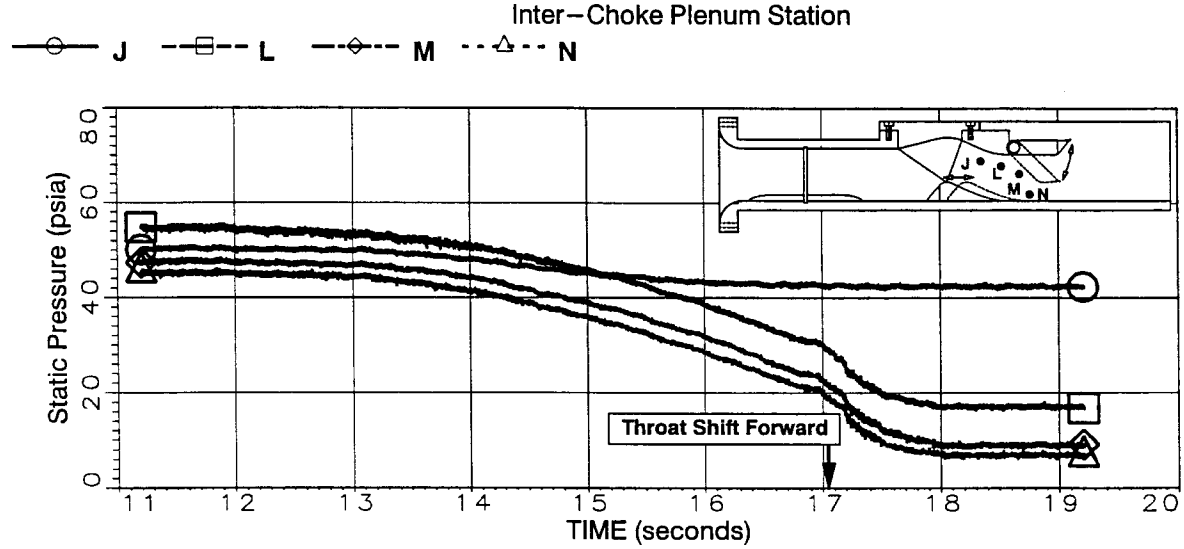

Figure 26. High Response Static Pressures for Fixed Chute Configuration with 10 Chutes (FC–1). Aft Throat Convergent Flap and Translating Plug Moved In Concert to Maintain Constant Pressure ("5") Upstream of the Forward Throat. NPR = 3. Digitial Data Transient #392 in Test Log. (Continued)

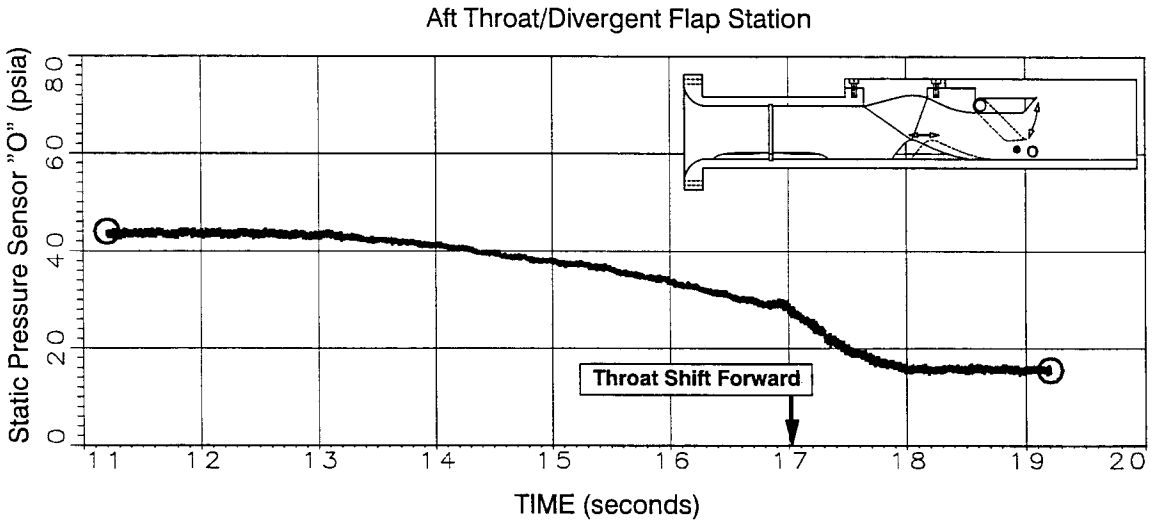

Figure 26. High Response Static Pressures for Fixed Chute Configuration with 10 Chutes (FC−1). Aft Throat Convergent Flap and Translating Plug Moved In Concert to Maintain Constant Pressure ("5") Upstream of the Forward Throat. NPR = 3. Digitial Data Transient #392 in Test Log. (Concluded)

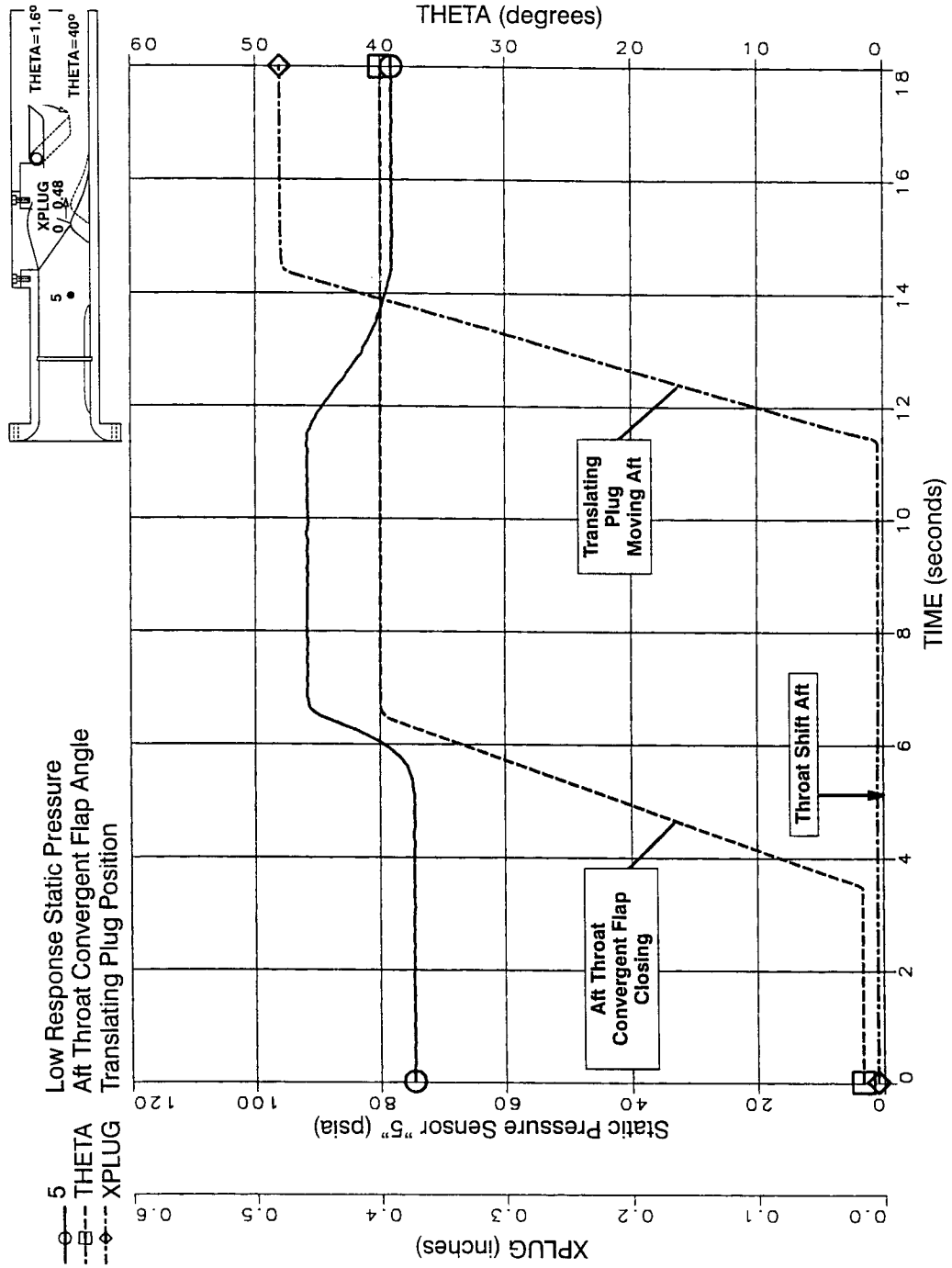

Figure 27. Effect on Low Response Pressure Sensor "5" of Aft Throat Convergent Flap Closing Then Translating Plug Moving Aft. Dynamic Stability Rig in the Fixed Chute Configuration with 10 Chutes (FC–1). NPR=5.1. Digital Data Transient No. 184.

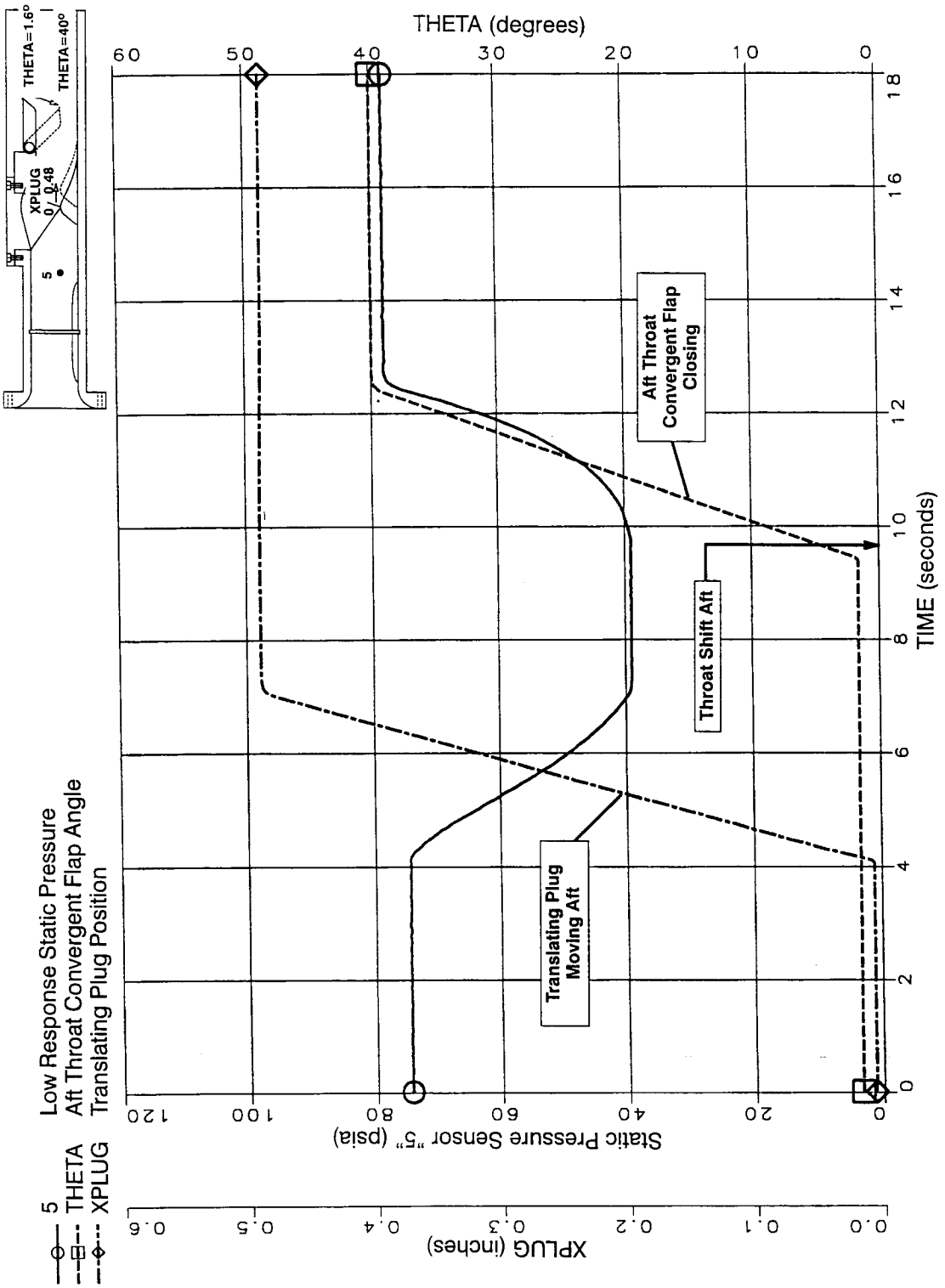

Figure 28. Effect on Low Response Pressure Sensor "5" of Moving Translating Plug Aft Then Aft Throat Convergent Flap Closing. Dynamic Stability Rig in the Fixed Chute Configuration with 10 Chutes (FC–1). NPR=5.1. Digital Data Transient No. 185.

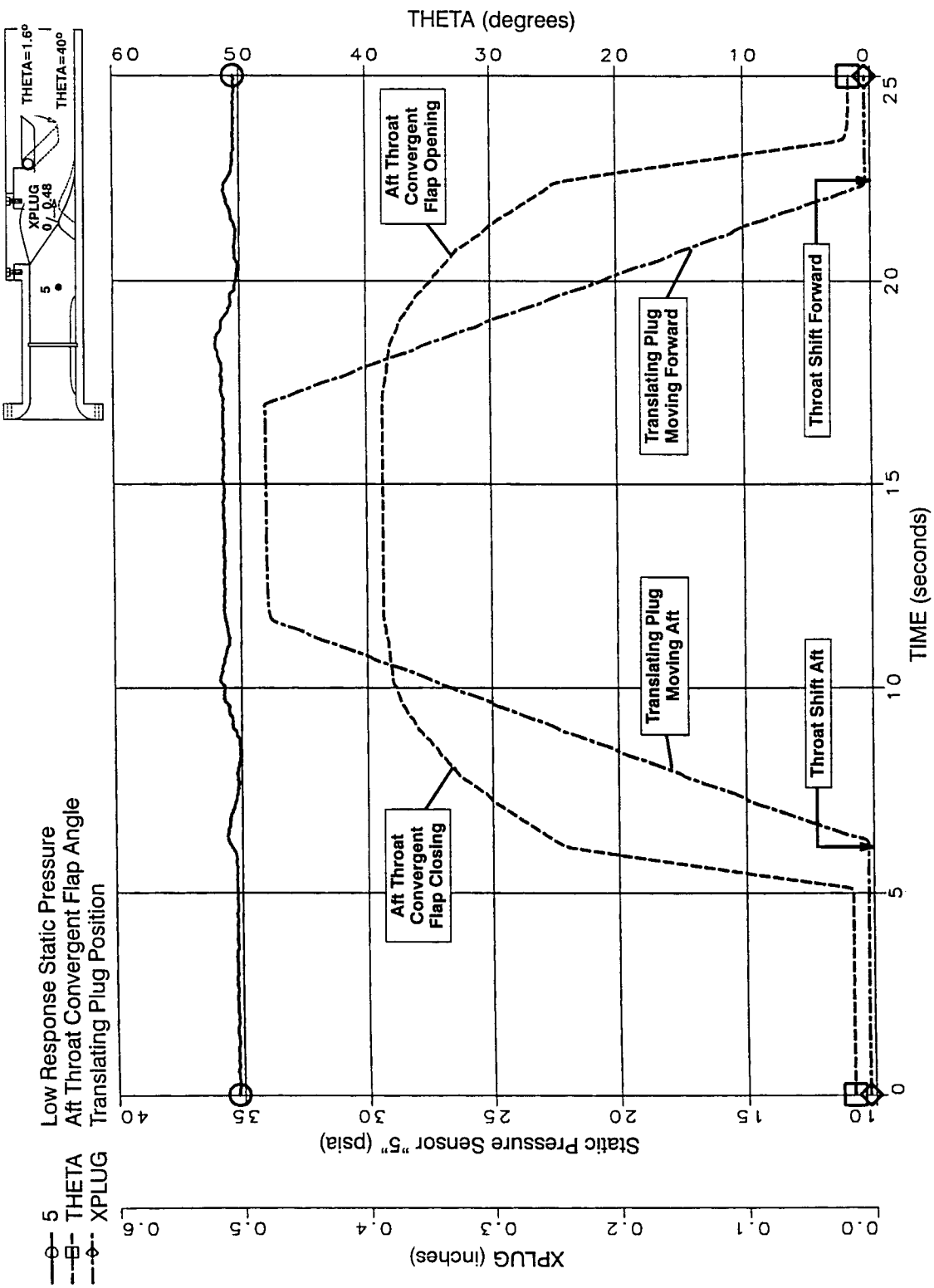

Figure 29. Effect on Low Response Pressure Sensor "5" of Aft Throat Convergent Flap and Translating Plug Moving in Concert to Shift the Throat Aft Then Forward While Maintaining a Constant Upstream Pressure ("5"). Dynamic Stability Rig in the Fixed Chute Configuration with 10 Chutes (FC–1). NPR = 2.4. Digital Data Transient No. 388.

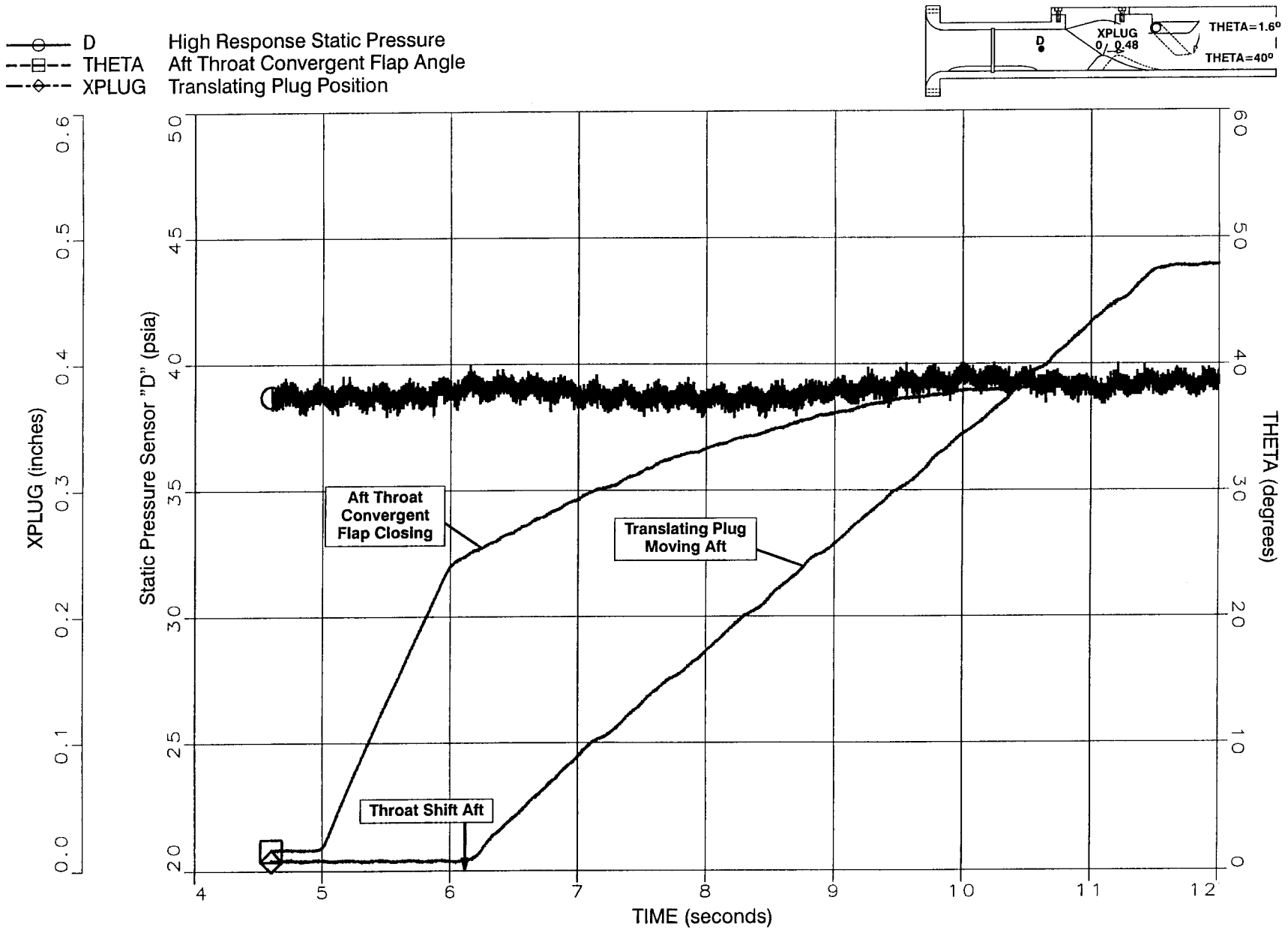

Figure 30. Effect on High Response Pressure Sensor "D" of Aft Throat Convergent Flap and Translating Plug Moving in Concert to Shift the Throat Aft While Maintaining a Constant Upstream Pressure ("5"). Dynamic Stability Rig in the Fixed Chute Configuration with 10 Chutes (FC−1). NPR = 2.4. Digital DataTransient No. 388.

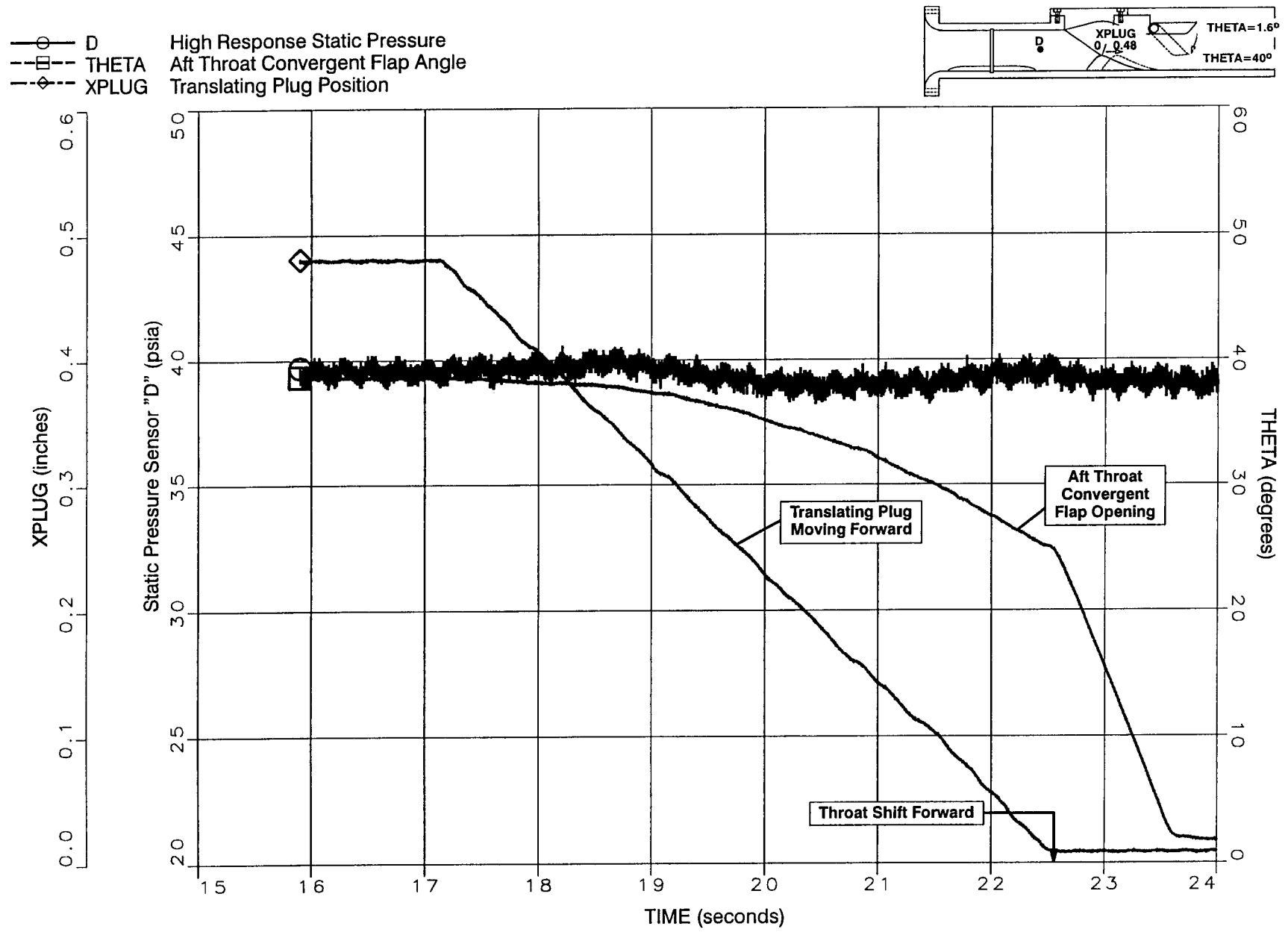

Figure 30. Effect on High Response Pressure Sensor "D" of Aft Throat Convergent Flap and Translating Plug Moving in Concert to Shift the Throat Forward While Maintaining a Constant Upstream Pressure ("5"). Dynamic Stability Rig in the Fixed Chute Configuration with 10 Chutes (FC−1). NPR=2.4. Digital DataTransient No. 388. (Concluded).

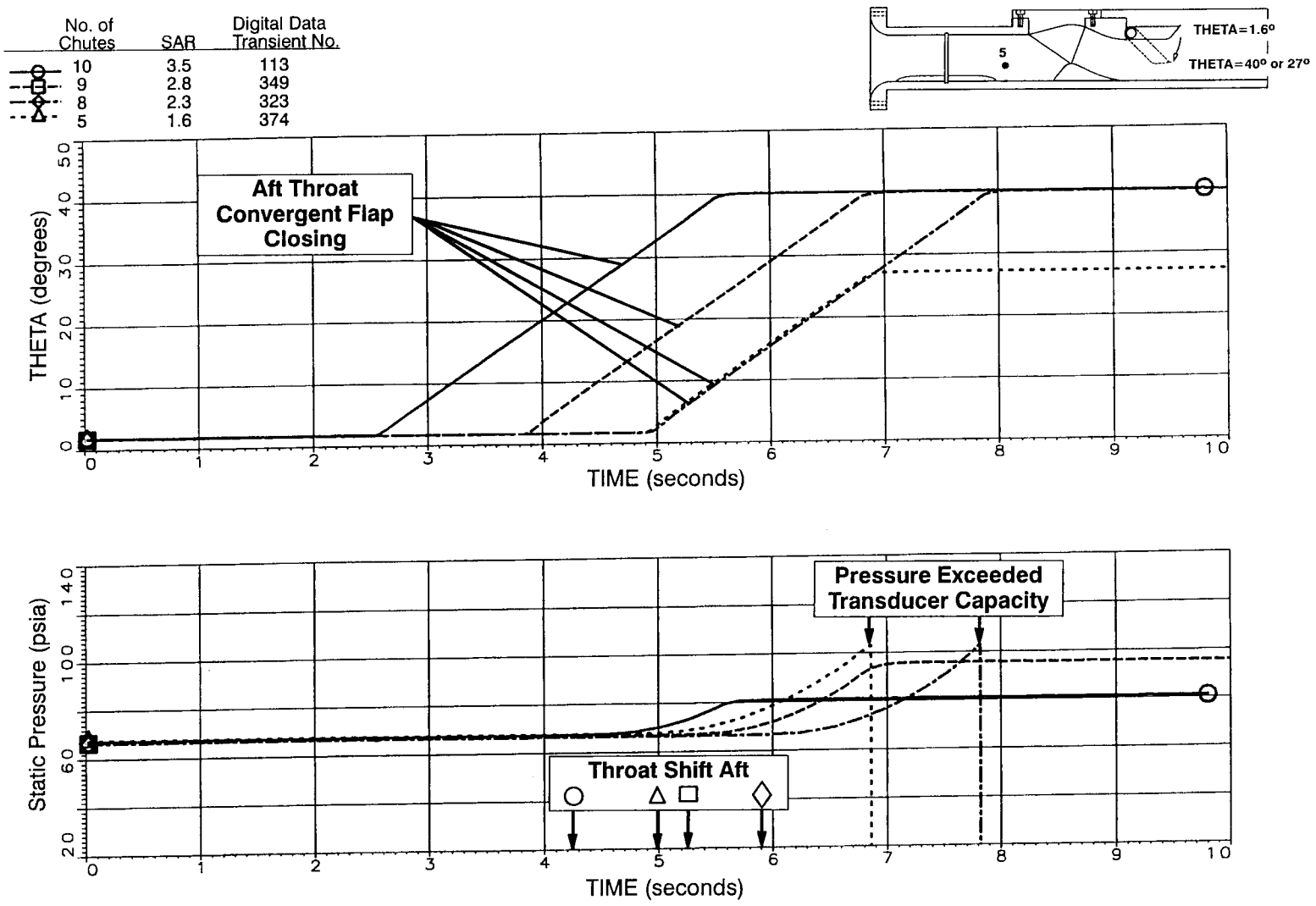

Figure 31. Effect on Low Response Static Pressure "5" of Varying the Number of Chutes in the Dynamic Stability Rig in the Fixed Chute Configuration. NPR = 4.6. Plug Fixed Forward Under the Chutes. Aft Throat Convergent Flap Closing. Actuation Time = 3 seconds.

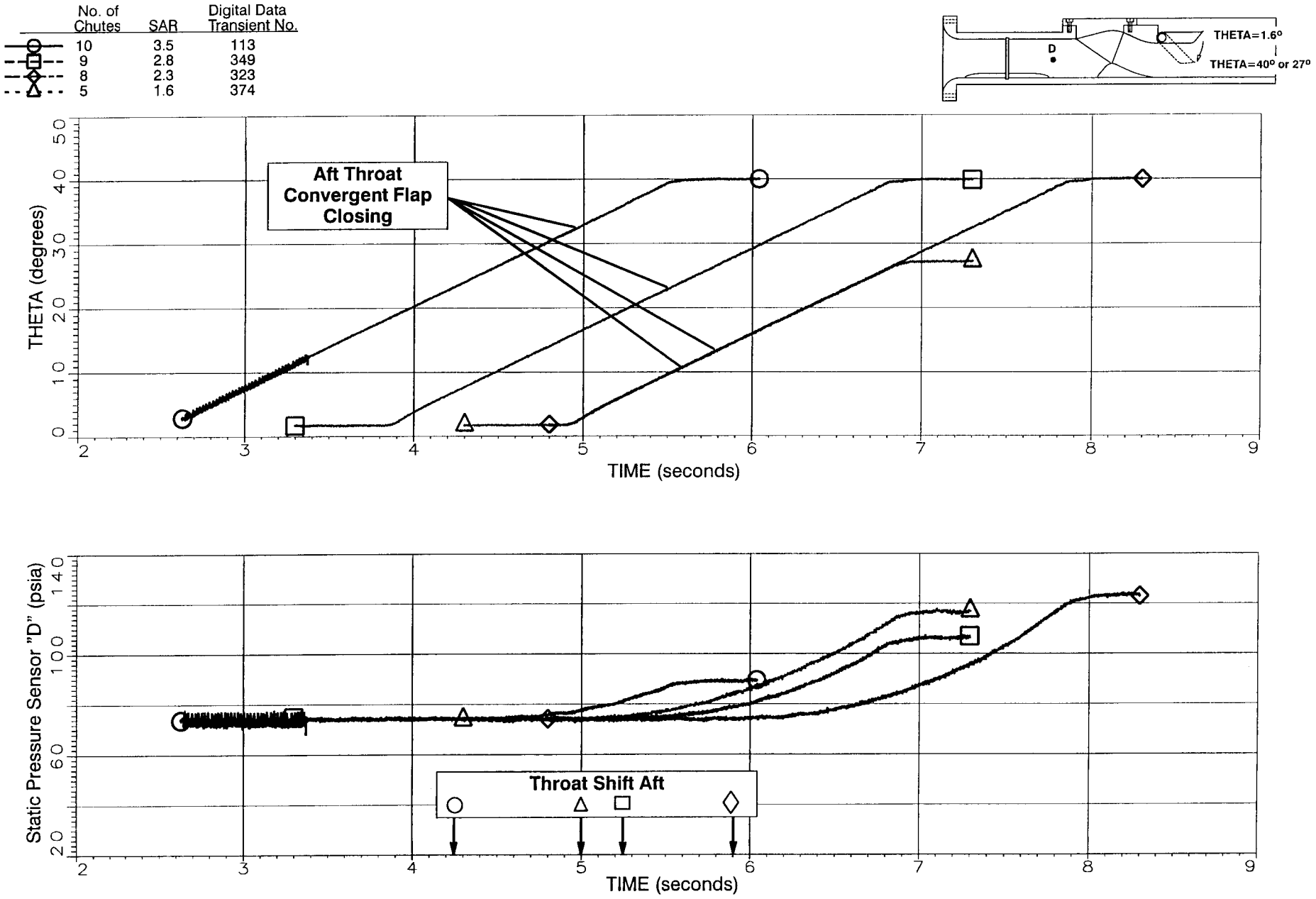

Figure 32. Effect on High Response Pressure Sensor "D" of Varying the Number of Chutes in the Dynamic Stability Rig in the Fixed Chute Configuration. NPR = 4.6. Plug Fixed Forward Under the Chutes. Aft Throat Convergent Flap Closing. Actuation Time = 3 seconds.

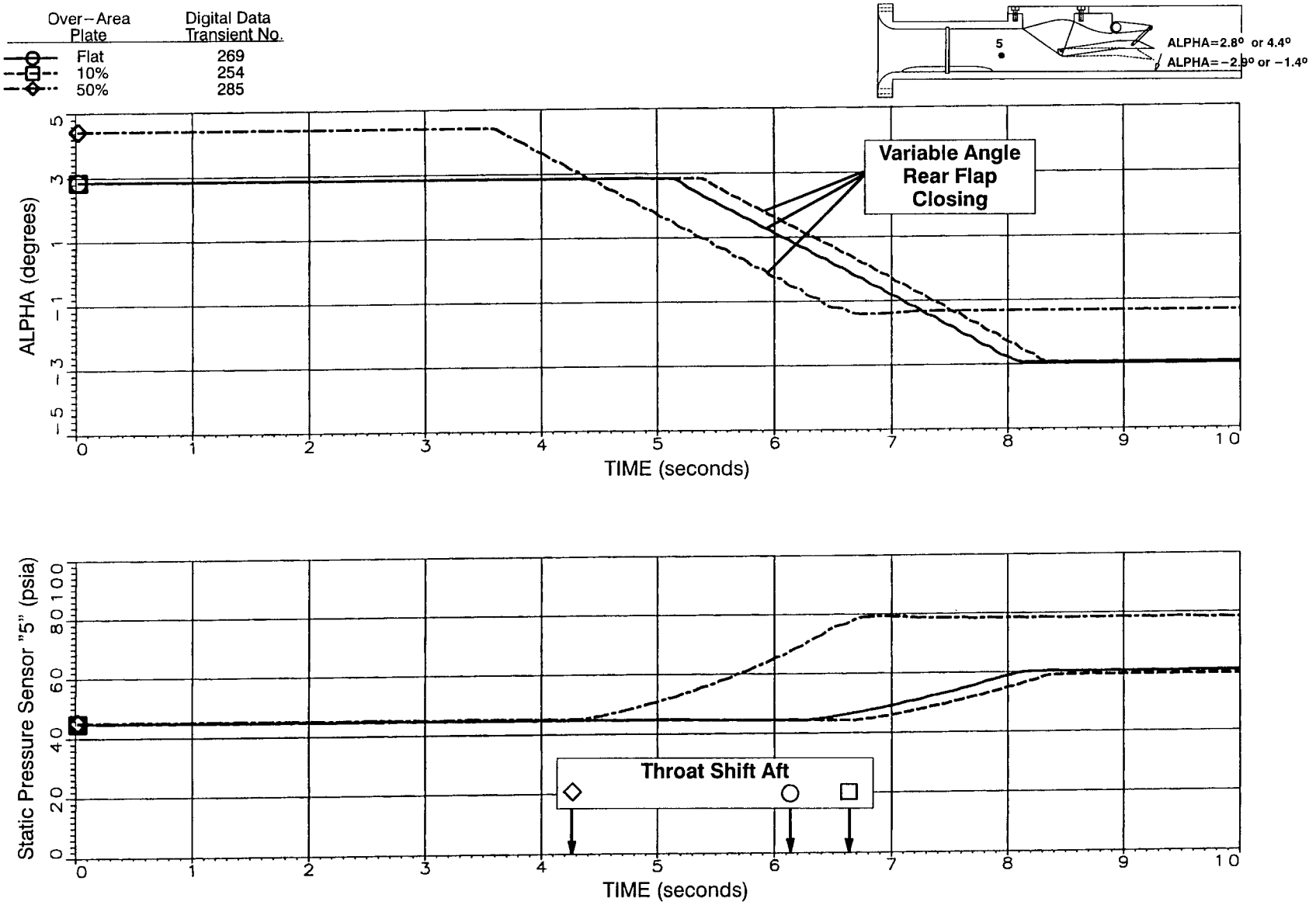

Figure 33. Effect on Low Response Pressure Sensor "5" of Varying Small Over–Area for Dynamic Stability Rig in the DSM Configuration. NPR = 3. Variable Angle Rear Flap Closing. Actuation Time = 3 seconds.

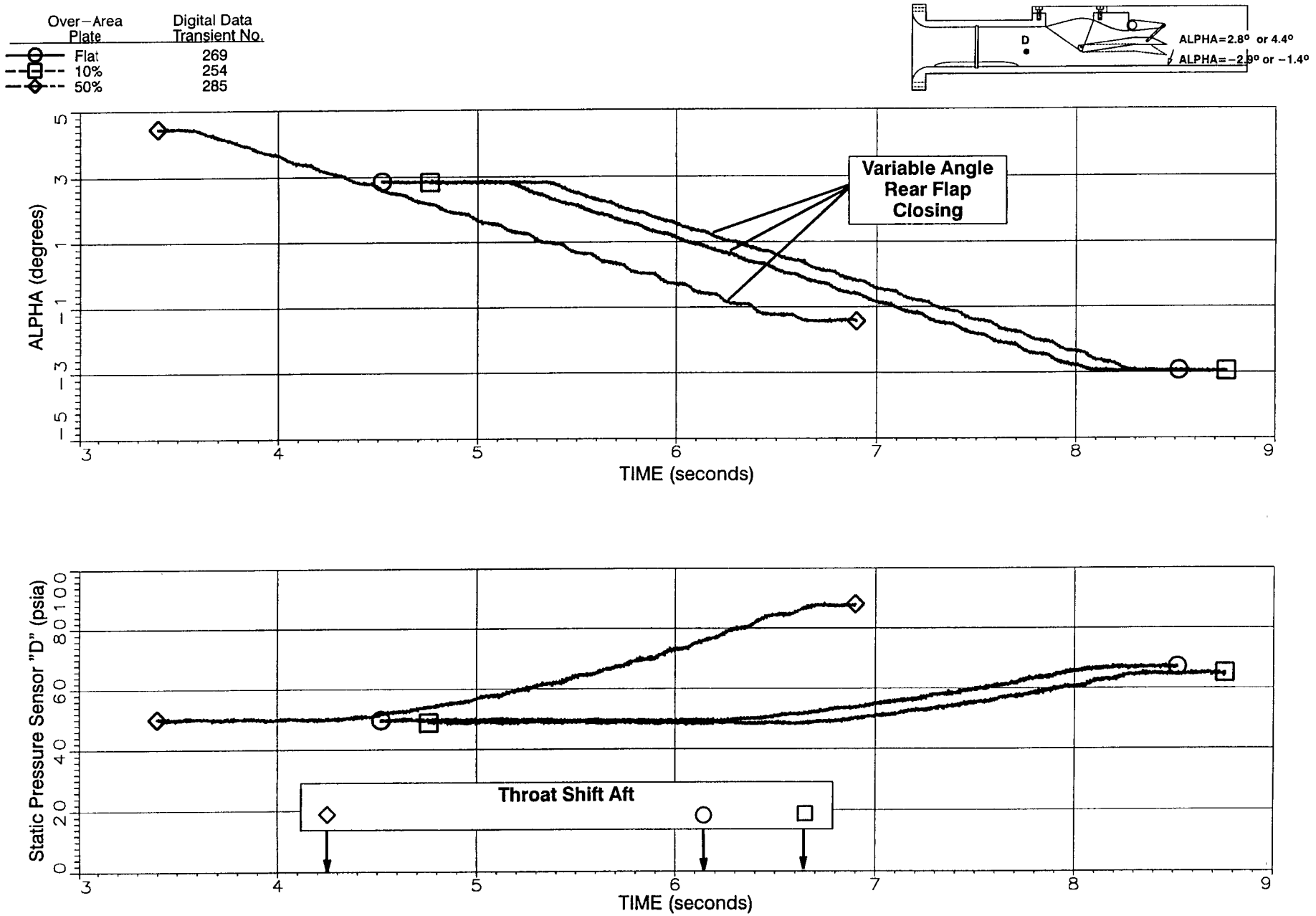

Figure 34. Effect on High Response Pressure Sensor "D" of Varying Small Over–Area for Dynamic Stability Rig in the DSM Configuration. NPR = 3. Variable Angle Rear Flap Closing. Actuation Time = 3 seconds.

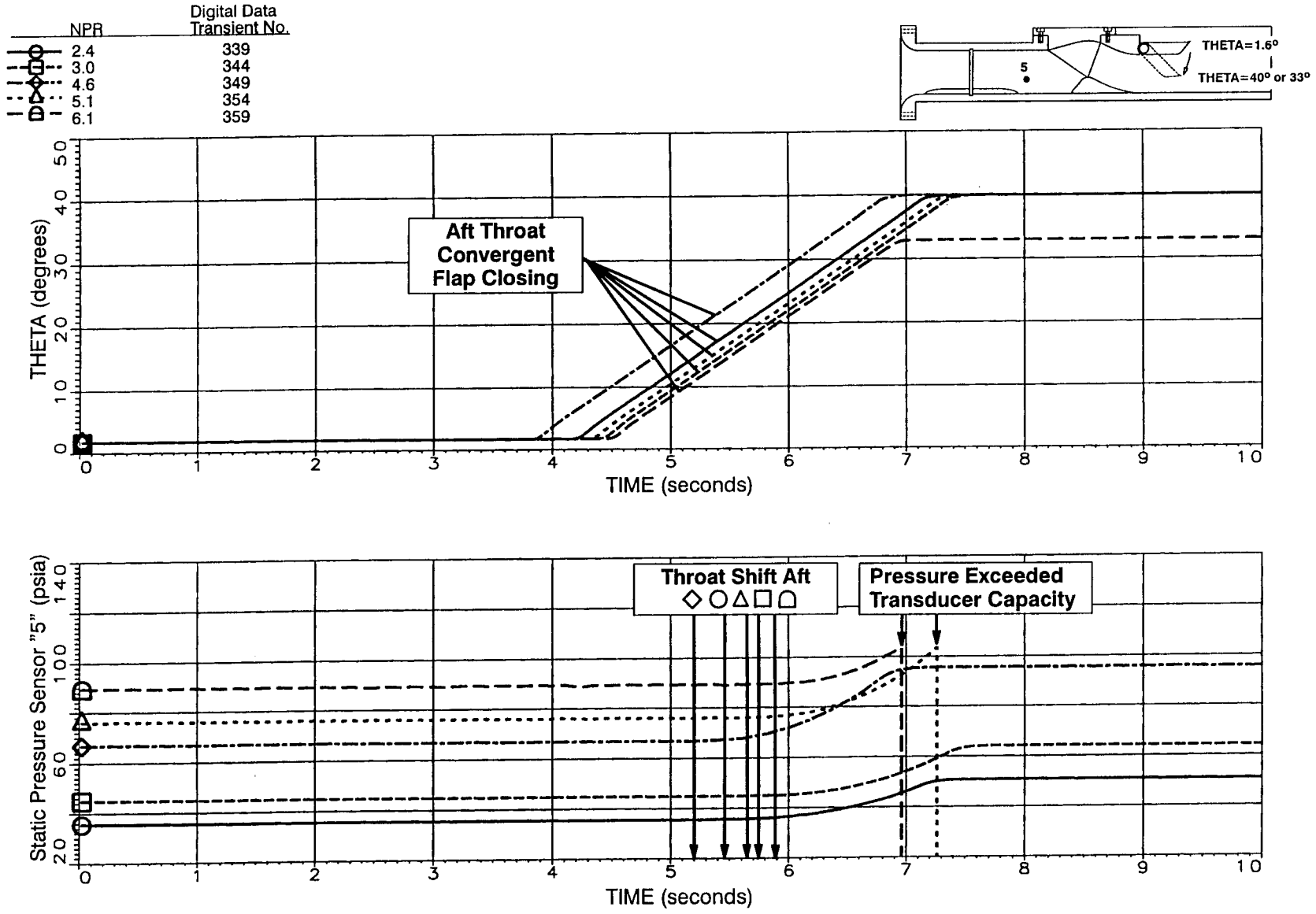

Figure 35. Effect on Low Response Pressure Sensor "5" of Varying NPR for Dynamic Stability Rig in the Fixed Chute Configuration with 9 Chutes (FC−2). Plug Fixed Forward Under the Chutes, Aft Throat Convergent Flap Closing. Actuation Time = 3 seconds.

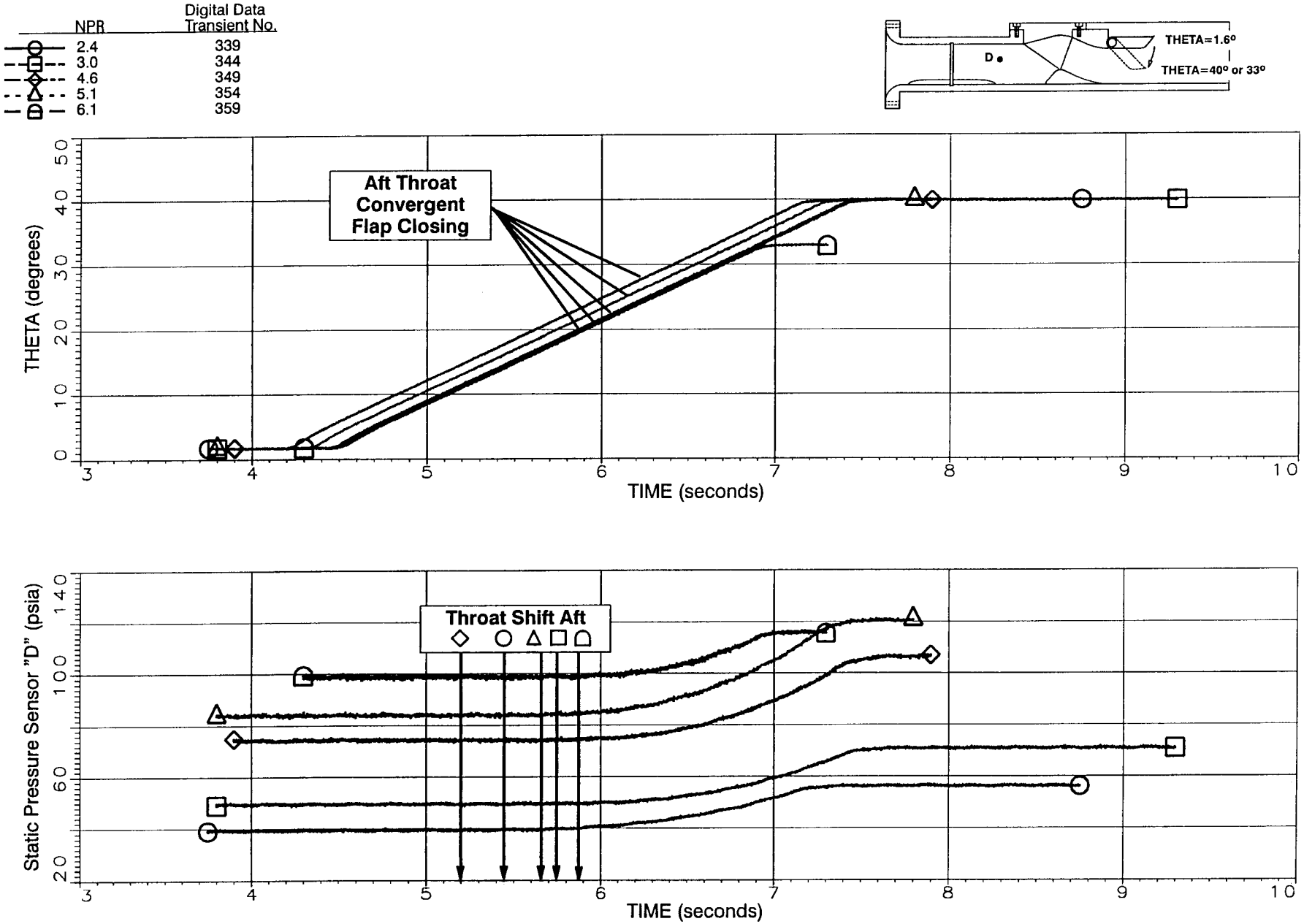

Figure 36. Effect on High Response Pressure Sensor "D" of Varying NPR for Dynamic Stability Rig in the Fixed Chute Configuration with 9 Chutes (FC–2). Plug Fixed Forward Under the Chutes, Aft Throat Convergent Flap Closing. Actuation Time = 3 seconds.

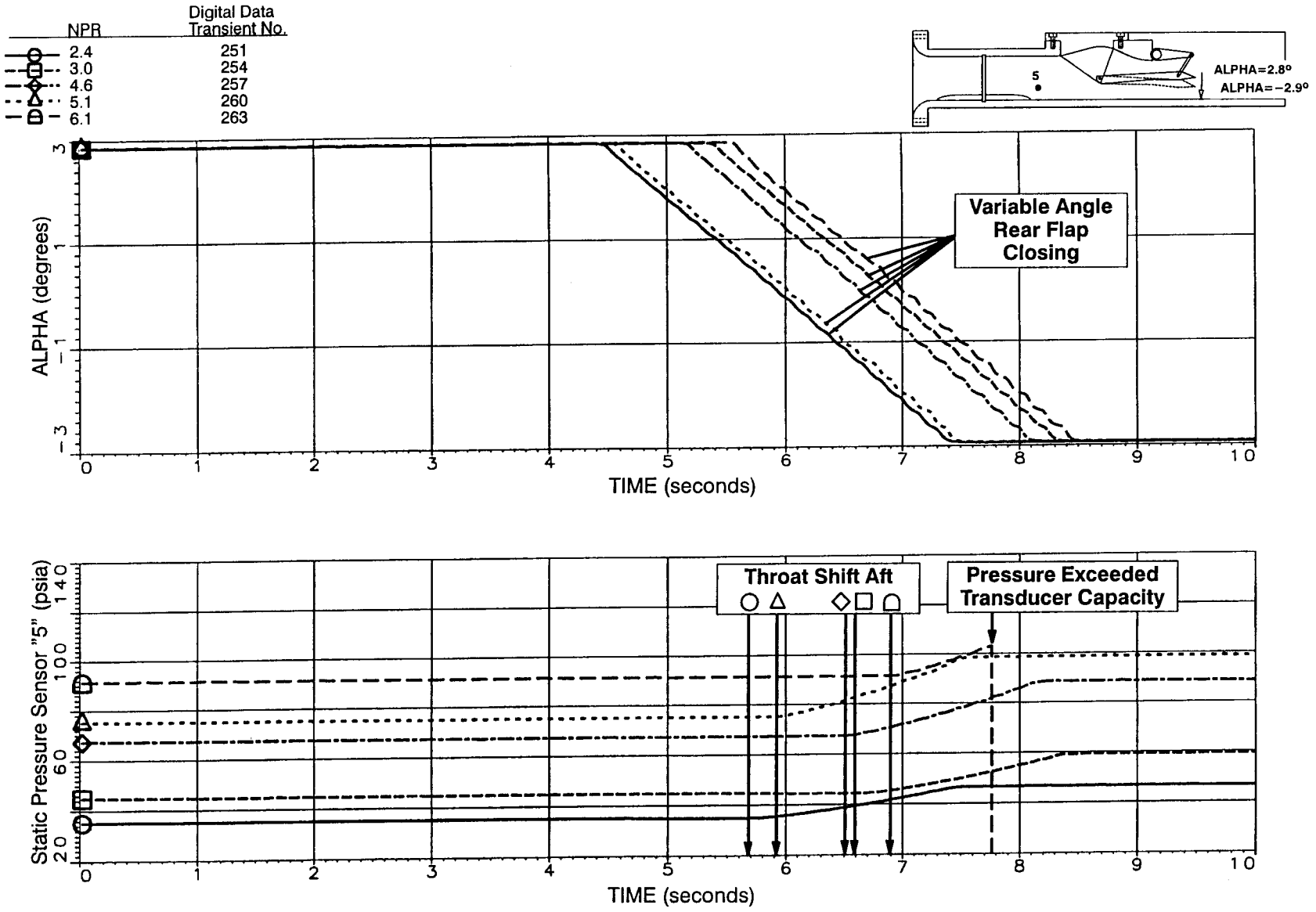

Figure 37. Effect on Low Response Pressure Sensor "5" of Varying NPR for the Dynamic Stability Rig in the DSM Configuration with 10% Over−Area Plate (DSM−2). Variable Angle Rear Flap Closing. Actuation Time = 3 sec.

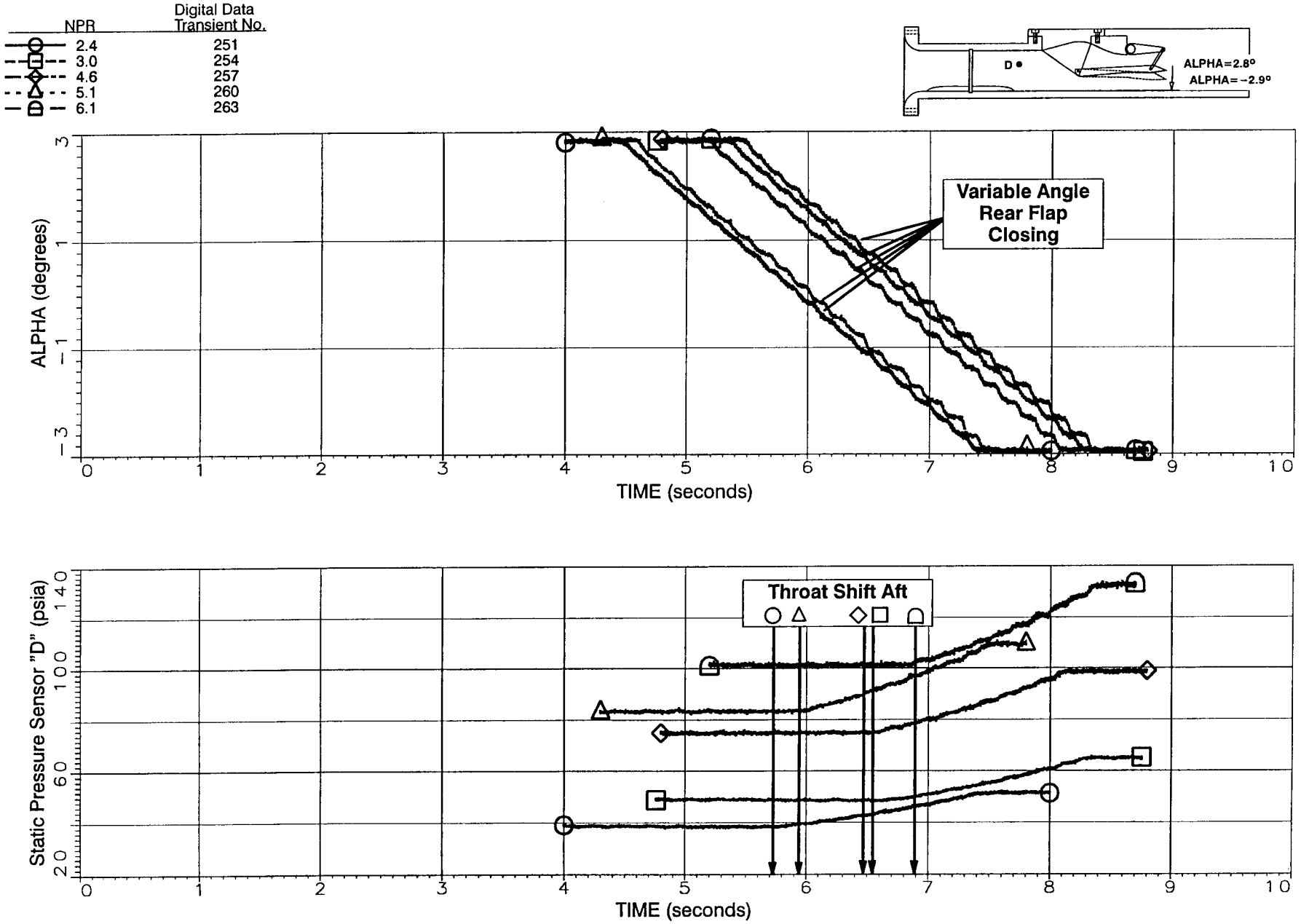

Figure 38. Effect on High Response Pressure Sensor "D" of Varying NPR for the Dynamic Stability Rig in the DSM Con–figuration with 10% Over–Area Plate (DSM–2). Variable Angle Rear Flap Closing. Actuation Time = 3 sec.

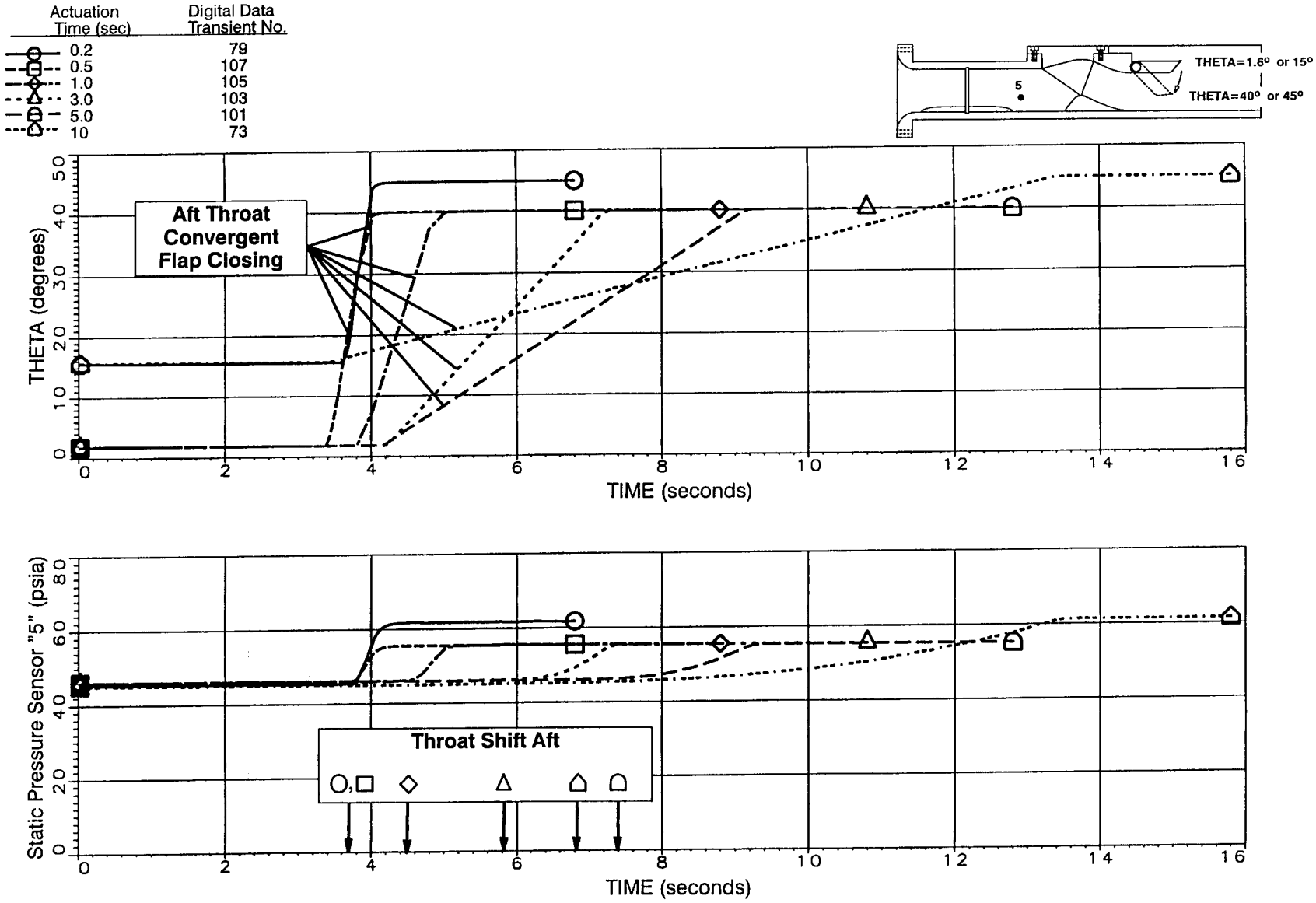

Figure 39. Effect on Low Response Pressure Sensor "5" of Varying Actuation Time for Dynamic Stability Rig in the Fixed Chute Configuration with 10 Chutes (FC−1). NPR = 3. Plug Fixed Forward Under the Chutes. Aft Throat Convergent Flap Closing.

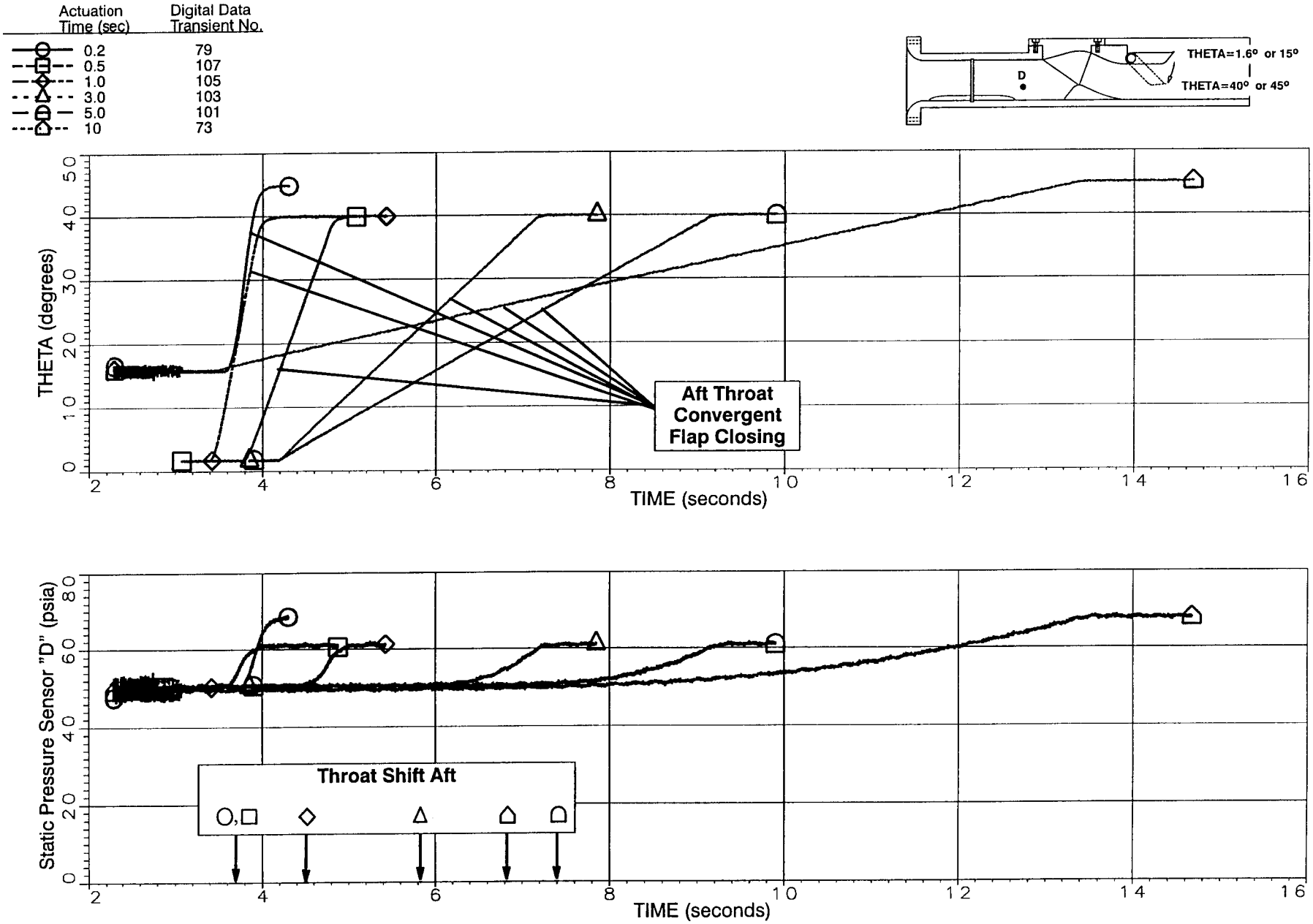

Figure 40. Effect on High Response Pressure Sensor "D" of Varying Actuation Time for Dynamic Stability Rig in the Fixed Chute Configuration with 10 Chutes (FC−1). NPR = 3. Plug Fixed Forward Under the Chutes. Aft Throat Convergent Flap Closing.

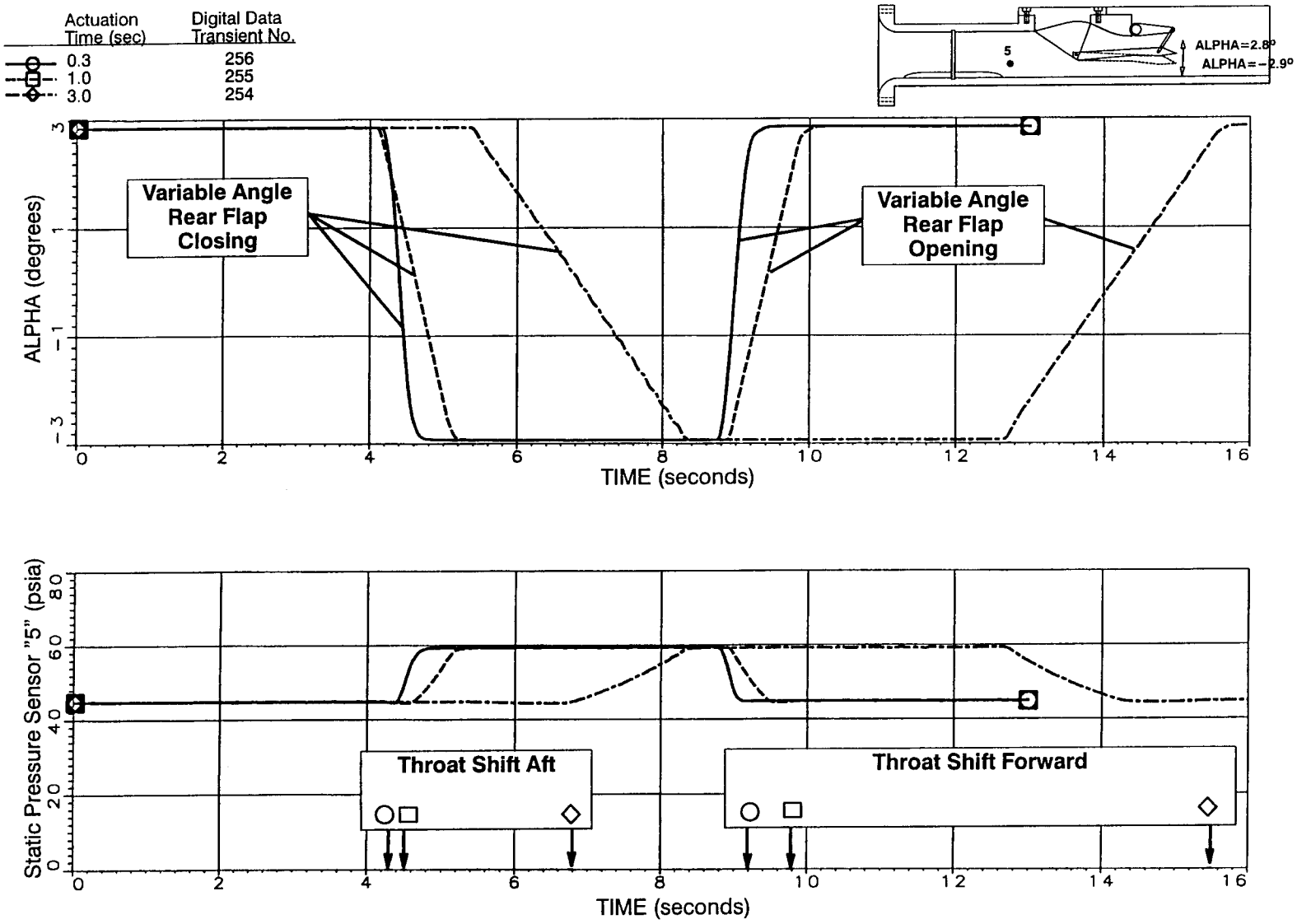

Figure 41. Effect on Low Response Pressure Sensor "5" of Varying Actuation Time for Dynamic Stability Rig in the DSM Configuration With 10% Over−Area Plate (DSM−2). NPR = 3. Variable Angle Rear Flap Closing Then Opening.

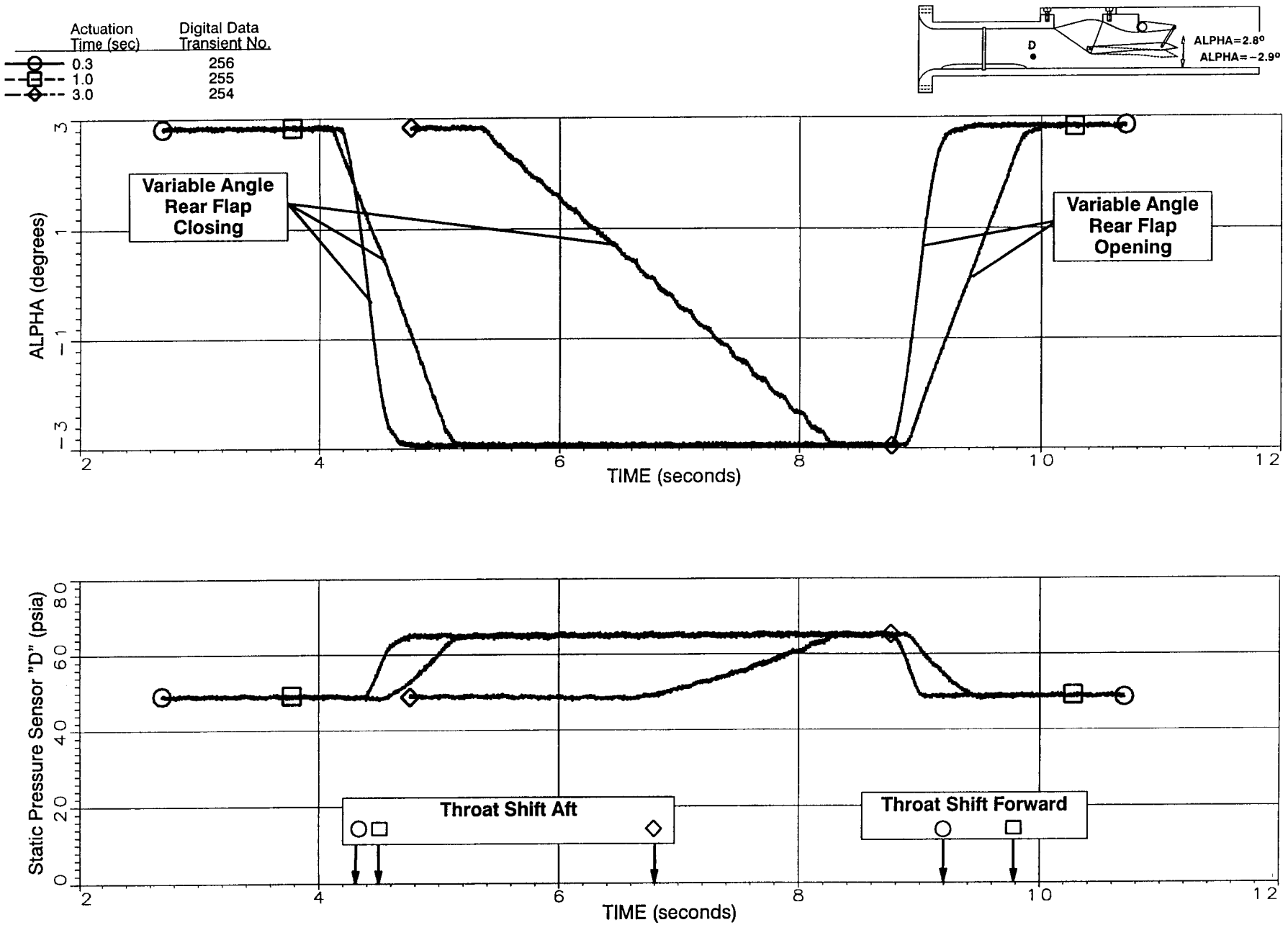

Figure 42. Effect on High Response Pressure Sensor "D" of Varying Actuation Time for Dynamic Stability Rig in the DSM Configuration With 10% Over–Area Plate (DSM–2). NPR = 3. Variable Angle Rear Flap Closing Then Opening.

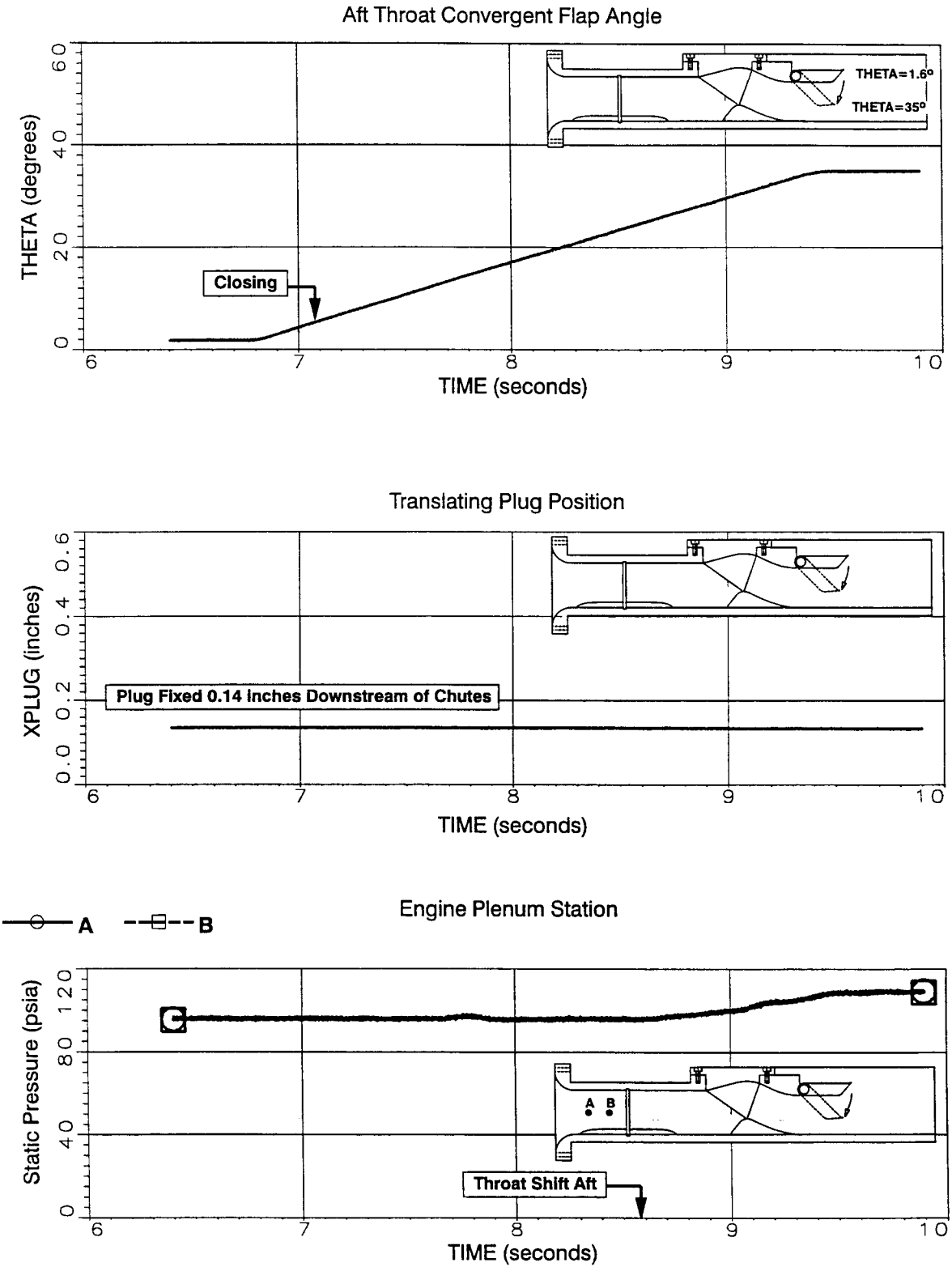

Figure 43. High Response Static Pressures for Fixed Chute Configuration with 10 Chutes (FC−1). Aft Throat Convergent Flap Closing and Translating Plug Fixed 0.14 inches Downstream from the Chutes. Actuation Time = 3 seconds. NPR = 5.4. Digital Data Transient #137 in Test Log.

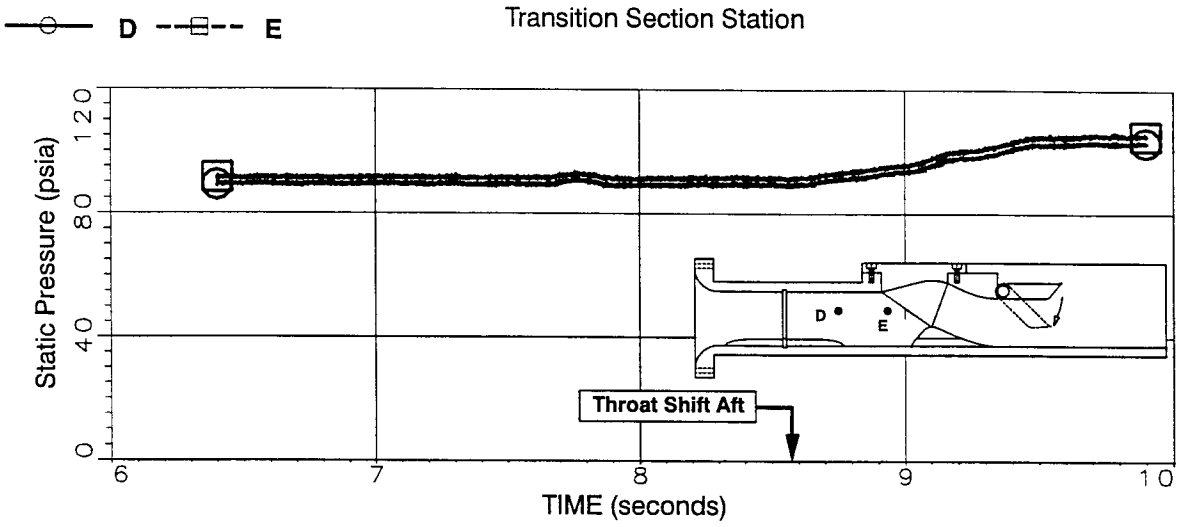

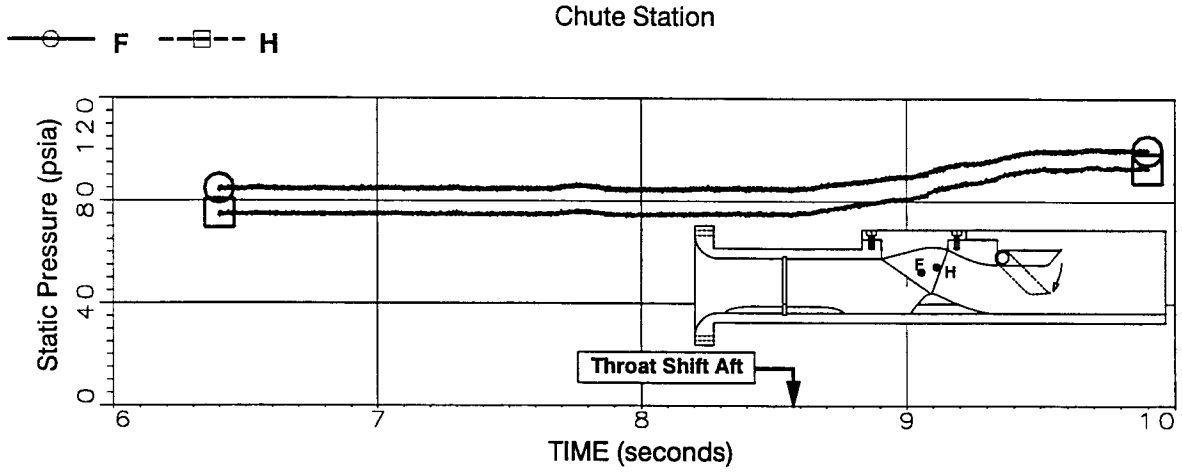

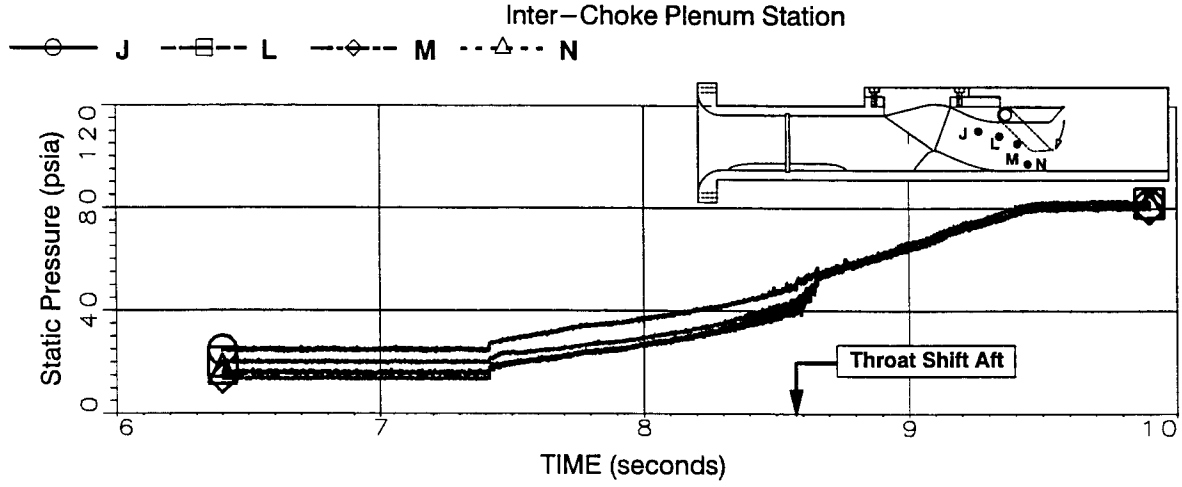

Figure 43. High Response Static Pressures for Fixed Chute Configuration with 10 Chutes (FC–1). Aft Throat Convergent Flap Closing and Translating Plug Fixed 0.14 inches Downstream from the Chutes. Actuation Time = 3 seconds. NPR = 5.4. Digital Data Transient #137 in Test Log. (Continued).

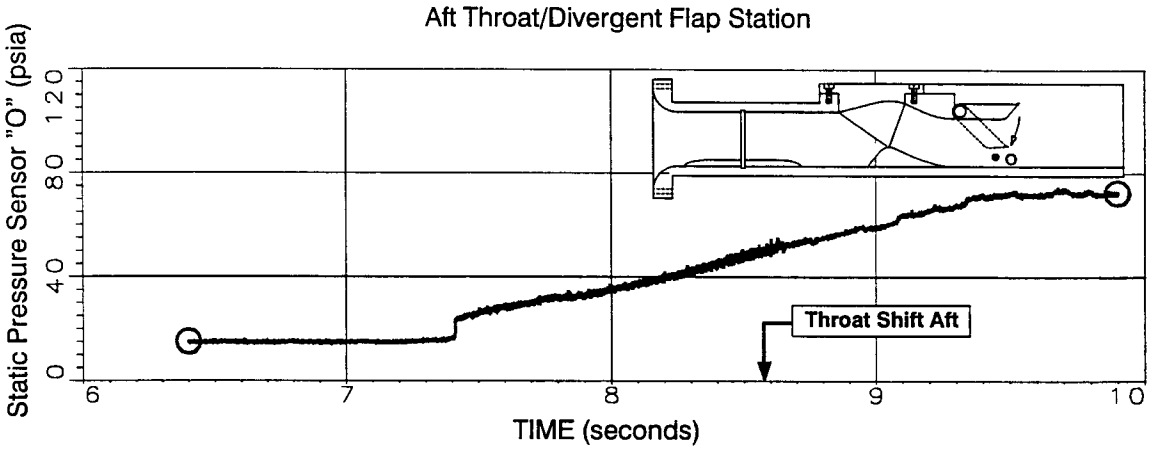

Figure 43. High Response Static Pressures for Fixed Chute Configuration with 10 Chutes (FC−1). Aft Throat Convergent Flap Closing and Translating Plug Fixed 0.14 inches Downstream from the Chutes. Actuation Time = 3 seconds. NPR= 5.4. Digital Data Transient #137 in Test Log. (Concluded).

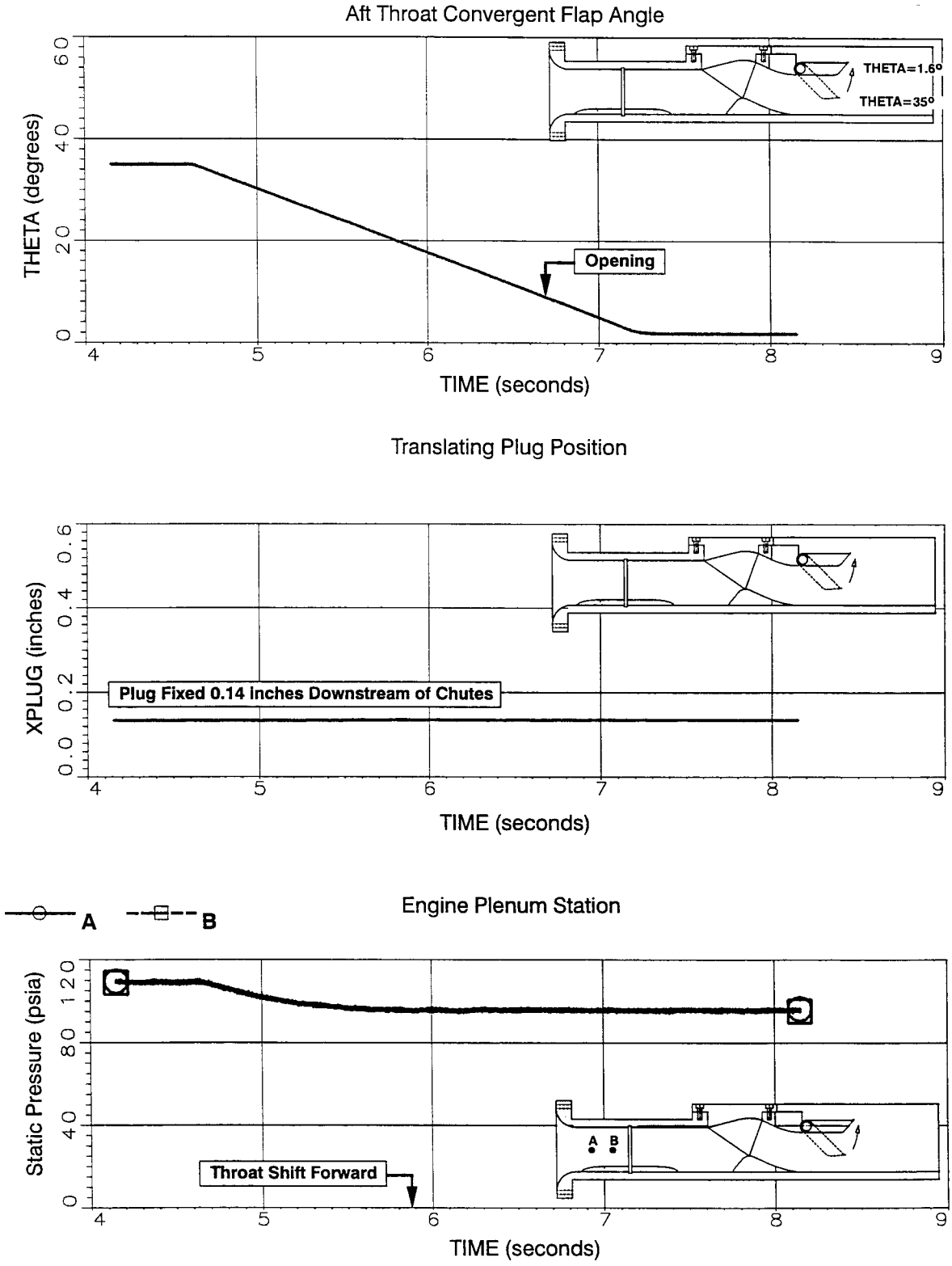

Figure 44. High Response Static Pressures for Fixed Chute Configuration with 10 Chutes (FC−1). Aft Throat Convergent Flap Opening and Translating Plug Fixed 0.14 inches Downstream from the Chutes. Actuation Time = 3 seconds. NPR = 5.4. Digital Data Transient #138 in Test Log.

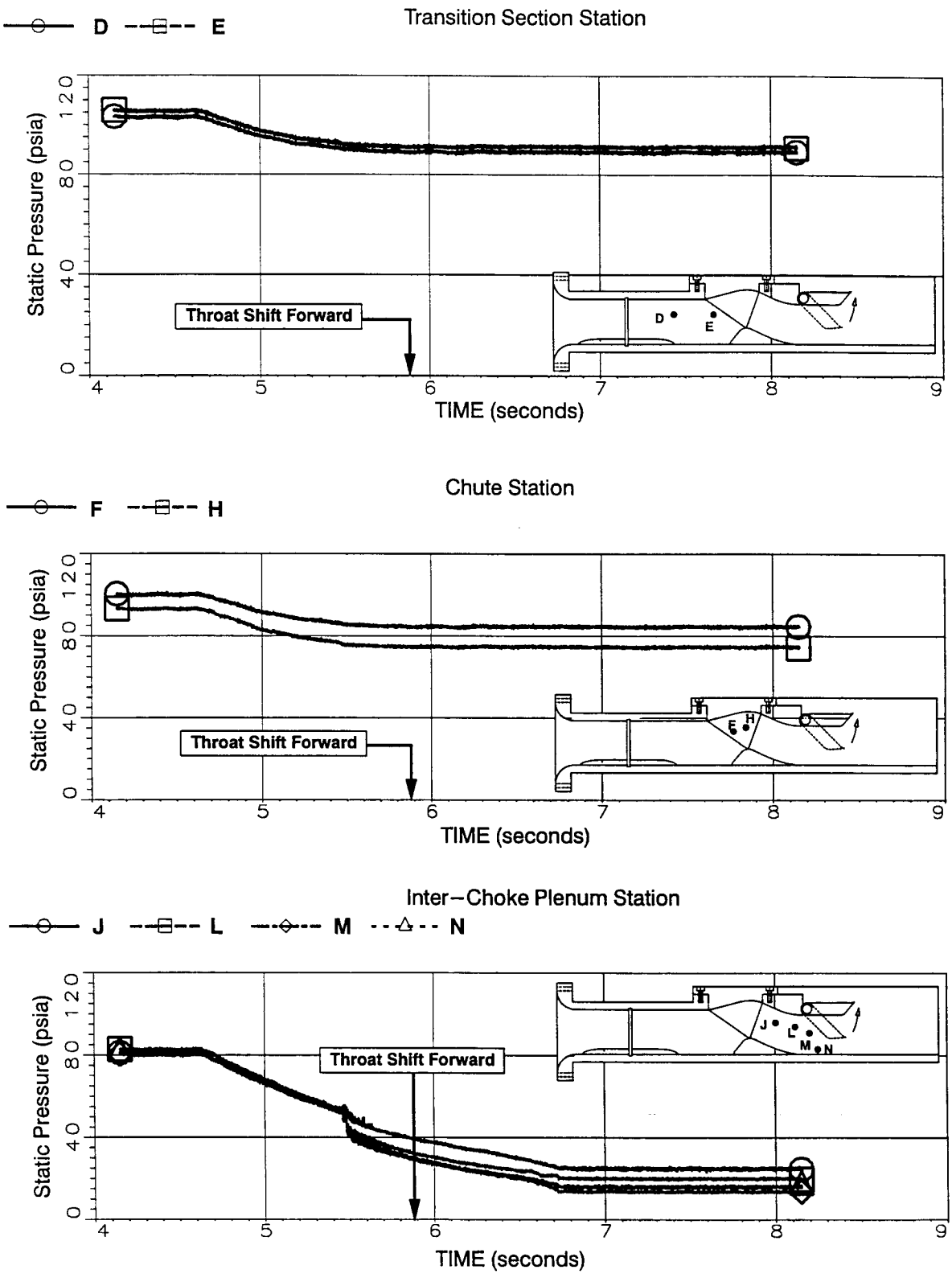

Figure 44. High Response Static Pressures for Fixed Chute Configuration with 10 Chutes (FC–1). Aft Throat Convergent Flap Opening and Translating Plug Fixed 0.14 inches Downstream from the Chutes. Actuation Time = 3 seconds. NPR= 5.4. Digital Data Transient #138 in Test Log. (Continued).

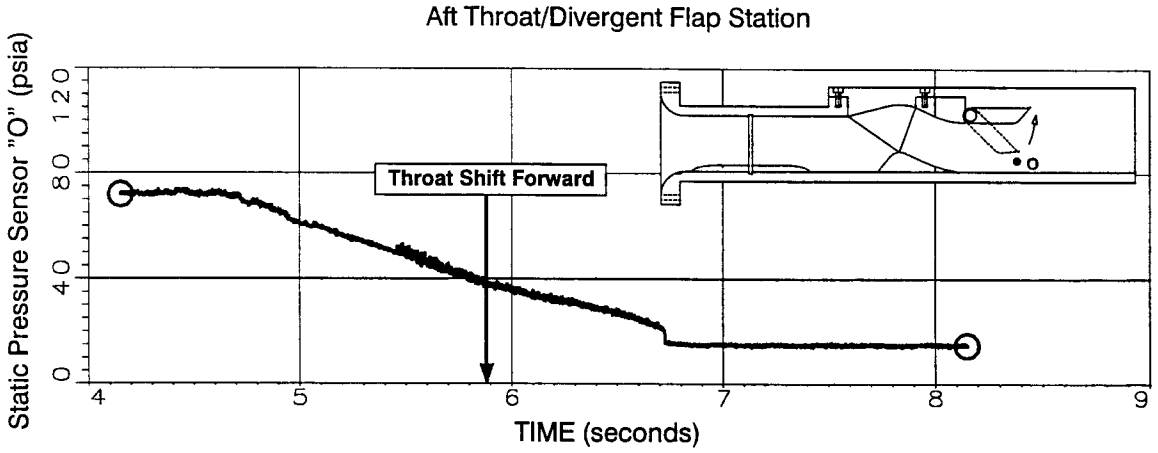

Figure 44. High Response Static Pressures for Fixed Chute Configuration with 10 Chutes (FC−1). Aft Throat Convergent Flap Opening and Translating Plug Fixed 0.14 inches Downstream from the Chutes. Actuation Time = 3 seconds. NPR= 5.4. Digital Data Transient #138 in Test Log. (Concluded).

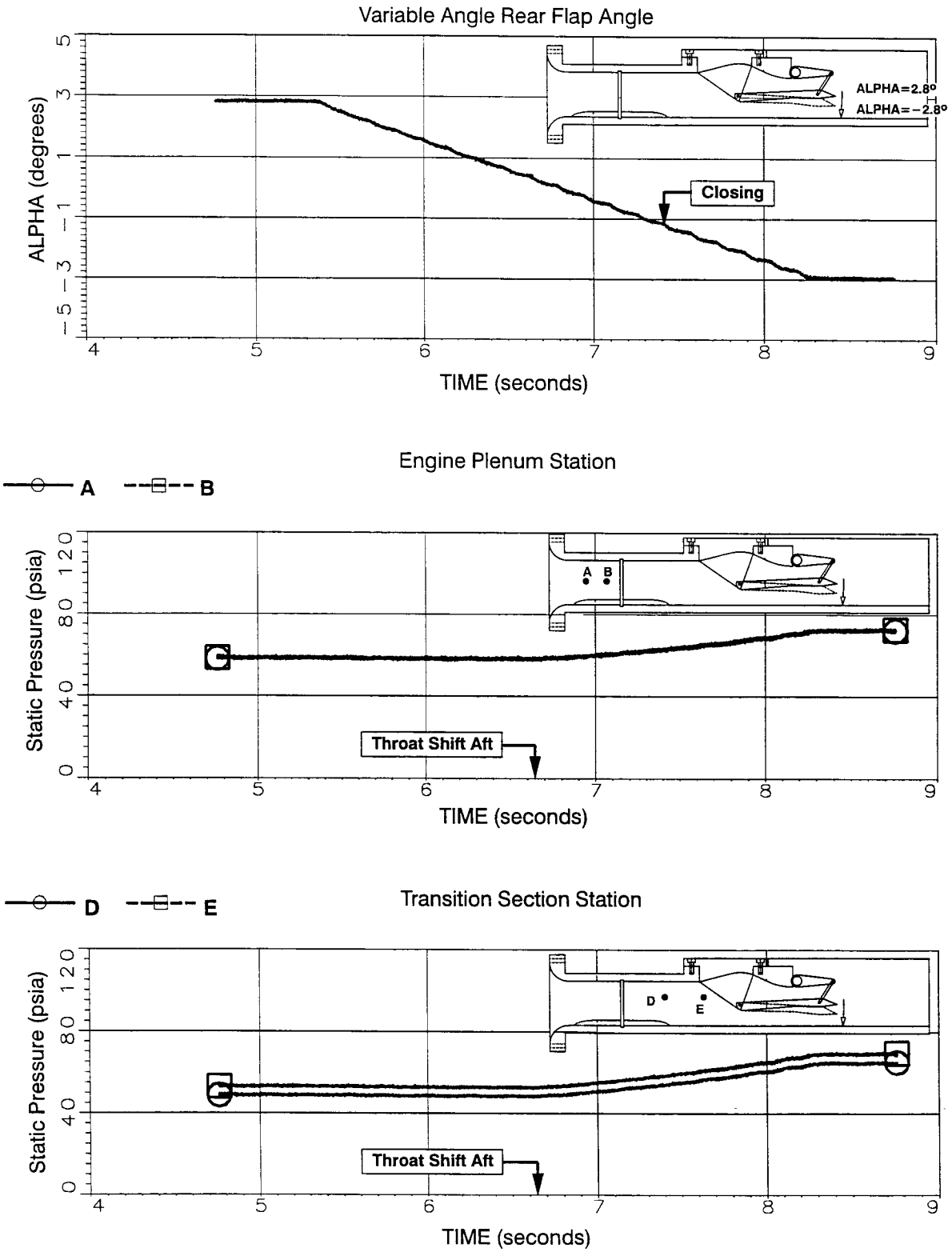

Figure 45. High Response Static Pressures for DSM Configuration with 10% Over–Area Plate (DSM–2). Variable Angle Rear Flap Closing. Actuation Time=3 seconds. NPR = 3. Digital Data Transient #254 in Test Log.

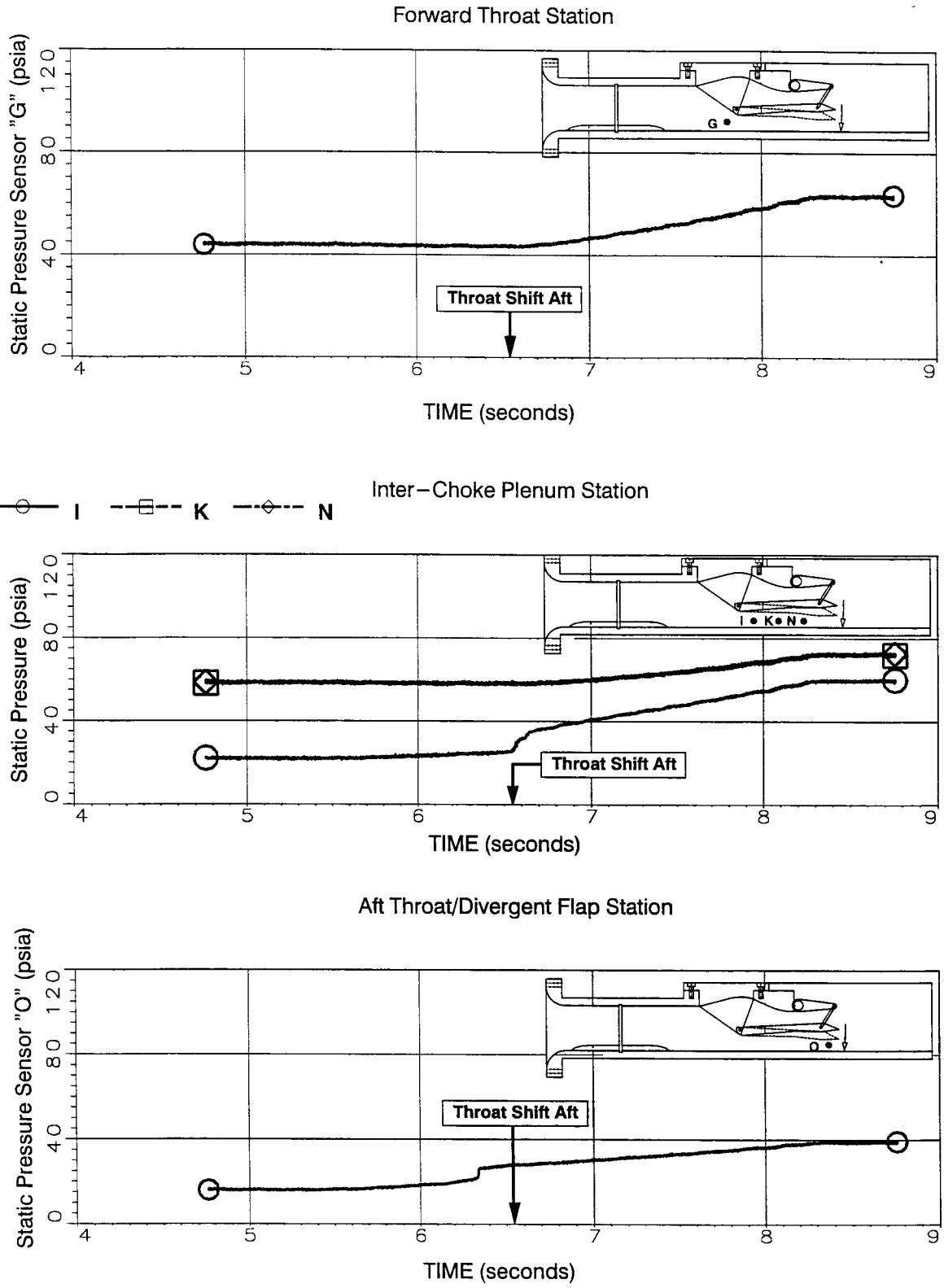

Figure 45. High Response Static Pressures for DSM Configuration with 10% Over–Area Plate (DSM–2). Variable Angle Rear Flap Closing. Actuation Time=3 seconds. NPR = 3. Digital Data Transient #254 in Test Log. (Concluded).

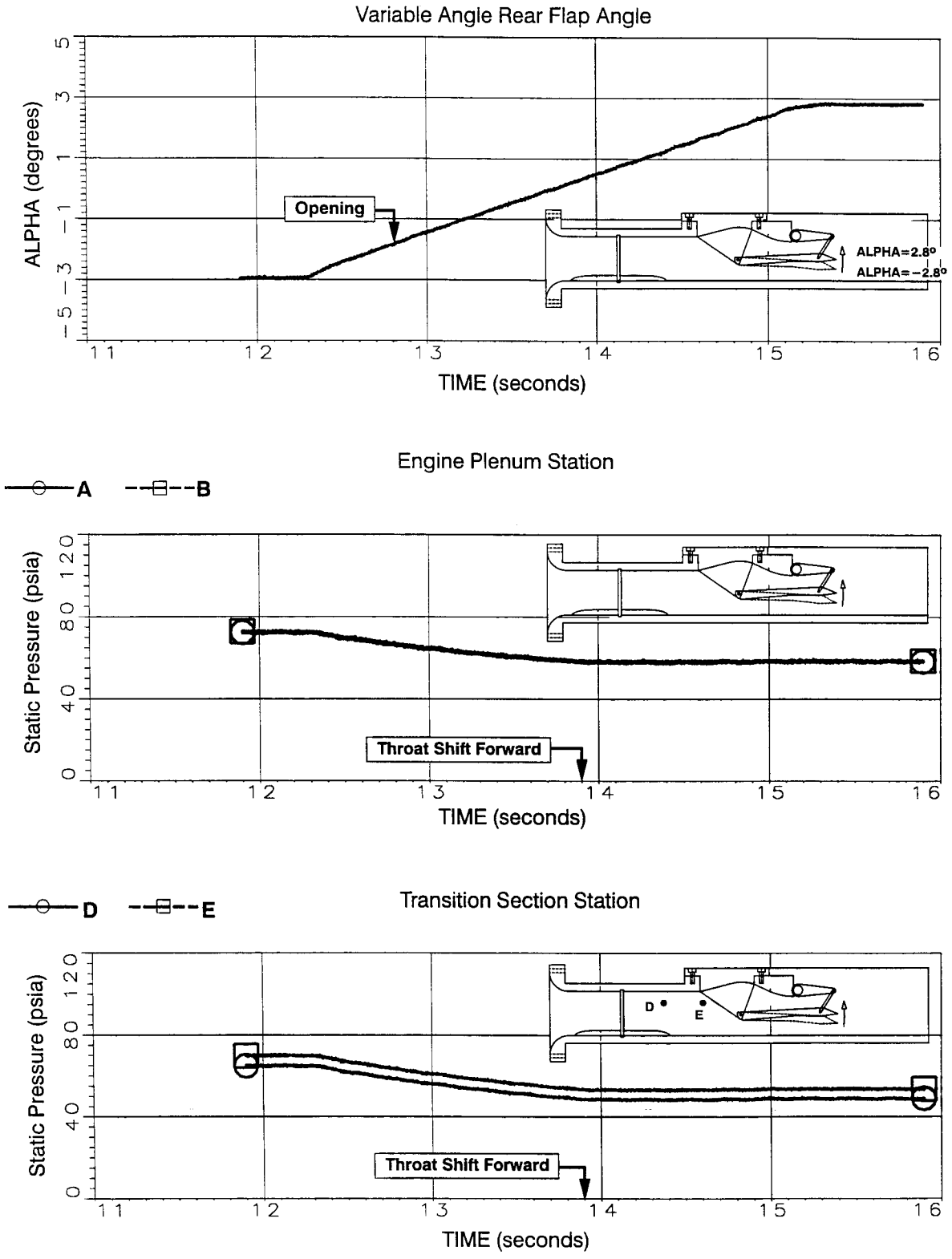

Figure 46. High Response Static Pressures for DSM Configuration with 10% Over−Area Plate (DSM−2). Variable Angle Rear Flap Closing. Actuation Time=3 seconds. NPR = 3. Digital Data Transient #254 in Test Log.

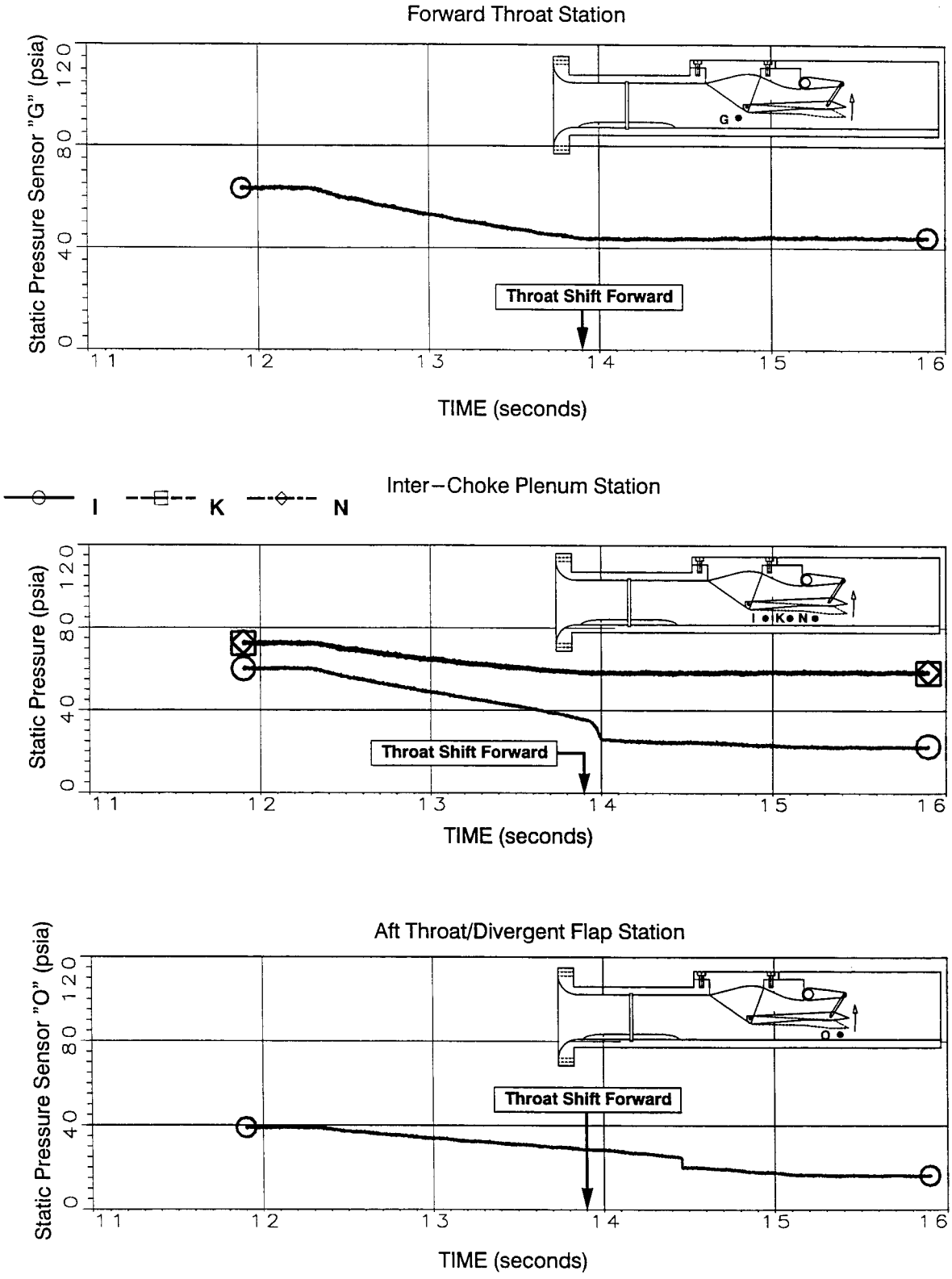

Figure 46. High Response Static Pressures for DSM Configuration with 10% Over–Area Plate (DSM–2). Variable Angle Rear Flap Closing. Actuation Time=3 seconds. NPR = 3. Digital Data Transient #254 in Test Log. (Concluded).

REPORT DOCUMENTATION PAGE

Form Approved
OMB No. 0704-0188

1. AGENCY USE ONLY (*Leave blank*)	2. REPORT DATE	3. REPORT TYPE AND DATES COVERED
	February 2005	Final Contractor Report

4. TITLE AND SUBTITLE

Nozzle Aerodynamic Stability During a Throat Shift

5. FUNDING NUMBERS

WBS–22–714–09–46
NAS3–26618

6. AUTHOR(S)

Edwin J. Kawecki and Gregg L. Ribeiro

7. PERFORMING ORGANIZATION NAME(S) AND ADDRESS(ES)

United Technologies Corporation
Pratt & Whitney
Government Engines & Space Propulsion
411 Silver Lane
East Hartford, Connecticut 06108

8. PERFORMING ORGANIZATION REPORT NUMBER

E–14803

9. SPONSORING/MONITORING AGENCY NAME(S) AND ADDRESS(ES)

National Aeronautics and Space Administration
Washington, DC 20546–0001

10. SPONSORING/MONITORING AGENCY REPORT NUMBER

NASA CR—2005-213333

11. SUPPLEMENTARY NOTES

This research was originally published internally as HSR026 in January 1996. Responsible person, Diane Chapman, Ultra-Efficient Engine Technology Program Office, NASA Glenn Research Center, organization code PA, 216–433–2309.

12a. DISTRIBUTION/AVAILABILITY STATEMENT

Unclassified - Unlimited
Subject Categories: 01, 02, 05, and 07

Available electronically at http://gltrs.grc.nasa.gov

This publication is available from the NASA Center for AeroSpace Information, 301–621–0390.

12b. DISTRIBUTION CODE

13. ABSTRACT ***(Maximum 200 words)***

An experimental investigation was conducted on the internal aerodynamic stability of a family of two-dimensional (2–D) High Speed Civil Transport (HSCT) nozzle concepts. These nozzles function during takeoff as mixer-ejectors to meet acoustic requirements, and then convert to conventional high-performance convergent-divergent (CD) nozzles at cruise. The transition between takeoff mode and cruise mode results in the aerodynamic throat and the minimum cross-sectional area that controls the engine backpressure shifting location within the nozzle. The stability and steadiness of the nozzle aerodynamics during this so called throat shift process can directly affect the engine aerodynamic stability, and the mechanical design of the nozzle. The objective of the study was to determine if pressure spikes or other perturbations occurred during the throat shift process and, if so, identify the caused mechanisms for the perturbations. The two nozzle concepts modeled in the test program were the fixed chute (FC) and downstream mixer (DSM). These 2–D nozzles differ principally in that the FC has a large over-area between the forward throat and aft throat locations, while the DSM has an over-area of only about 10 percent. The conclusions were that engine mass flow and backpressure can be held constant simultaneously during nozzle throat shifts on this class of nozzles, and mode shifts can be accomplished at a constant mass flow and engine backpressure without upstream pressure perturbations.

14. SUBJECT TERMS

High speed civil transport; Nozzles; Throat shift; Fixed chute; Downstream mixer

15. NUMBER OF PAGES

84

16. PRICE CODE

17. SECURITY CLASSIFICATION OF REPORT	18. SECURITY CLASSIFICATION OF THIS PAGE	19. SECURITY CLASSIFICATION OF ABSTRACT	20. LIMITATION OF ABSTRACT
Unclassified	Unclassified	Unclassified	